Linear and Nonlinear Rheological Properties of Scarcely Crosslinked Poly(dimethyl siloxane) Gels

Hideaki Takahashi

2009

Contents

CHAPTER 3

Examination of Gelation Process

CHAPTER 4

Linear Viscoelastic Behavior of Scarcely Crosslinked Poly(dimethyl siloxane) Gel

CHAPTER 6

Nonlinear Mechanical Behavior of Scarcely Crosslinked Poly (dimethyl siloxane) Gel: Effect of Strand Length Polydispersity

CHAPTER 7

List of Publications

CHAPTER 1

INTRODUCTION

1-1. Background

So called "crosslinked polymers" include various materials, e.g. thermoset polymers including epoxy resin, visible light curing resins, rubbers, and gels containing sol components. These materials are utilized in a wide area of industries because of their excellent properties such as mechanical properties, thermal stability, solvent resistance. These properties, in particular the mechanical (rheological) properties, have been extensively investigated. The results of these studies are summarized below.

1-1-1. Analysis of network structure with the rheological methods

The rubber elasticity, seen for usual rubbers and gels at room temperature, is the feature that rubbers/gels can be largely elongated/deformed, by rater small forces, without rupture and their shape can recover immediately on the removal of the force. These features have been one of the most important subjects of study in the field of industries and polymer physics. The relationship(s) between the mechanical properties and the network structure of rubbers/gels has been studied over several decades. In the early studies, Flory showed the relationship between the shear modulus and the molecular weight between crosslinks (M_c) for the affinely deformed network.[1)] James and Guth[2)] showed that the fluctuation of the crosslinking points reduces the equilibrium modulus compared to that expected for the affine displacements of these points. Langley[3)] and Dossin and Graessley[4)] demonstrated that the modulus is enhanced by the trapped entanglement (permanent knot) between the network strands. However, in these theories, the cross-linked rubber network was idealized as a network having tetrafunctional

connectivity and being composed of strands of equal length. Thus, the value of M_c obtained from the data through analysis utilizing those theories was just an average, and the distribution of M_c could not be determined.

In vulcanization of rubbers and polymerization/crosslinking reaction of reactive prepolymers, the network structure is mostly nonuniform because of random formation of the crosslinks, trapped entanglements, and dangling chains. However, this structural nonuniformity provides the rubbers/gels with useful functions, for example, high extensibility, large impact absorption, and so on.

For the investigation of network structure of crosslinked polymers, rheological and/or swelling methods as well as dynamic light scattering (DLS),[5,6] small angle X-ray scattering (SAXS),[7] small angle neutron scattering (SANS)[8] methods have been used. Among these methods, the rheological method is frequently used for analysis of the gelation process and investigation of viscoelastic properties of crosslinked polymers. The molecular weight between crosslinks can be estimated from the conventional expression of plateau modulus[1,9] G_e as well as the swelling method. On the other hands, from DLS, SAXS, SANS, the distance between crosslinks can be estimated from analysis of the variation of scattering intensity data with the scattering angle. However, again, the values obtained with these methods are just an average.

Murakami *et al.* suggested a chemo-rheological method for determining the molecular weight between crosslinks.[10] In this method, stress relaxation measurements were performed for the thermally degrading rubbers. The stress decay was attributed to chemical scission of the rubber strands. Murakami *et al.* suggested that the previous Tobolsky's theory[11] for the relationship between stress and the number of effective strands could describe the stress decay behavior only during an early stage of the strand scission. Then, they proposed a new

relationship to estimate the strand length distribution of rubbers. Fig.1-1 shows the distribution curves of the degree of polymerization between crosslinks of DCP (dicumyl peroxide)-cured rubbers degraded at various temperatures.[10] The bottom panel in Fig.1-1 shows the theoretical calculation of the distribution of the degree of polymerization x between crosslinks based on the Murakami theory.[10] The calculation looks reasonable, although no data are available for small x (because of lack of sensitivity for measuring a small stress at long times) and thus the theory cannot be tested for those x.

After these pioneering studies, several new aspects have been revealed for natural rubbers (crosslinked cis-polyisoprene). For example, Toki *et al.*[12] examined X-ray diffraction from natural rubbers exhibiting the elongation-induced crystallization to discuss the length distribution of the rubber strands.

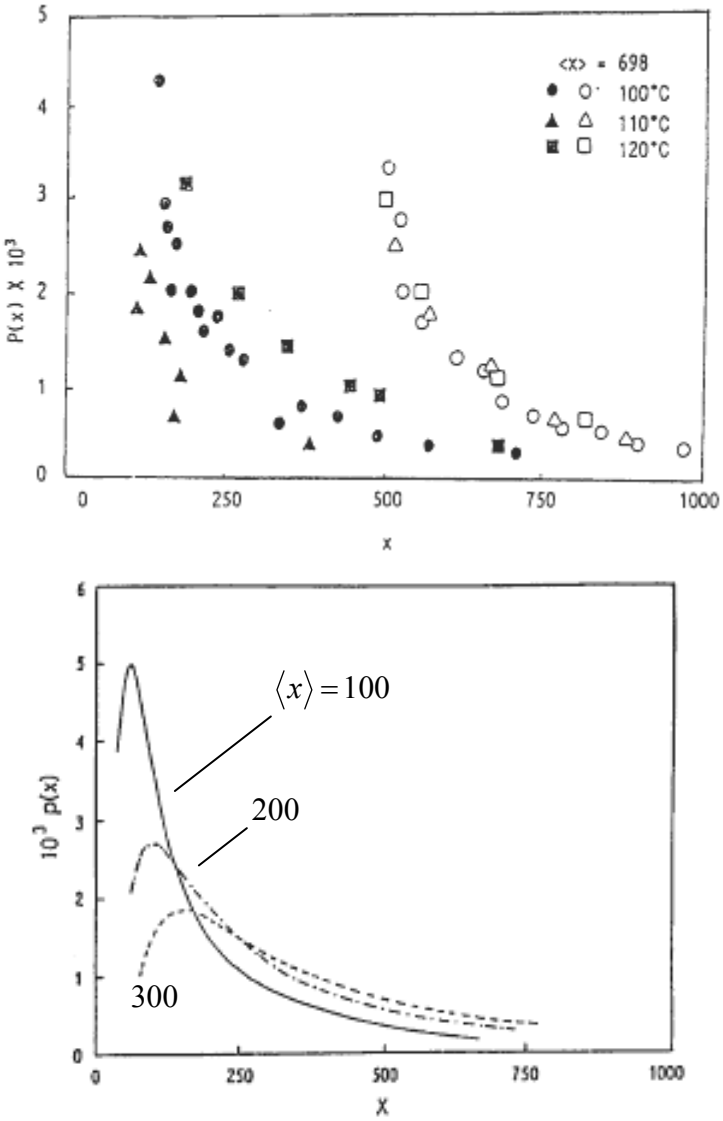

Figure 1-1 Distribution curves of the degree of polymerization between crosslinks of DCP-cured rubbers vulcanizate having the average of the degree of polymerization between crosslinks $\langle x \rangle = 698$ (top panel). The specimen was degraded at various temperatures. Unfilled symbols and filled symbols indicate the distribution obtained on the basis of Murakami's method[10] and Tobolsky's method.[11] Bottom panel shows theoretical calculation in Ref.10 with $\langle x \rangle$ values as indicated.

1-1-2. Properties of gels and rubbers with controlled network structure

The gels and rubbers having controlled network structure (gel strand length and crosslinking functionality) can be obtained with the "end-crosslinking" method. In this method, the prepolymers with well characterized molecular weight and reactive groups at their ends are allowed to react with a multifunctional crosslinker. The molecular weight between crosslinks (M_c) can be controlled by utilizing unimodal prepolymers. "Silicone gels" and "Silicone rubbers" are representative materials having the network formed with this end-crosslinking method. These materials are frequently utilized in the studies of the network structure of gels and rubbers, because they do not crystallize under large deformation (unlike natural rubbers).

There still remains a considerable debate and ongoing research concerning the validity of the rubber elasticity theory. "Well-characterized" networks have been prepared to test and evaluate these models. Patel *et al.* prepared successfully a model network through the end-linking hydrosilylation reaction of vinyl-terminated, monodisperse Poly(dimethyl siloxane) (PDMS) prepolymers with a tetrafunctional cross-linker.[13] Recently, Urayama *et al.* also synthesized the end-linked PDMS rubbers/gels containing the uniform network to extensively examine the properties of these rubbers/gels.[14-18]

The elastic free energy (W) governing stress-strain behavior of elastomer is used to predict the stresses (strains) under any type of strains (stresses). W can be theoretically formulated by considering a change of the number of conformations available for the network strands under deformation. However, early assessment of the molecular theories was ambiguous, because early studies utilized experimental data solely for the uniaxial deformation[19] measured for randomly crosslinked networks with obscure structure.[19-22] Urayama *et al.* examined the mechanical behavior of the uniform model PDMS network under biaxial deformations to demonstrate that the familiar Mooney-Rivlin (MR)[23,24] type

expression of W does not quantitatively reproduce the biaxial stress-strain data.[14-16)]

The significant deviation from the predictions of the classical theories of rubber elasticity (including the MR-type theory) seen for real rubbers/gels has been mostly attributed to the unrealistic assumption of "freely passing phantom networks" adopted in those theories.[23,24)] In real rubbers/gels, the network strands are mutually uncrossable to form the "trapped entanglement" in general. The modern molecular models of rubber elasticity consider the role of these entanglements in the rubber elasticity. However, these models were not clearly verified because of the restriction to the uniaxial elongational mode for randomly crosslinked networks in the earlier studies. Urayama *et al.*[14,17,18)] compared the mechanical behavior of the uniform model PDMS network under general uniaxial/biaxial elongational conditions with the predictions of five molecular models that differently treated the entanglement effects: These models included the diffused-constraint model[25)], the slip-link model[26)], and the tube models of several versions.[27-29)] It turned out that a version of slip-link model describes most successfully the experimental data for general uniaxial/biaxial elongational conditions.

Furthermore, Urayama *et al* investigated the dynamics of free guest chains trapped in uniform model networks in relation to the reputation concept (tube model).[30,31)] The crosslinked polymer network, giving an invariant topological environment for the guest chains, serves as a simpler experimental model system compared to polymer melts. Earlier studies[32-34)] for similar guest chains were not conclusive partly because of a chemical difference between the host and guest chains,[32)] polydispersity of the guest chains/host strands,[33,34)] and the necessity of stress subtraction in the analysis.[32,33)] (The relaxational stress of the guest chains could be obtained only after subtraction of the host stress from the measured stress data.) Urayama *et al.*[14,35)] overcame this difficulty by using their uniform model network and monodisperse linear guest chains, both having the same chemical structure (PDMS). They

investigated the guest/host pairs of different guest molecular weights M_g and host mesh sizes M_x (molecular weight between crosslinks). An example of their results is shown in Fig.1-2, where the dynamic Young's modulus (E') and loss tangent ($\tan\delta$) of these pairs are plotted against the angular frequency (ω). Clearly, the characteristic relaxation time of the guest chain τ_g strongly increases with increasing M_g, demonstrating the entanglement effect on the guest dynamics. It was also found that τ_g is longer in the host network having $M_x < M_e$ (M_e = entanglement spacing in bulk PDMS) than in the host with $M_x \cong M_e$. This difference represents the network effect (stronger constraint) for the guest dynamics.

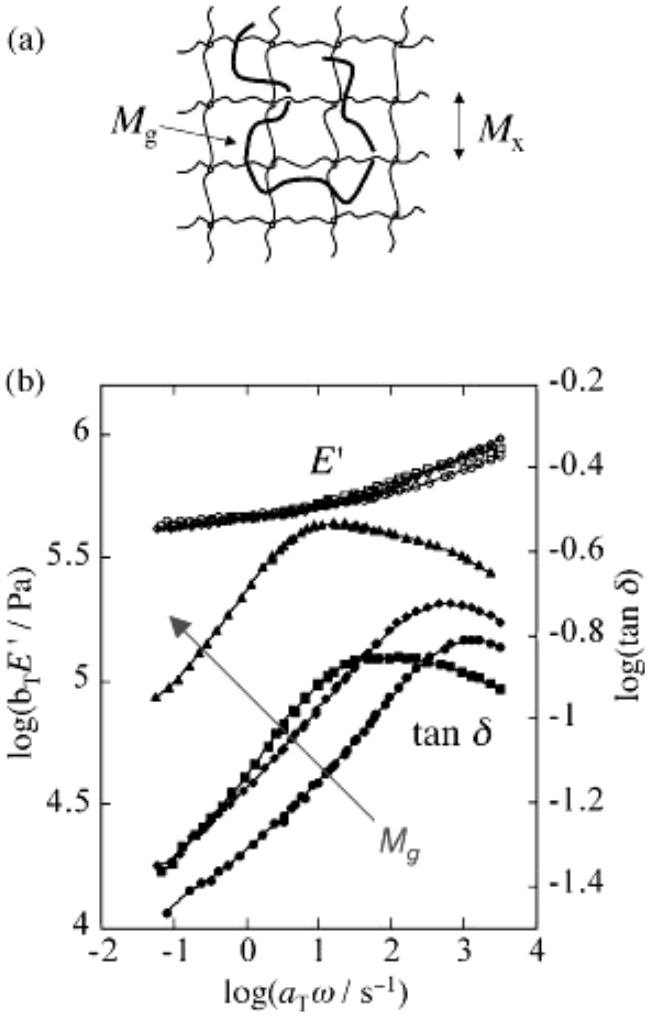

Figure 1-2 (a) Schematic illustration of a guest linear chain trapped in a host network.[14] (b) Master curves of dynamic storage Young's modulus E' (unfilled symbols) and the loss tangent $\tan\delta$ (filled symbols) for the entanglement-dominated PDMS network (with $M_x < M_e$) containing the guest linear PDMS chains of various M_g ($> M_e$). The reference temperature is 30℃.[14]

The classical theory of rubberlike elasticity assumes that four strands diverge from each crosslinking points (tetrafunctional crosslink), all strands are equal in length, and dangling chains are negligible. However, industrially produced rubbers/gels are composed of polydisperse strands and contain dangling tail/loop chains, as explained earlier. For these rubbers/gels, the relationships between material properties and network structure cannot be well analyzed because of difficulties in characterization of the network strand length distribution.

In relation of this point, the effect of molecular weight distribution of the network strands on the rubber elasticity has been investigated extensively for model PDMS rubbers/gels.[36-42] Mark *et al.* utilized the end-crosslinking method to prepare the bimodal networks composed of very short and relatively long PDMS strands and examine the relationship between this distribution and modulus/deformation of the rubbers.[37-40] The elongational stress of this bimodal rubber was found to exhibit non-Gaussian feature (significantly sigmoidal stress-strain relationship), which was in contrast to the Gaussian feature seen for the rubber composed of unimodal strands. This difference can be attributed to non-affine deformation of particular strands (early full stretch of short strands) under large strains. However, their model rubbers were not free from the trapped entanglements and the effect of the strand length distribution could be clearly resolved only after an analysis of the effects of the trapped entanglements.

Theoretically, the maximum attainable elongational ratio λ_{max} of rubbers free from the trapped entanglement can be evaluated as a full-stretch ratio of each strand:

$$\lambda_{max} = R_{max} / \left\langle R_c^2 \right\rangle^{1/2} = (bN_m)/(bN_m{}^{1/2}) = N_m{}^{1/2} \tag{1.1}$$

Here, $\left\langle R_c^2 \right\rangle^{1/2}$ and R_{max}, respectively, are the mean-square end-to-end distance and the full-stretch end-to-end length of the strand, and b and N_m are the monomer step length and the number of monomers per strand. This theoretical λ_{max} can easily reach 20, while the actual λ_{max} measured for usual rubbers hardly reach 10 because of the trapped entanglements therein.[43] In the presence of the entanglement, λ_{max} is governed by the number N_e of monomers per entanglement and the corresponding expression, $\lambda_{max} = N_e^{1/2}$ (Eq.(1.1) with N_m being replaced by N_e) is in accord with experiments.[44]

In relation to this point, Obuknov *et al.*[45] predicted that deswollen networks with supercoiled strands could be highly elongated even compared to the network composed of entanglement-free, random Gaussian strands. Urayama *et al.* actually prepared such a supercoiled network first by allowing end-crosslinking of monodisperse prepolymers in dilute solutions (where the entanglement is hardly formed) and then fully remove the solvent under vacuum.[14,46-48] The crosslinked gel largely decreased its volume on this solvent removal, and the resulting dry, deswollen rubber contains supercoiled strands. This supercoiled rubber had λ_{max} as large as 30,[14,46-48] lending support to the molecular view of supercoil proposed by Obuknov *et al.*[45]

Impact absorption (damping) is also a specific, useful function of rubbers/gels. Damping materials are used in various fields, for example, seismic isolation of buildings and protection of electronic parts. As electronic parts are improved and highly integrated for these days, the parts may be exposed to the complicated vibration in a wide range of frequency. However, since the electronic parts are fragile against the vibration, a damping material with high performance is desired for protection of those parts. The loss tangent $\tan\delta$ is often employed as a measure of dissipation of deformation energy.[9] The $\tan\delta$ value for a damping material is desired to be large and constant in wide ranges of temperature and frequency. To achieve this

property, earlier studies attempted to broaden the glass transition zone (where $\tan\delta$ is enlarged) as well as to optimize the location of the glass transition temperature T_g to the desired temperatures by blending[49] or interdegitating[50,51] chemically different polymers having different T_g's. However, as long as the tuning of damping relies on the glass transition, the optimized transition zone could not be significantly broadened/flattened. Furthermore, an unavoidable, large decrease of E' at around T_g is not desired for a damping material. As an alternative method, impregnation of high-viscosity oils for enhancement of damping was also attempted.[13,35,52,53] However, the oils could be extracted from materials, allowing the material to be used only in enclosed systems.

Urayama *et al.* prepared a damping material composed solely of an irregular network with many pendant chains through end-linking of a mixture of bifunctional and monofunctional end-reactive linear prepolymers (PDMS) with a tri-functional crosslinker and/or end-linking of the bifunctional prepolymers with the crosslinker at an off-stoichiometric composition.[14,54] These materials exhibited large $\tan\delta$ values (~ 0.3) over wide ranges of temperature and frequency. This temperature- and frequency-insensitive damping was attributable to a broad relaxation spectrum of irregular networks having the pendant chains of various length/degree of branching. The topological control thus achieved through the control of end-linking reaction offers a new route for functionalizing polymer networks.

1-2. Scope of this thesis

As explained in the previous section, extensive experimental studies for model rubbers/gels (made through end-linking of prepolymers) have improved the molecular

understanding of polymer networks to a considerable depth. Nevertheless, for rubbers having nonuniform network structure, complete characterization of their structure and analysis of the structure-property relationship cannot be easily made.

This thesis does not claim to have all necessary approaches for this complete characterization/analysis. Instead, it aims to add several new insights to advance the existing knowledge. For this purpose, the focus of this thesis is placed on the gelation process and the rheological, swelling, and mechanical properties of scarcely crosslinked poly(dimethyl siloxane) PDMS gels made from a double-liquid reaction of two prepolymers having monomethylsilyl group in the chain backbone and vinyl group at the chain end. The gelation occurs mainly through the reaction of these functional groups.

This thesis is divided into seven chapters including this introductory part as the first chapter. Chapter 2 describes details of the methods of preparation and characterization of the PDMS gel samples as well as the principles and methods of experiments employed in the studies.

Chapter 3 investigates the linear viscoelastic behavior during a gelation process of two PDMS prepolymers. For further examination of the gelation process, the reacting prepolymer mixture was collected at several reaction times t_r and the molecular characteristics of toluene-soluble sol chains therein and a fraction of the remaining (unreacted) monomethylsilyl group ϕ_{HMeSi} were examined. The results are used to discuss the mechanism of forming the scarcely crosslinked PDMS gel.

Chapter 4 investigates the viscoelastic behavior of the scarcely crosslinked PDMS gel. The gel exhibited the fast and slow relaxation processes characterized with different types of power-law behavior of the loss modulus, G''. The equilibrium plateau modulus G_e as well as the equilibrium swelling ratio were used to characterize the gel network structure. From the

analysis of the storage and loss moduli, G' and G'', the origin of the two relaxation processes related to the gel network dynamics is discussed.

Chapter 5 examines further details of the linear viscoelastic behavior of scarcely crosslinked PDMS gels. For this purpose, the behavior is compared for the gel between before and after extraction of sol chains. The result confirms the origin of the two relaxation processes characterized with the power-law behavior of G''. Furthermore, the effect of the gel strand length on the relaxation behavior is also examined.

Chapter 6 examines nonlinear mechanical behavior of a scarcely crosslinked PDMS gel under constant-rate elongation and large step shear strains. In particular, the extensional behavior was compared for the gels with/without a strand length distribution to examine the role of this distribution in the mechanical rupture. Analysis of the linear viscoelastic moduli of the gel after imposition of large shear strains is used to further discuss the process of strand scission.

Finally, Chapter 7 gives a summary of the findings of this thesis.

References

1) Flory PJ, "*Principles of Polymer Chemistry*", Cornell University Press, Ithaca, New York (1953).
2) James HM, Guth EJ, *J Chem Phys* , **15**, 669 (1947).
3) Langley NR, *Macromolecules*, **1**, 348 (1968).
4) Dossin LM, Graessley WW, *Macromolecules*, **12**, 123 (1979).
5) Orakdogen N, Okay O, *Polym Bull*, **57**,631 (2006).
6) Kuru EA, Orakdgen N, Okay O, *Eur Polym J*, **43**, 2913 (2007).

7) Urayama K, Kawamura T, Hirata Y, Kohjiya S, *Polymer*, **39**, 3827 (1998).

8) Horkay F, Hecht AM, Zrinyi M, Geisser E, *Polymer Gels and Networks*, **4**, 451 (1996).

9) Ferry JD, *VIscoelastic Properties of Polymers, 3rd ed*., Wiley, New York (1980).

10) Murakami K, Oikawa H, Suh KD, *Nihon Reoroji Gakkaishi (J Soc Rheol Jpn)*, **17**, 13 (1989).

11) Tobolsky AV, *Properties and Structure of Polymers*, p233, John Wiley (1960).

12) Toki S, Sics I, Ran S, Liu L, and Hsiao BS, *Polymer*, **44**, 6003 (2003).

13) Patel SK, Marons S, Cohen C, Gillmor JR and Colby RH, *Macromolecules*, **25**, 5241 (1992).

14) Urayama K, *Polym J*, **40**, 669 (2008).

15) Kawamura T, Urayama K, Kohjiya S, *Macromolecules*, **34**, 8252 (2001).

16) Kawamura T, Urayama K, Kohjiya S, *J Polym Sci, Part B, Polym Phys*, **40**, 2780 (2002).

17) Urayama K, Kawamura T, Kohjiya S, *Macromolecules*, **34**, 8261 (2001).

18) Urayama K, Kawamura T, Kohjiya S, *J Chem Phys*, **118**, 5658 (2003).

19) Gottlieb M, Gaylord RJ, *Polymer*, **24**, 1644 (1983).

20) Higgs PG, Gaylord RJ, *Polymer*, **31**, 70 (1990).

21) Meissner B, *Polymer*, **41**, 7827 (2000).

22) Gottlieb M, Gaylord RJ, *Macromolecules*, **20**, 130 (1987).

23) Treloar LRG, *The Physics of Rubber Elasity 3rd ed.*, Oxford University Press: Oxford, England (1975).

24) Erman B, Mark JE, "*Structure and Properties of Rubberlike Netwoks*", Oxford University Press: Oxford, England (1997).

25) Kloczkowski A, Mark JE, Erman B, *Macromolecules*, **28**, 5089 (1995).

26) Edwards SF, Vilgis TA, *Polymer*, **27**, 483 (1986).

27) Gaylord RJ, Douglas JF, *Polym Bull*, **23**, 529 (1990).

28) Kaliske M, Heinrich G, *Rubber Chem Technol*, **72**, 602 (1999).

29) Rubinstein M, Panyukov S, *Macromolecules*, **30**, 8036 (1997).

30) de Gennes PJ, *J Chem Phys*., **55**, 572 (1971).

31) Doi M, Edwards SF, *The Theory of Polymer Dynamics*, Clarendon Press, Oxford (1986).

32) Kan HC, Ferry JD, Fetters LJ, *Macromolecules*, **13**, 1571 (1980).

33) Granick S, Pederson S, Nelb GW, Ferry JD, *J Polym Sci ,Polym Phys Ed.*, **19**, 1745 (1981).

34) Poh BT, Adachi K, Kotaka T, *Macromolecules*, **20**, 2569 (1987).

35) Urayama K, Yokoyama K, Kojiya S, *Macromolecules*, **34**, 4513 (2001).

36) Schimmel KH, Heinrich G , *Colloid Polym Sci* , **269**, 1003 (1991).

37) Mark JE, *Adv Polym Sci*, **44**, 1 (1982).

38) Llorente MA, Andrady AL, and Mark JE, *J Polym Sci ,Polym Phys Ed*, **19**, 621 (1981).

39) Mark JE, *Acc Chem Res* ,**27**,271 (1984).

40) Mark JE, *Rubber Chem Technol* , **72**, 465 (1999).

41) Mark JE, *Macromol Symp*, **201**, 77 (2003).

42) Smith TL, Haidar B, Hedrick JL , *Rubber Chem Technol*, **63**,256 (1990).

43) Kotani T, Kawashima M, Suzuki S, *Nippon Gomu Kyokaishi*, **12**, 1030 (1969).

44) Fetters LJ, Lohse DJ, Colby RH, *Chain Dimension and Entanglement Spacing, in Mark JE ed. Physical Properties of Polymers Handbook (2nd ed.)*, Springer, New York (2007).

45) S.P.Obknov, M.Rubinstein, R.H.Colby, *Macromolecules*, **27**, 3191 (1994).

46) K.Urayama, S.Kojiya, *Polymer*, **38**, 955 (1997).

47) K.Urayama, S.Kojiya, *Eur.Phys.J. B*, **2**, 75 (1998).

48) Urayama K, *Kobunshi*, **47**, 572 (1998).

49) J.A.Grates, D.A.Thomas, E.C.Hickey, L.H.Sperling, *J.Appl.Polym.Sci.*, **19**, 1731 (1975).

50) Nagatani A, *Nippon Gomu Kyokaishi*, **74**, 237 (2001).

51) Inoue K, Ito T, Sumita M, *Nippon Gomu Kyokaishi*, **74**, 186 (2001).

52) M.A.Bibbó, E.M.Vallés, *Macromolecules*, **17**, 360 (1984).

53) C.P.Yang, C.Y.Ting, *J. Appl. Polym. Sci*, **49**, 1019 (1993).

54) Urayama K, Miki T, Takigawa T, Kojiya S, *Chem Mat*, **16**, 173 (2004).

CHAPTER 2

Materials and Measurements

2-1. Introduction

In this thesis, commercially available two vinyl-terminated poly(dimethyl siloxane) prepolymers were used. Scarcely crosslinked PDMS gels were prepared with a double-liquid reaction of these prepolymers in bulk without utilizing solvent and multi-functional crosslinkers. The gel samples were subjected to rheological, swelling, and GPC measurements. A PDMS gel sample being composed of monodisperse strands, generously supplied from Prof. Urayama at Kyoto University, was also used as a reference material in Chapter 6. This sample was subjected to rheological measurements.

This chapter highlights the synthesis and characterization of the samples as well as the principles and methods of the measurements.

2-2. Synthesis and Characterization

2-2-1. Synthesis

Two linear PDMS prepolymers (SE1886; Toray-Dow Corning Silicone Co. Ltd; currently Dow Corning-Toray Co. Ltd) were utilized. The prepolymer A, a neat PDMS having vinyl groups at the ends, had the weight-average molecular weight and polydispersity index of $M_w = 34.7\times10^3$ and $M_w/M_n = 2.6$. The prepolymer B, a chemically modified PDMS with a small fraction (0.7 mol%) of the dimethylsilyl units being replaced by monomethylsilyl (HMeSi) units, had $M_w = 35.1\times10^3$ and $M_w/M_n = 3.1$. As judged from the degree of polymerization of the prepolymer B, $N_w \cong 470$ (evaluated from its M_w), each prepolymer B chain contained, on average, $\cong 3$ monomethylsilyl (HMeSi) groups in its backbone.

The mixture of two prepolymers A and B were allowed to react at 50˚C for 6h and at 120℃ for 3h, respectively, to prepare the PDMS gels examined in Chapter 3 and Chapters 4 – 6. Some details of the double-liquid crosslinking reaction (catalyzed with a trace amount of Pt complex contained in the prepolymer A) are shown in Scheme 2-1: The vinyl group at a prepolymer end reacts with the monomethylsilyl group in the prepolymer B as well as with the end vinyl group of the other prepolymers. The former route of the reaction, occurring more frequently than the latter,[1] gives a dangling prepolymer grafted onto a middle of the other prepolymer if the reaction efficiency is low, which was the case for the gel examined in Chapters 3-6.

The Gel-U utilized in Chapter 6 was prepared by Prof. Urayama at Kyoto University.[2] He obtained Gel-U from the stoichiometric end-linking reaction of monodisperse PDMS chains (M_n=84,000) and tetrafunctional crosslinkers. Gel-U contained a small amount (15 vol%) of guest linear PDMS chains (M_g= 138×10^3) in its uniform network.[2]

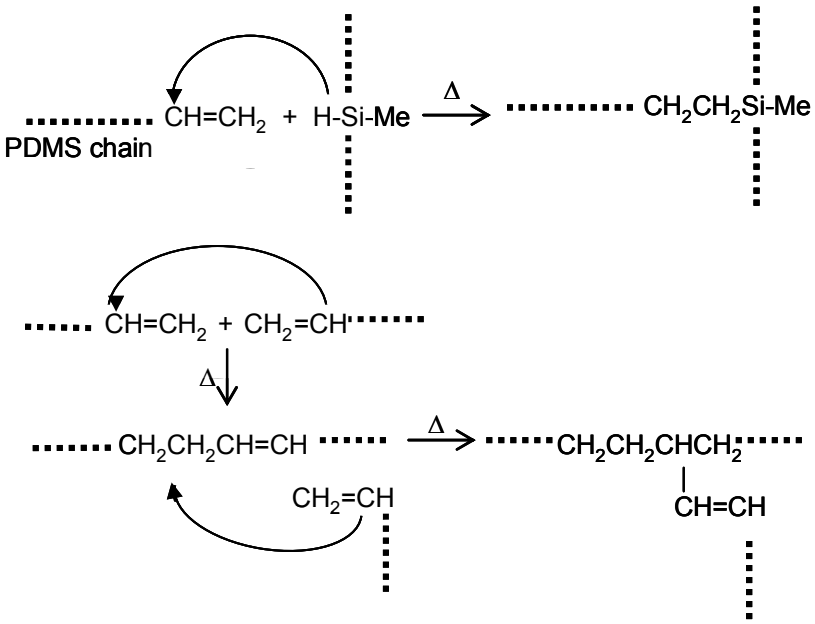

Scheme 2-1 Double-liquid crosslinking reaction of two types of vinyl terminated PDMS prepolymers in bulk. The upper route of the reaction (main reaction) gives a dangling prepolymer grafted onto a middle of the other prepolymer if the reaction efficiency is low.

2-2-2. Characterization

The gel samples utilized in Chapters 3-6 contained a large amount of sol chains. These sol chains were recovered by soaking the as-prepared gel samples (in a sheet-like form) in fresh toluene (good solvent for PDMS) for 48 h or 72 h, with toluene being replaced in every 12 h. All sol chains were extracted with this procedure, and the weight fraction ϕ_{sol} of the sol chains in the as-prepared gel was evaluated from the masses of the dry gel specimen before and after the sol extraction. The extracted sol chains were subjected to gel permeation chromatography (GPC) and low-angle light scattering (LALS) measurements to determine their weight-average molecular weight M_w and the molecular weight distribution. The principles and actual methods of these measurements are explained later.

The as-prepared gel samples (and a sample after the sol extraction) were subjected to viscoelastic and swelling experiments to determine an average molecular weight between crosslinks, M_c. The principles, analyses, and actual methods of these measurements are explained later.

For the gel samples utilized in Chapters 3-6, Tables 2.1-2.3 summarize the ϕ_{sol} and M_w data of the sol chains and the M_c data for the gel network obtained from the above measurements.

Table 2.1 Characteristics of a PDMS gel Used in Chapter 4.

sample code	w_A/w_B ratio[a]	ϕ_{sol}[b]	$10^{-3}M_{w,sol}$[c]	$10^{-3}M_c$[d]
Gel-1[e]	1/1	0.58	50.3	340

a: weight ratio of prepolymers A and B.
b: sol fraction in as-prepared gels determined after extraction of sol chains with toluene.
c: weight-average molecular weight of sol chains in as-prepared gels determined with GPC-LALS.
d: molecular weight between crosslinks determined from the equilibrium plateau modulus.
e: prepared in Chapter 4.

Table 2.2 Characteristics of PDMS gels Used in Chapter 5.

sample code	w_A/w_B ratio[a]	ϕ_{sol}[b]	$10^{-3}M_{w,sol}$[c]	$10^{-3}M_c$[d]
Gel-1[e]	1/1	0.58	50.3	340
Gel-2[f]	1/2	0.34	38.5	64
Gel-3[f]	2/1	0.92	81.8	——
Gel-1E[f,g]	1/1	0	——	340

a: weight ratio of prepolymers A and B.
b: sol fraction in as-prepared gel determined after extraction of sol chains with toluene.
c: weight-average molecular weight of sol chains in as-prepared gel determined with GPC-LALS.
d: molecular weight between crosslinks determined from the equilibrium plateau modulus.
e: prepared in Chapter 4.
f: prepared in Chapter 5.
g: gel sample containing no sol chains obtained after the sol extraction from Gel-1 sample.

Table 2.3 Characteristics of PDMS gels Used in Chapter 6.

sample code	w_A/w_B ratio	ϕ_{sol}	$10^{-3}M_{w,sol}$	$10^{-3}M_c$ [a]
Gel-1/1 [b]	1/1 [c]	0.47 [d]	45.8 [e]	190
Gel-U [f]	——	0.15 [f]	138 [g]	15

a: molecular weight between crosslinks determined from the equilibrium plateau modulus.
b: prepared in Chapter 6.
c: weight ratio of prepolymers A and B.
d: sol fraction in as-prepared gel determined after extraction of sol chains with toluene.
e: weight-average molecular weight of sol chains in as-prepared gels determined with GPC-LALS.
f: supplied from Prof. Urayama, Kyoto University.
g: from Ref.1.

2-3. Gel Permeation Chromatography (GPC) and Low-Angle Light Scattering (LALS)

2-3-1. Principle of GPC

GPC (Gel Permeation Chromatography) is a kind of liquid chromatography called "SEC (Size Elution Chromatography)". GPC is frequently used to determine molecular weight distribution (MWD) and the corresponding number- and weight-average molecular weights, M_n and M_w.

Fig. 2-1 shows the principle of SEC schematically.[3] When a polymer solution sample is injected into a column packed with granular gels having micro/nano-pores almost as large as the hydrodynamic volume of polymers, the polymer molecules are separated according to the hydrodynamic volumes. Polymer coils larger than the largest pores of the gels cannot enter the

pores and they are eluted at the interstitial volume V_i. On the other hand, molecules small enough to access the entire pore volume V_p are eluted at the sum of V_i and V_p. Molecules of a size between these extremes have access only to a part of the pore volume; hence they are eluted at an elution volume $V_e = V_i + K_g V_p$. Here, K_g is the partition coefficient of a sample in SEC[4] ($0 < K_g < 1$). Among the molecules that can enter the pores, a molecule being larger in size is eluted earlier.

M_w and MWD of a homopolymer sample are usually determined by use of a relationship between molecular weight M and the elution volume V_e (so-called calibration relationship). This relationship is obtained for standard polymers that are chemically identical to the sample and have known molecular weights and narrow, unimodal MWD (or, monodisperse MWD). The molecular weight $M_i(V_i)$ of a fraction of the sample eluted at a volume V_i is evaluated from the calibration relationship, and the concentration C_i of this fraction is proportional to the intensity h_i^{RI} of the refractive index (RI) increment signal at this V_i. (If the polymer exhibits UV adsorption, the UV signal can be utilized instead of the RI signal.) From the $\{h_i^{RI}, M_i\}$ data, M_w and M_n of the sample are determined as

$$M_w = \frac{\sum_i h_i^{RI} M_i}{\sum_i h_i^{RI}}, \quad M_n = \frac{\sum_i h_i^{RI}}{\sum_i h_i^{RI} / M_i} \tag{2.1}$$

The above calibration method works only when the standard polymers have the same chemical structure and topological architecture (e.g., linear, regularly star-branched, etc) as the examined sample. If the degree of branching of the sample is unknown, the calibration method (utilizing linear polymer standards) cannot easily apply. However, even for this case, the molecular weight M_i of the fraction of the sample at the elution volume V_i can be

determined, on the absolute basis, from the RI and low-angle light scattering (LALS) signals at this V_i. The principle of this absolute LALS method is explained below.

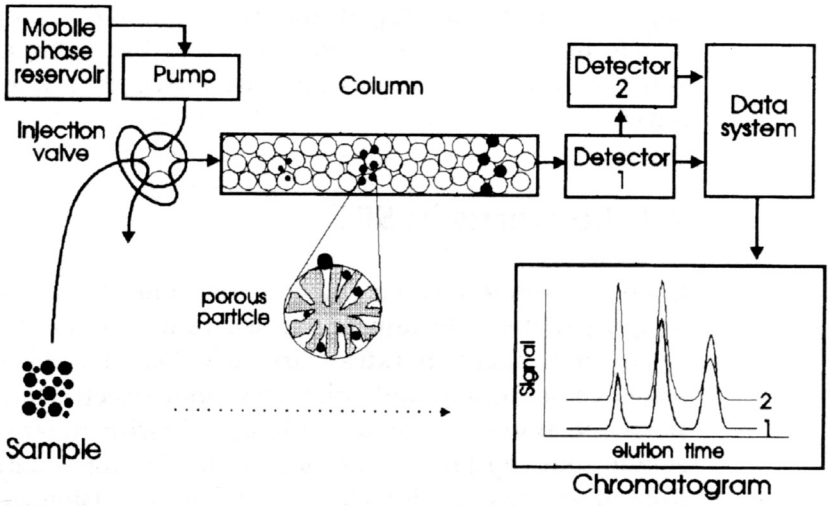

Figure 2-1 Principle of size exclusion chromatography.[3)]

2-3-2. Principle of LALS

When polymer chains in a dilute solution are exposed to light, the intensity of the light scattered from the chains is generally proportional to the number and size of the polymers. The Reyleigh ratio R is defined as $R = (I_s r^2)/(I_i V_s)$, where I_i and I_s denote the intensities of incident and scattered light beams, respectively, V_s is the scattering volume in the solution, and r is the distance from the scattering point to a detector. This R is usually dependent on the angle between the incident and scattered light beams, θ, and expressed, after subtraction of the background scattering from the solvent, as

$$\frac{K_1 C}{R(\theta)} = \left[\frac{1}{M_W} + 2A_2 C + 3A_3 C^2 + \cdots\right]\left[\frac{1}{P(\theta)}\right] \tag{2.2}$$

Here, M_w and C denote the weight-average molecular weight and mass concentration of the polymer sample, respectively, A_2 and A_3 are the second and third virial coefficients. K_1 is a numerical factor determined by the refractive index of the solvent n, the refractive index increment dn/dC, Avogadro constant N_A, and the wavelength of incident light λ_i:

$$K_1 = \frac{2\pi^2 n^2 (\mathrm{d}n/\mathrm{d}C)^2}{N_A \lambda_i^4} \tag{2.3}$$

The function $P(\theta)$ appearing in Eq.(2.2) is a form factor reflecting a spatial distribution of the scattering points within a polymer molecule, i.e., the polymer chain conformation. For small scattering angle θ, $P(\theta)$ is expressed as

$$\frac{1}{P(\theta)} = 1 + \left(\frac{1}{3}\right)\left\langle S^2 \right\rangle_z q^2 \quad \text{for small } \theta \tag{2.4}$$

where $\langle S^2 \rangle_z$ is the z-average mean-square radius of gyration, and q is a scattering vector defined by

$$q = \frac{4\pi n}{\lambda_i} \sin\left(\frac{\theta}{2}\right) \tag{2.5}$$

At infinite dilution ($C \to 0$) and low angle ($\theta \to 0$), the form factor reduces to $P(\theta) = 1$, and the terms in Eq.(2.2) containing A_2 and A_3 vanish. Then, Eq.(2.2) becomes

$$\frac{K_1 C}{R(\theta)} = \frac{1}{M_{\mathrm{w}}} \tag{2.6}$$

Thus, the value of M_{w} is determined from the low-angle light scattering (LALS) intensity from dilute solutions.

The above LALS method requires the solvent refractive index, n, and its increment ratio for the polymer, (dn/dC), to be determined from separate experiments. With the n and (dn/dC) data, Eqs.(2.3) and (2.6) allows absolute determination of M_{w} requiring no reference polymer. However, the determination of M_{w} becomes easier if a reference polymer is utilized. For example, for chemically identical reference and sample polymers, M_{w} of the sample is easily determined from the $R(\theta)/C$ ratio measured at low θ and C and the reference molecular weight $M_{\mathrm{w,ref}}$ as

$$M_{\mathrm{w}} = \frac{\left[R(\theta)/C\right]^{\mathrm{sample}}_{\theta,C\to 0}}{\left[R(\theta)/C\right]^{\mathrm{ref}}_{\theta,C\to 0}} M_{\mathrm{w,ref}} \tag{2.7}$$

This reference method can apply even if the reference polymer is chemically different from the sample polymer. For this case, Eq.(2.7) is modified as (cf. Eqs.(2.3) ad (2.6))

$$M_{\mathrm{w}} = \frac{\left[\dfrac{R(\theta)}{C\{\mathrm{d}n/\mathrm{d}C\}^2}\right]^{\mathrm{sample}}_{\theta,C\to 0}}{\left[\dfrac{R(\theta)}{C\{\mathrm{d}n/\mathrm{d}C\}^2}\right]^{\mathrm{ref}}_{\theta,C\to 0}} M_{\mathrm{w,ref}} \tag{2.8}$$

Namely, M_{w} of the sample polymer can be determined from the (dn/dC) data for the sample and reference in addition to the $M_{\mathrm{w,ref}}$ data.

The above reference method can apply to the polymer sample in either an isolated LALS photometer or a photometer connected to GPC equipped with the refractive index (RI) increment detector. In particular, for the latter case, the molecular weight can be determined for the sample as a whole as well as each sample fraction at the elution volume V_i. Namely, from the RI and LALS signal intensities h_i^{RI} and h_i^{LS} of the fraction at V_i, M_{i} of this fraction is evaluated as

$$M_{\mathrm{i}} = \frac{(\mathrm{d}n/\mathrm{d}C)_{\mathrm{ref}}}{(\mathrm{d}n/\mathrm{d}C)_{\mathrm{sample}}} \frac{\left[h_i^{\mathrm{LS}}/h_i^{\mathrm{RI}}\right]^{\mathrm{sample}}}{\left[A_{\mathrm{ref}}^{\mathrm{LS}}/A_{\mathrm{ref}}^{\mathrm{RI}}\right]} M_{\mathrm{w,ref}} \tag{2.9}$$

where $A_{\mathrm{ref}}^{\mathrm{RI}}$ and $A_{\mathrm{ref}}^{\mathrm{LS}}$ are the integrated RI and LALS signals obtained from the GPC-LALS measurement for the reference solution, and $(\mathrm{d}n/\mathrm{d}C)_{\mathrm{sample}}$ and $(\mathrm{d}n/\mathrm{d}C)_{\mathrm{ref}}$ are the RI increment ratios for the sample and reference. The $(\mathrm{d}n/\mathrm{d}C)_{\mathrm{ref}}/(\mathrm{d}n/\mathrm{d}C)_{\mathrm{sample}}$ ratio appearing in Eq.(2.9) is easily evaluated from the integrated RI signals of the sample and reference solutions of known concentration C as

$$\frac{(\mathrm{d}n/\mathrm{d}C)_{\mathrm{ref}}}{(\mathrm{d}n/\mathrm{d}C)_{\mathrm{sample}}} = \frac{\left[A^{\mathrm{RI}}/C\right]^{\mathrm{ref}}}{\left[A^{\mathrm{RI}}/C\right]^{sample}} \tag{2.10}$$

(If the reference is chemically identical to the sample, $(\mathrm{d}n/\mathrm{d}C)_{\mathrm{ref}}/(\mathrm{d}n/\mathrm{d}C)_{\mathrm{sample}} = 1$ and Eq.(2.9) is further simplified.) Thus, the GPC-LALS method gives a easy/simple route for determination of M_{i} of the sample fraction. From this M_{i} and the RI signal intensity h_i^{RI}, M_{w} and M_{n} of the sample as a whole as well as the polydispersity index $M_{\mathrm{w}}/M_{\mathrm{n}}$ can be straightforwardly evaluated through Eq.(2.1).

2-3-3. Method

In Chapter 3, the PDMS prepolymer reaction mixture during the gelation process was collected, and the sol chains therein were characterized with the GPC-LALS measurement. The measurement was conducted with a GPC system (Model 515; Waters Co. Ltd) equipped with a gel column (TSK-gel-GMHXL) and connected to a multi-angle light scattering (MALS) photometer (DAWN-EOS, Wyatt Technology Co., Ltd) covering low to high scattering angles. The solvent was toluene (a good solvent for PDMS). Commercially available linear PDMS chains (Polymer Source Inc.) were utilized as the elution/LALS standards, and the sol data were analyzed on the basis of Eq.(2.9) (with $(dn/dC)_{ref}/(dn/dC)_{sample} = 1$ because the sample and reference were chemically identical) and Eq.(2.1) to determine M_w and M_w/M_n of the sol chains. In addition, the RI signal recorded as a function of elution volume was converted to the molecular weight distribution function representing the weight fraction as a function of the molecular weight. In the actual measurement, the toluene solution of the collected reaction mixture was filtered with Millipore unit (0.2μm) to remove the insoluble gel component formed in a late stage of reaction. Thus, the sol concentration in the sample solution was smaller than a nominal concentration determined from the mass of the collected reaction mixture. This sol concentration was determined from the integrated RI signal intensity with the aid of the intensity-concentration calibration made for the prepolymer A.

In Chapters 4-6, the sol was extracted from the sample after full gelation. These sol chains were characterized with the GPC-LALS measurements. The measurements were conducted with the GPC system (Model 515; Waters Co. Ltd) equipped with the gel column (TSK-gel-GMHXL) and connected to a LALS photometer (KMX-6; Chromatrix Co., Ltd) detecting low-angle scattering data. The solvent was toluene, and the prepolymer A (with M_w determined from LALS) and commercially available polystyrenes (PS) of known M_w (TSK;

Toso Co., Ltd) were utilized as the elution/LALS standards. The data were analyzed on the basis of Eqs.(2.9) and (2.1) to determine M_w and M_w/M_n of the sol chains. (The $(dn/dC)_{ref}/(dn/dC)_{sample}$ ratio was evaluated for the prepolymer A and PS references; cf. Eq.(2.10).)

2-4. Rheological Measurements

2-4-1. Concept

Rheology is the science of deformation and flow of matter. In this thesis, the matter is polymeric samples. The rheological character of the sample, specified by a stress-strain relationship, can be conveniently determined with a device called rheometer (Fig.2-2).

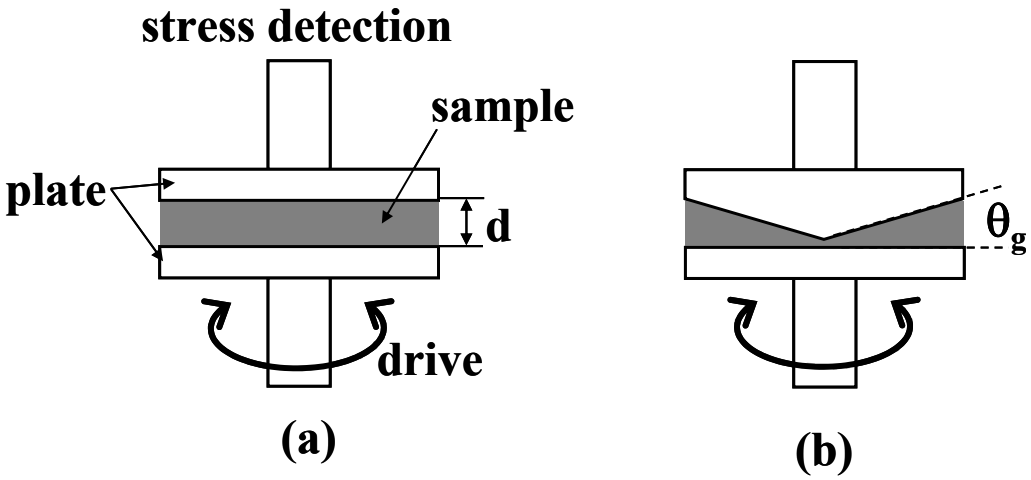

Figure 2-2 Schematic illustration of the rheological device: (a) parallel plate (gap d), (b) cone/plate (gap angle θ_g)

2-4-2. Principle of linear viscoelastic measurement

When a material is abruptly subjected to a small shear strain γ at a time $t = 0$, the

resulting shear stress $\sigma(t)$ at $t > 0$ is proportional to the strain and can be written as

$$\sigma(t) = G(t)\gamma \tag{2.11}$$

Here, $G(t)$ is the linear viscoelastic relaxation modulus of the material being independent of γ.

In the linear viscoelastic regime, $\sigma(t)$ for a shear strain $\gamma(t)$ of arbitrary history (t dependence) can be conveniently expressed in terms of $G(t)$ through the Boltzmann's superposition principle:[5)]

$$\sigma(t) = \int_{-\infty}^{t} G(t-t')\dot{\gamma}(t')\mathrm{d}t' \tag{2.12}$$

Here, $\dot{\gamma}(t')$ is the strain rate at a past time $t' < t$, and the term $\dot{\gamma}(t')\mathrm{d}t'$ represents an infinitesimal step strain imposed at that time.

In general, $G(t)$ has a distribution of relaxation modes that can be represented with a discretized relaxation spectrum $\{h_p, \tau_p\}$, with h_p and τ_p being the intensity and characteristic time of the p-th relaxation mode, as[5,6)]

$$\begin{aligned} G(t) &= G_\mathrm{e} + \sum_{p\geq 1} h_p \exp(-t/\tau_p) \quad \text{for a solid} \\ G(t) &= \sum_{p\geq 1} h_p \exp(-t/\tau_p) \qquad\quad \text{for a liquid} \end{aligned} \tag{2.13}$$

where G_e represents the equilibrium modulus (of a solid). τ_p is defined in the order of $\tau_1 > \tau_2 > \tau_3$, and τ_1 represents the longest relaxation time.

The linear viscoelastic measurements are usually conducted under sinusoidal shear strain that oscillates with time at an angular frequency ω and amplitude γ_0 ($<< 1$) as

$$\gamma(t) = \gamma_0 \sin(\omega t) \tag{2.14}$$

As noted from Eqs.(2.12) and (2.14), $\sigma(t)$ in a stationary state oscillates at the same ω but with

a phase different from $\gamma(t)$:

$$\sigma(t) = \gamma_0 \left[G'(\omega) \sin(\omega t) + G''(\omega) \cos(\omega t) \right] \tag{2.15}$$

The storage and loss moduli appearing in Eq.(2.15), $G'(\omega)$ and $G''(\omega)$, represent the elastic and viscous components of the stress that are in-phase and out-of-phase with respect to the sinusoidal strain, respectively. These moduli can be related to the relaxation modulus $G(t)$ through Fourier transformation

$$G'(\omega) = \omega \int_0^\infty G(t) \sin(\omega t) \mathrm{d}t, \quad G''(\omega) = \omega \int_0^\infty G(t) \cos(\omega t) \mathrm{d}t \tag{2.16}$$

Thus, $G'(\omega)$ and $G''(\omega)$ are equivalent to $G(t)$ and fully represent the linear viscoelastic feature of the material. From Eqs.(2.12)-(2.15), $G'(\omega)$ and $G''(\omega)$ can be also expressed in terms of the relaxation spectrum $\{h_p, \tau_p\}$. For a liquid and a solid, this expression is given by

$$\begin{aligned} G'(\omega) &= \sum_p h_p \frac{(\omega\tau_p)^2}{1+(\omega\tau_p)^2}, \qquad G''(\omega) = \sum_p h_p \frac{\omega\tau_p}{1+(\omega\tau_p)^2} \quad \text{for a liquid} \\ G'(\omega) &= G_\mathrm{e} + \sum_p h_p \frac{(\omega\tau_p)^2}{1+(\omega\tau_p)^2}, \; G''(\omega) = \sum_p h_p \frac{\omega\tau_p}{1+(\omega\tau_p)^2} \quad \text{for a solid} \end{aligned} \tag{2.17}$$

At sufficiently low ω ($<< 1/\tau_1$, with τ_1 being the longest relaxation time), Eq.(2.17) gives simple proportionalities,

$$\begin{aligned} &G'(\omega) \propto \omega^2, G''(\omega) \propto \omega \quad \text{for a liquid} \\ &G'(\omega) = G_\mathrm{e}, G''(\omega) \propto \omega \quad \text{for a solid} \end{aligned} \tag{2.18}$$

The relaxation of a given sample is not completed in a range of ω where these proportionalities have not been observed.

In a stress relaxation test, a step strain is abruptly applied at time 0 and the shear stress $\sigma(t)$ (= $G(t)\gamma$, cf. Eq.(2.11)) is measured at $t > 0$. Alternatively, the linear viscoelastic

behavior can be also characterized by applying a step shear stress σ at time 0 and measuring the following evolution of strain $\gamma(t)$ at $t > 0$. The material function obtained from this creep test is the creep compliance defined by

$$J(t) = \gamma(t) / \sigma \tag{2.19}$$

$J(t)$ is related to the relaxation modulus through a general expression, $\int_0^t G(t')J(t-t')\mathrm{d}t' = t$. Thus, $J(t)$ is equivalent to $G(t)$.

2-4-3. Principle of elongational test

If an isotropic specimen is elongated in one direction, it usually shrinks equally in the other two directions. In this experiment referred to as a simple elongation experiment, a linear relationship is observed between the elongational stress $\sigma_E(t)$ and the tensile strain ε (Hencky strain; $\varepsilon = \ln \lambda$ with λ being the elongational ratio) if the strain is small.[5] For an incompressible material, this relationship is simply expressed in terms of the relaxation modulus $G(t)$ defined for the shear strain as

$$\sigma_E(t) = 3\int_{-\infty}^{t} G(t-t')\,\dot{\varepsilon}(t')\mathrm{d}t' \tag{2.20}$$

For this case, the tensile relaxation modulus or Young relaxation modulus, $E(t)$, coincides with $3G(t)$. The dynamic Young modulus is defined by Eq.(2.16) with $G(t)$ therein being replaced by $E(t)$. The dynamic Young modulus is also expressed in terms of the tensile relaxation spectrum $\{3h_p, \tau_p\}$ through Eq.(2.17) with h_p therein being replaced by $3h_p$.

2-4-4. Principle of time-temperature superposition

For a material characterized with the relaxation spectrum $\{h_p, \tau_p\}$, the thermo-rheological

simplicity is observed for its linear viscoelastic properties [5] if all relaxation modes have the same temperature dependence in their characteristic times τ_p and intensities h_p and these $\tau_p(T)$ and $h_p(T)$ at a temperature T are expressed as

$$h_p(T) = b_T h_p(T_r), \tau_p(T) = a_T \tau_p(T_r) \tag{2.21}$$

Here, T_r is a reference temperature, and a_T and b_T are the T-dependent but p-independent shift factors. Substitution of Eq.(2.21) into Eq.(2.17) gives a relationship of the dynamic moduli at different temperature T and T_r,

$$G'(\omega)\big|_{\text{at } T} = b_T G'(\omega a_T)\big|_{\text{at } Tr}, G''(\omega)\big|_{\text{at } T} = b_T G''(\omega a_T)\big|_{\text{at } Tr} \tag{2.22}$$

Eq.(2.22) means that the moduli data at the temperature T and angular frequency ω are equivalent to the data at the reference temperature T_r and a frequency ωa_T, which allows construction of a master curve of the moduli at T_r covering a wide range of ω by shifting/superposing the data at various T along the ω axis as well as the modulus axis, although the shift along the latter axis is usually small.

This shift usually works for homogeneous polymeric liquids because the viscoelastic relaxation of this material occurs through accumulation of a local motion and its mode distribution merely reflects the distribution of the length scale of relaxation, not a distribution of the activation energy. The modulus shift factor b_T is known to be close to $T\rho(T)/T_r\rho(T_r)$, with $\rho(T)$ being the mass density at the temperature T. The WLF-type frequency shift factor, represented as $\log a_T = -C_1(T-T_r)/(C_2+T-T_r)$ (with C_1, C_2 = constant), is frequently observed at T not very higher than the glass transition temperature, but the Arrhenius-type shift factor ($\ln a_T = \Delta E\{T^{-1}-T_r^{-1}\}$) is also noted at high T. Thus, the frequency shift factor is to be experimentally determined as the factor giving the best superposition for respective materials.

2-4-5. Method

Dynamic viscoelastic measurements were conducted with a strain-controlled commercial rheometer, MR-300 Soliquid-meter (Reoroji Co.Ltd) in Chapter 3, and with MR-500 Soliquid-meter (Reoroji Co.Ltd) in Chapters 4-6. The experimental conditions were summarized in Table 2.4. The measurements were made in the linear viscoelastic regime (under small strain amplitudes). In Chapters 4 and 5, measurements for the gel specimen were made under slight compression (with a normal stress < 0.15 Pa) in order to prevent the sample slippage. The $G'(\omega)$ and $G''(\omega)$ data measured for the PDMS network after full gelation (Chapters 4-6) exhibited the thermo-rheological simplicity, and the data at different T were superposed to construct the master curves at 20˚C (cf. section 2-4-4.)

Table 2.4 Experimental Conditions in Dynamic Viscoelastic Measurements in Chapters 3 – 6.

Chapter	geometry	γ_0	ω /s^{-1}	temperature /℃
3	PP [a]	≤ 0.2	0.13 – 13	50
4	PP [b]	< 0.2	0.063 – 63	-40 – 100
5	PP [b]	< 0.2	0.063 – 63	-40 – 100
6	CP [c]	≤ 0.3	0.063 – 63	20

a: parallel-plate (round disk) of the diameter = 18 mm.
b: parallel-plate (round disk) of the diameter = 20 mm.
c: cone-plate of the diameter = 20 mm and gap angle = 2 deg.

In Chapters 4 and 5, creep tests were conducted for the gel specimens with a laboratory stress rheometer (RS600; Haake Co. Ltd) to determine the creep compliance $J(t)$ at 20˚C. A

parallel-plate fixture of a diameter = 20 mm was used, and the measurement was conducted at a shear stress of 50 Pa that was well in the linear viscoelastic regime for the gel. The $J(t)$ data covering up to $t = 10^4$ s were converted to the storage and loss modulus $G'(\omega)$ and $G''(\omega)$, which was helpful for extending the master curves of $G'(\omega)$ and $G''(\omega)$ to lower ω.

In Chapter 6, step shear tests were conducted for the gel specimens at 20˚C (room temperature) with a cone-plate (CP) fixture of diameter = 20 mm and gap angle = 2 deg mounted on a laboratory rheometer (MR-500 Soliquid-meter; Reoroji Co. Ltd). Each specimen was subjected to a step shear strain γ in a range of γ = 0.01-5.1, and the shear stress σ was measured as a function of time t (up to 10^4 s) after imposition of the strain. The measured σ was not proportional to γ, and this nonlinearity was represented through the *nonlinear* relaxation modulus, $G(t,\gamma) = \sigma(t,\gamma)/\gamma$. For each run of the step shear test, the specimen was freshly prepared in the CP fixture with the method explained earlier.

In all these measurements, a specimen was sandwiched between the plates or between cone and plate, and either the upper plate (RS600; Haake Co. Ltd) or lower plate (MR-300 Soliquid-meter, MR-500 Soliquid-meter; Reoroji Co. Ltd) was driven to deform the specimen; cf. Fig.2-2. The mechanical response, detected with a force transducer and/or a position sensor, was converted into the dynamic moduli according to Eq.(2.15), the creep compliance according to Eq.(2.19), and the nonlinear relaxation modulus $G(t,\gamma) = \sigma(t,\gamma)/\gamma$.

Elongational tests in Chapter 6 were conducted for rectangular gel specimens at 20˚C (room temperature) with an extensional viscosity fixture (EVF) attached to a laboratory rheometer (ARES, Rheometrics Co. Ltd; currently TA Instruments). The elongational strain rate $\dot{\varepsilon}$ was set constant at $\dot{\varepsilon}$=0.01 and 0.1 s^{-1}. The true elongational stress σ_E (not the engineering stress reduced to unit cross-sectional area before the elongation) was measured. In EVF, the specimen was wound onto a rotating shaft to be subjected to the constant-rate

elongation. Small ledges made of a silicone adhesive were attached to the pulling edges of the specimen, and the specimen was gripped at these ledges by metal pins of EVF. These ledges were helpful for start-up of winding without slippage of the specimen.

2-5. Evaluation of Molecular Weight between Crosslinks M_c

2-5-1. Use of theory of rubber elasticity

For crosslinked gels/rubbers, the network therein is frequently assumed to be composed of monodisperse Gaussian strands being tetrafunctionally crosslinked to each other (without forming the dangling tails/loops) and the crosslinking points are assumed to affinely displaced on application of the macroscopic (external) strain without exhibiting spatial fluctuation. Under these assumptions the strand molecular weight between crosslinks is related to the equilibrium plateau modulus G_e and mass density of the network ρ as[7)]

$$M_c = \frac{\rho RT}{G_e} \tag{2.23}$$

Here, R is the gas constant and T is the absolute temperature.

Although the PDMS gels examined in this thesis were composed of polydisperse strands and the above assumptions were not valid, the M_c given by Eq.(2.23) is still useful as a measure for the average molecular weight between crosslinks in those gels. Thus, the M_c evaluated from the G_e data is utilized to discuss the network structure of the PDMS gel in Chapters 3-6.

2-5-2. Use of theory of network swelling

Rubbers usually absorb a solvent in contact to increase their volumes. On this swelling

phenomenon, the network strands between crosslinks are forced to expand/stretch. At the same time, the entropic force acting along the strand tends to shrink the strand. These two forces are in balance at the swelling equilibrium.

For the network composed of monodisperse Gaussian strands (without forming dangling tails/loops), the swelling behavior is described within the same thermodynamic framework as that utilized for formulation of the equilibrium modulus (Eq.(2.23)). In this framework known as the Flory-Rehner theory,[7] the equilibrium volume ratio V_R and the equilibrium swelling ratio Q_{eq} defined by $V_R = 1/Q_{eq} = V_0/V$, with V_0 and V the network volume before and after full swelling, are related to the number density of active strands n_e as

$$n_e = -\frac{V_0}{\upsilon_s}\frac{\ln(1-V_R)+V_R+\chi V_R^{\,2}}{\left(V_R^{\,1/3}-V_R/2\right)} \tag{2.24}$$

Here, χ and υ_s represent the interaction parameter between polymer and solvent and the molar volume of solvent, respectively. Scarcely crosslinked networks (typically having $M_c \geq 10000$) exhibit significant swelling to have $V_R << 1$. For this case, Eq.(2.24) can be satisfactorily approximated as

$$n_e = \frac{V_0 V_R^{5/3}}{v_s}\left(\frac{1}{2}-\chi\right) \qquad (\text{for } V_R^{\,1/3} >> V_R/2) \tag{2.25}$$

From this n_e and the specific volume of a crosslinked polymer, υ_p, M_c is obtained as

$$M_c = \frac{V_0}{\upsilon_p n_e} \tag{2.26}$$

This M_c can be obtained from the V_R data through Eqs.(2.24) - (2.26).

Although the PDMS gels examined in this thesis were not composed of monodisperse strands and the above assumptions were not valid, the M_c given by Eq.(2.26) is still a useful measure for the average molecular weight between crosslinks. This M_c, evaluated from the

measured swelling ratio at equilibrium, is later utilized to discuss the network structure of the PDMS gel.

References

1) Macosko CW, Benjamin GS, *Pure Appl Chem*, **53**, 1505 (1981).

2) Urayama K, Yokoyama K, and Kohjiya S, *Macromolecules*, **34**, 4513 (2001).

3) Pasch H, Trathnigg B, "*HPLC of Polymers*", Springer, Berlin (1999).

4) Skoog DA, Holler FJ, Nieman TA, "*Principles of Instrumental Analysis, 5th ed.*", Harcourt Brace & Company, Florida (1998).

5) Ferry JD, *Viscoelastic Properties of Polymers, 3rd ed*., Wiley, New York (1980).

6) H. Watanabe, *Prog. Polym. Sci.*, **24**, 1253 (1999).

7) Flory PJ, *Principles of Polymer Chemistry*, Cornell University Press, Ithaca, New York (1953).

CHAPTER 3

Examination of Gelation Process

3-1. Introduction

Gelation is a phenomenon of converting a "sol" having fluidity to a "gel" with no fluidity under an infinitesimal stress. The gelation in polymeric systems is usually associated with formation of chemical/physical crosslinks through which the polymer chains are incorporated in the gel network as the constituent strands. The gelation was first analyzed by Flory[1)] and Stockmayer[2)] through the branched chain models and later by Stauffer[3,4)] through the percolation model, with the effects of the excluded volume and the loop-type strands on gelation being better analyzed in the latter model. Since the properties of polymeric systems drastically change on gelation, the gelation has been regarded as a critical phenomenon within the framework of the percolation model. Specifically, self-similarly branched structure at the critical gelation point has been characterized with a fractal exponent,[5,6)] and the viscoelastic property at this point has been described in terms of this exponent.[7,8)] However, this exponent does not have a universal value applicable to all gelation systems, and theoretical analysis is still being continued for this problem.

Gelation through formation of chemical crosslinks has been viscoelastically investigated for various polymeric systems including epoxy resions,[9-18)] polyurethane,[19-21)] and poly(acryl amide).[22)] Winter and coworkers[23-25)] showed that at the critical gelation point the storage and loss moduli $G'(\omega)$ and $G''(\omega)$ exhibit the power-law dependence on the angular frequency ω reflecting the fractal structure of the gel network at this point:

$$G''(\omega) = G'(\omega)\tan\delta \propto \omega^{n_g} \ (0 < n_g < 1), \ \tan\delta = n_g\pi/2 \tag{3.1}$$

This simple power-law dependence stimulated extensive studies. Tordjeman *et al.*[26,27] focused on the exponent n_g appearing in Eq.(3.1) to discuss the gel structure in model systems obtained through end-crosslinking of telechelic prepolymers. Braun *et al.*[28] made a simulation for molecular weight distribution and concentration of the soluble chains (sol chains) during a gelation process and compared the results with experiments. They also evaluated, from the simulation, the fractions of dangling chains and loops during the gelation to discuss a change in the network structure on gelation. Thus, the molecular understanding of gel has been significantly refined on the basis of the power-law relationship, Eq.(3.1). However, it should be also emphasized that the critical gelation characterized by Eq.(3.1) does not necessarily occur in all systems. In fact, Winter and Mours pointed out that non-critical gelation is desirable for preparation of high damping materials.[29]

Concerning the above features of gelation, this Chapter examines the rheological behavior during the gelation (crosslinking) process of a PDMS gel prepared through a double-liquid reaction of two PDMS preplymers. A gel obtained from 1:1 mixture of the prepolymers (hereafter referred to as Gel-1) was found to have a considerably large sol fraction ($\phi_{sol} = 0.66$), and its equilibrium modulus G_e was much smaller than the nominal modulus calculated from the number average molecular weight $M_{n,pre}$ of the prepolymers, $G_e^o = (1-\phi_{sol})\rho RT/M_{n,pre}$. The mechanism of formation of such a "scarce" gel having $G_e << G_e^o$ was also examined. Specifically, the sol chains collected at several stages in the crosslinking process were characterized and the results were compared with the viscoelastic behavior at those stages. It turned out that the crosslinking occurred in two steps to result in the large polydispersity of the gel strands. This two-step crosslinking also appeared to provide Gel-1 with a non-critical character (invalidity of Eq.(3.1)). Details of these results are presented below.

3-2. Experimental

3-2-1. Material

Commercially available two vinyl-terminated PDMS prepolymers (SE1886; Dow Corning Toray Co.,Ltd) were used, as explained in Chapter 2. The prepolymer A, a neat PDMS having vinyl-groups at the ends, had the weight average molecular weight and polydispersity index of $M_{w,pre} = 34.7\times10^3$ and $M_{w,pre}/M_{n,pre} = 2.6$. The prepolymer B, a chemically modified PDMS with a small fraction (0.7 mol%) of the dimethylsilyl units being replaced by monomethylsilyl units, had $M_{w,pre} = 35.1\times10^3$ and $M_{w,pre}/M_{n,pre} = 3.1$. As judged from the degree of polymerization of the prepolymer B, $N_w \cong 470$ (evaluated from its $M_{w,pre}$), each prepolymer B chain contained, on average, $\cong 3$ monomethylsilyl (HMeSi) groups in its backbone.

The Gel-1 was prepared from a 1/1 (wt/wt) mixture of the prepolymers A and B. The gelation (crosslinking) occurred mainly through a reaction of the (HMeSi) groups in the backbone of the prepolymer B with the vinyl groups at the chain ends of A and B, as illustrated in the top part of Scheme 2-1. A minor reaction between vinyl groups also occurred to some extent; cf. bottom part.

The Gel-1 sample was prepared in a rheometer at 50˚C. At this temperature, the crosslinking reaction was rather slow so that the reaction mixture at several stages in the gelation process could be easily collected (for molecular characterization) without disturbing much the viscoelastic measurement: The mixture was placed between the parallel plates in the rheometer chamber (for the measurement) as well as on a horizontal part of an inner wall of the chamber (the part not disturbing the measurement) for collection of the mixture. The linear viscoelastic measurement was repeatedly conducted throughout the gelation process except for a sample collection period: At a given reaction time (curing time) t_r, the chamber

was narrowly opened to collect a small amount (~ 0.1 g) of the mixture and then quickly closed to conduct the viscoelastic measurement. The chamber was opened just for ~20 sec or less on each sample collection, and a change of the sample temperature was not significant (a decease by ~ 3 degree that was recovered in 30 sec after closing the chamber). The collected material was subjected to GPC/NMR measurements, as explained below in more detail.

3-2-2. Measurements

During the whole course of the gelation at 50˚C except the sample collection period explained above, the storage and loss moduli $G'(\omega)$ and $G''(\omega)$ were *repeatedly* measured in the direction of decreasing angular frequency ω with a commercial rheometer, MR-300 Soliquid-meter (Reoroji Co., Ltd) in the condition shown in Table 2.4. The measurement has been made in the linear viscoelastic regime (strain amplitude ≤ 0.2). The isochronal moduli for a given ω value at a given reaction time t_r were evaluated from interpolation of the data recorded as functions of reaction time.

The 1:1 prepolymer mixture collected at given t_r was quenched with liquid nitrogen, weighed (after returning to room temperature), and subjected to GPC and ^{1}H-NMR measurements. For comparison, the unreacted prepolymers were also subjected to the measurements.

The GPC measurement was conducted with Model 515 (Waters Co. Ltd) equipped with a gel column (TSK-gel-GMHXL) and connected to a multi-angle light scattering (MALS) photometer DAWN-EOS (Wyatt Technology Co., Ltd) under the condition described in section 2-3-3. The solvent was toluene (a good solvent for PDMS).

^{1}H-NMR measurement was conducted with Varian MERCURY plus AS400 spectrometer to determine the number ratio $r(t_r)$ of H in the HMeSi group to H in the dimethylsilyl (Me_2Si) group. This ratio was utilized to calculate the fraction of the unreacted HMeSi group at

given t_r. A static magnetic field was set at 9.4 T, and the resonance frequency was 400.0 MHz. The pulse width (flip angle), pulse repetition, and number of scan were 6.25 μs (45 deg), 1 min, and 4, respectively. The collected materials were dissolved in deuterated chloroform, filtered with Millipore unit (0.2μm), and then subjected to the measurements. Thus, the ratio $r(t_r)$ characterized the chemical composition of the sol component in the collected material. The number fraction $n_{HMeSi}(t_r)$ of the unreacted HMeSi group in the sol component at given t_r was evaluated as $n_{HMeSi}(t_r) = r(t_r)/r(0)$, where $r(0)$ is the H number ratio measured for the 1:1 mixture of the prepolymers before the reaction at 50˚C.

3-3. Results and Discussion

3-3-1. Viscoelastic behavior

Fig.3-1 shows the storage and loss moduli, G' and G'', of the 1:1 mixture of the prepolymers during the gelation process at reaction times t_r as indicated. These G' and G'' data were obtained after interpolation of the data (repeatedly measured as functions of time) to the given t_r, as explained earlier. The data are double-logarithmically plotted against the angular frequency ω with an arbitrary frequency shift factor A as indicated.

In the range of ω examined, respective prepolymers and their mixture at 50˚C exhibited the terminal relaxation (flow) behavior characterized by the power-law relationships, $G' \propto \omega^2$ and $G'' \propto \omega$; cf. Eq.(2.18). This behavior is noted also for the 1:1 prepolymer mixture allowed to react at 50˚C for t_r = 54 min; see Fig.3-1. At t_r = 60 min, G'' remains almost proportional to ω but the ω dependence of G' becomes considerably weaker than the ω^2 dependence, indicating that a weak but slow relaxation process prevails at this t_r. The ω dependence weakens even for G'' on a further increase of t_r ($\geq$ 65 min), suggesting the formation of a 3-dimensional microgel at those t_r. In fact, for $t_r \geq$ 65 min, the GPC

measurement confirmed existence of a toluene-insoluble microgel, as explained later in more detail. The slow relaxation seen at $t_r \geq 65$ min can be related to these microgels. Finally, at $t_r = 308$ min, the gelation is almost completed to exhibit the ω-insensitive plateau of G' and much smaller G'' at low ω. The equilibrium plateau modulus at $t_r = 308$ min (where the gelation was almost completed and the reaction mixture had $\phi_{sol} = 0.66$), $G_e = 450$ Pa (cf. Fig.1), was considerably smaller than the nominal modulus calculated from $M_{n,pre}$ of the prepolymers, $G_e^o = (1-\phi_{sol})\rho RT/M_{n,pre} = 740\times10^3$ Pa with ρ, R, T being the density, gas constant, and absolute temperature (cf. Eq.(2.23)). This result indicates that a scarce gel network having a very low number density of its effective strands was formed on completion of the reaction.

In relation to this gelation behavior, it should be noted that the critical gelation characterized with the ω-independent $\tan\delta$ (Eq.(3.1)) was not observed for Gel-1; see Fig.3-2 where the $\tan\delta$ data at several representative ω values are plotted against t_r. This result strongly suggests that the gelation of Gel-1 occurred without forming a huge, self-similarly branched critical gel chains. This lack of critical gelation is in harmony with the molecular characteristics of the sol chains explained below.

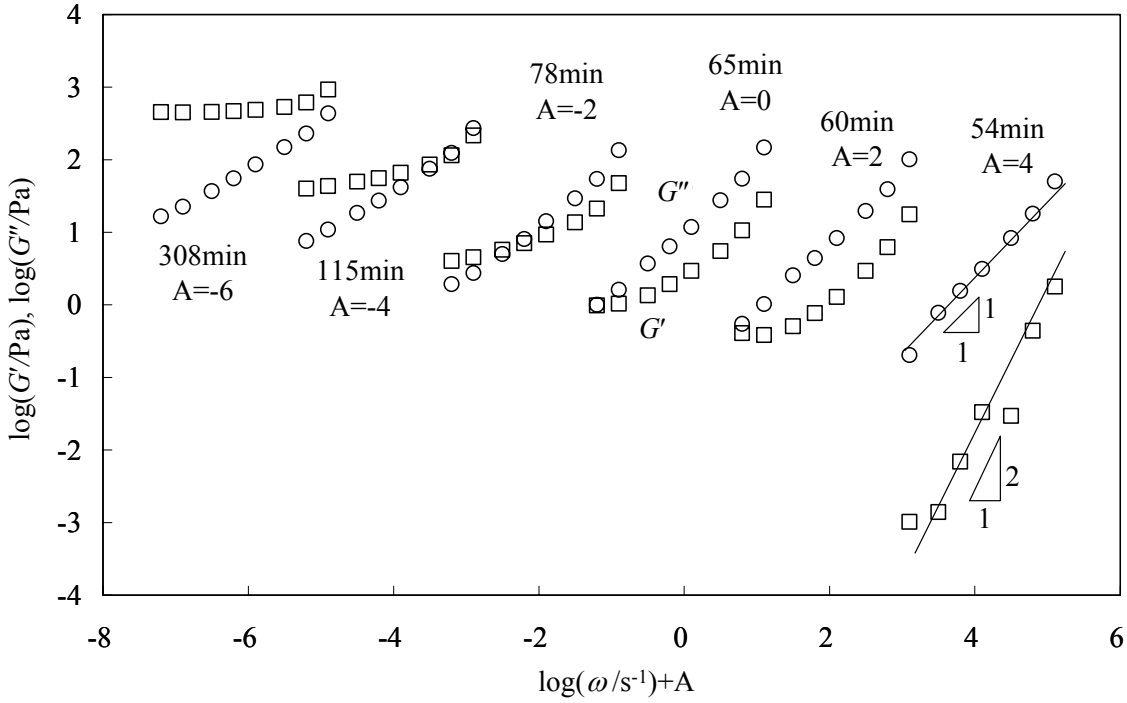

Figure 3-1 Change in frequency dependence of storage and loss moduli, *G*' and *G*", at various curing times as indicated. The reaction (curing) temperature was 50℃.

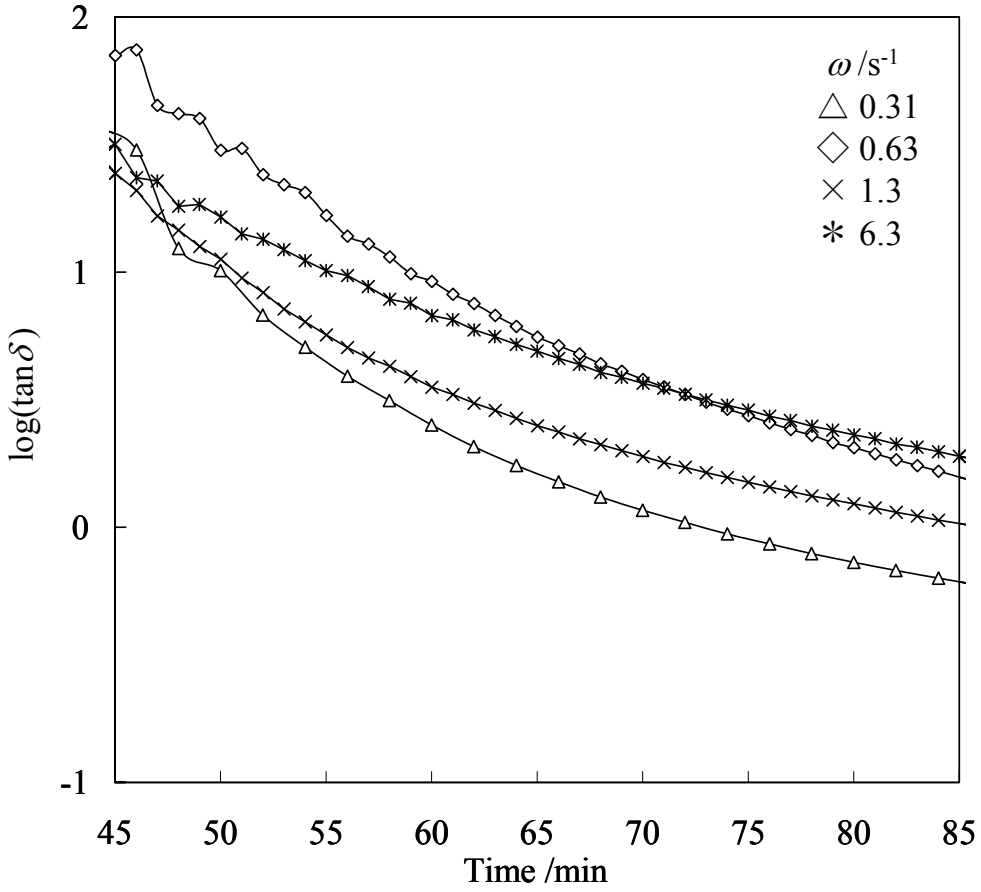

Figure 3-2 Time dependence of loss tangent (tanδ) measured at 50℃ at various angular frequencies as indicated. ω = 0.31s^{-1}(△), 0.63s^{-1}(◇), 1.3s^{-1}(×), 6.3s^{-1}(*).

3-3-2. Characterization of sol and gel components

The top panel of Fig.3-3 shows the GPC profile (refractive index (RI) increment signal) of the toluene-soluble sol component in the 1:1 prepolymer mixture collected at the reaction times t_r as indicated. For comparison, the profile is also shown for the prepolymer A ($t_r = 0$). (The profile of the prepolymer B was close to that of the prepolymer A). The molecular weight M utilized in the abscissa axis was determined from the RI and light scattering (LS) signals and thus the absolute molecular weight. The GPC profiles are normalized by their integrated intensity so that the changes in the molecular weight distribution of the sol component with t_r can be visually/easily observed.

As noted in the top panel of Fig.3-3, the GPC profile for the sol component tails to a larger M side (almost reaching $M = 1\times10^7$) with increasing t_r up to 65 min and then this high-M tail vanishes on a further increase of t_r to 308 min. This result clearly indicates that huge sol chains were formed in an early stage of the gelation reaction and these sol chains were incorporated in the insoluble gel network in the late stage.

The high-M tail thus formed during the reaction may contain densely branched chains (pre-gel chains). For characterization of this tail, it is useful to focus on an elution volume difference, $\Delta V_e(M,\mathrm{sol}) \equiv V_e(M,\mathrm{sol}) - V_e(M,\mathrm{linear})$, for each section of the GPC profile. Here, $V_e(M,\mathrm{sol})$ is the elution volume of the sol component having the molecular weight M (absolute molecular weight determined from RI/LS signals), and $V_e(M,\mathrm{linear})$ is the elution volume of a linear PDMS chain having the same M. $V_e(M,\mathrm{linear})$ was evaluated from the elution calibration for the linear PDMS standards. The bottom panel of Fig.3-3 shows plots of $\Delta V_e(M,\mathrm{sol})$ at respective t_r against log M. The branching in the sol component can be examined for this plot, as explained below.

In general, the GPC elution volume V_e is determined by a hydrodynamic volume of the polymer coil, as explained in Chapter 2. This hydrodynamic volume is reflected in the

intrinsic viscosity $[\eta]$, and the universal linear relationship holds between $\log [\eta]M$ and V_e:[31] $\log [\eta]M = -V_e/K + B$ with K (> 0) and B being constants. If the sol chain is a regularly branched f-arm star chain and the excluded volume effect is not significant, its $\Delta V_e(M,\mathrm{sol})$ is evaluated from this relationship as[32]

$$\begin{aligned} \Delta V_e(M,\mathrm{sol}) &= K \log [\eta]_{\mathrm{linear}}/[\eta]_{\mathrm{star}} \\ &= K \log [0.586\,(f/2)^{3/2}/\{0.390(f-1)+0.196\}] \\ &\cong K \log [1.5(f/2)^{3/2}] \quad \text{for } f >> 1 \end{aligned} \tag{3.2}$$

Namely, $\Delta V_e(M,\mathrm{sol})$ increases logarithmically with f for this case. Although actual sol chains quite possibly have an irregularly multi-branched structure and the excluded volume is not negligible for PDMS in toluene, $\Delta V_e(M,\mathrm{sol})$ should be larger, in general, for the sol chains having more branches. Thus, $\Delta V_e(M,\mathrm{sol})$ can be utilized as a measure for the degree of branching for the sol component in the reaction mixture.

As noted in the bottom panel of Fig.3-3, the sol component has $\Delta V_e(M,\mathrm{sol}) \cong 0$ at $M \leq 3\times10^4 \cong M_{w,\mathrm{pre}}$ ($\log M < 4.5$) irrespective of t_r and the sol chains included in this section of M are linear chains (mostly unreacted prepolymers). In contrast, $\Delta V_e(M,\mathrm{sol})$ is larger than zero and increases with increasing $M > 3\times10^4$, suggesting that the sol chains in this section of M are mostly branched chains and their degree of branching is larger for larger M. In the late stage of gelation reaction, these high-M branched sol chains should have been incorporated in the gel network and the main portion of the sol component becomes the linear chains, as evidenced from the top panel of Fig.3-3 where the fraction of the high-M tail (in particular for $M > 10^5$) is noted to decrease significantly with increasing t_r/min from 65 to 308.

Corresponding to the above change of the sol component during the gelation reaction, a toluene-insoluble gel component was formed at $t_r \geq 65$ min. For characterization of this gel

formation, the GPC signal intensity was calibrated (with the signal for the prepolymer A being utilized as a reference) to evaluate the weight fraction $\phi_{sol}(t_r)$ of the sol in the reaction mixture at respective t_r. For the sol component, the number ratio $r(t_r)$ of the HMeSi group to the chemically inert Me_2Si group in the chain backbone was also determined from the ^{1}H-NMR measurement. The $r(t_r)/r(0)$ ratio coincides with a number fraction $n_{HMeSi}(t_r)$ of unreacted HMeSi group in the sol component at t_r. This $n_{HMeSi}(t_r)$ should be smaller for the gel component than for the sol component, although $n_{HMeSi}(t_r)$ could not be determined for the insoluble gel component.

Figs.3-4 and 3-5, respectively, show plots of $\phi_{sol}(t_r)$ and $n_{HMeSi}(t_r)$ against t_r. Clearly, $n_{HMeSi}(t_r)$ of the sol component rapidly decreases from 1 to $\cong$ 0.3 on an increase of t_r/min from 0 to 65, i.e., in the early stage of gelation reaction, and then gradually decreases to zero at longer t_r (in the late stage); see Fig.3-5. In contrast, the sol fraction $\phi_{sol}(t_r)$ remains close to unity in the early stage, and the decrease of $\phi_{sol}(t_r)$ is noted only in the late stage; see Fig.3-4. Thus, the insoluble gel was formed only after consumption of the majority of the HMeSi group. This result, being consistent with that seen in Fig.3-3, suggests a scenario of the gelation mechanism illustrated in Fig.3-6: In the early stage, highly branched but soluble chains (pre-gel chains) of the molecular weight almost reaching $M_{sol\text{-}tail} = 1\times10^7$ are formed through consumption of the majority of HMeSi group; see the top-to-middle part of Fig.3-6. The high-M tail of this pre-gel is composed of $M_{sol\text{-}tail}/M_{w,pre} \cong 300$ prepolymer chains. In the late stage at $t_r > 65$ min, $\phi_{sol}(t_r)$ largely decreases while $n_{HMeSi}(t_r)$ gradually decreases with t_r (cf. Figs.3-4 and 3-5). Thus, the pre-gel chains should have been mutually linked through the remaining HMeSi groups to form 3-dimensional, insoluble gel network, as illustrated in the middle-to-bottom part of Fig.3-6. Since $n_{HMeSi}(t_r)$ for the sol chains is small at long t_r ($n_{HMeSi}(t_r) < 0.1$ for $t_r > 100$ min; cf. Fig.3-5) and $n_{HMeSi}(t_r)$ for the gel component should be even smaller, the pre-gel chains can be mutually linked only scarcely in the late stage.

Furthermore, the sol component at long t_r (= 308 min) is mainly composed of linear chains (mostly prepolymer chains), as explained for Fig.3-3. Thus, in the late stage, the huge pre-gel chains appear to be preferentially linked to form the gel without involving much of those low-M linear sol chains, as illustrated in the middle-to-bottom part of Fig.3-6.

In relation to the above scenario, it is noted that a small fraction of the HMeSi group (≅ 0.1) remains unreacted even at t_r = 120 min (Fig.3-5) but the gelation slows considerably at around this t_r (Fig.3-4). This slowing should have occurred not because of the full consumption of the HMeSi group but possibly due to the steric hindrance: Namely, the sol chains would not easily approach the reactive sites (HMeSi and/or vinyl groups) remaining inside of the highly branched pre-gel chains because of the steric repulsion, thereby kinetically retarding the reaction. In fact, on (practical) completion of the gelation, the sol fraction was considerably ($\phi_{sol}(\infty) = 0.58$) possibly because of this kinetic factor.

The above gelation scenario, formation of densely branched pre-gel chains (having M as large as 1×10^7) followed by scarce linking of these chains, suggests a difference of the degree of branching at length scales below and above the size of the pre-gels chains. Thus, in this type of gelation, the *self-similarly* hyper-branched chains of infinitely large molecular weight is not formed, which naturally results in the lack of the critical gelation behavior seen in Fig.3-2. It is also noted that most of the prepolymer chains should be involved in the gel network as the dangling loops/tails for the case of the two-step gelation, as illustrated in Fig.3-6. The elasticity at low ω is sustained only by a small fraction of the prepolymer chains involved in the scarcely percolated links between the pre-gel chains, which naturally results in the "average" molecular weight between effective crosslinks considerably larger than $M_{n,pre}$ and the measured equilibrium modulus considerably smaller than the nominal modulus, $G_e^o = (1-\phi_{sol})\rho RT/M_{n,pre}$.

Finally, it is informative to examine the mole ratio $r_{HMeSi/vinyl}$ of the HMeSi group to the

vinyl group (at the prepolymer chain end). For the 1/1 wt/wt reaction mixture examined here, the $r_{\mathrm{HMeSi/vinyl}}$ ratio is close to 1/3 (calculated from M_{n} of the prepolymers and the HMeSi content (0.7 mol%) in the prepolymer B). This off-stoichiometric ratio may appear to have led to the formation of very scarce effective strands giving $G_{\mathrm{e}} <<$ nominal modulus $G_{\mathrm{e}}^{\mathrm{o}} = (1-\phi_{\mathrm{sol}})\rho RT/M_{\mathrm{n,pre}}$. However, the plateau modulus expected for this $r_{\mathrm{HMeSi/vinyl}}$ value is of the order of $r_{\mathrm{HMeSi/vinyl}}G_{\mathrm{e}}^{\mathrm{o}} \cong 250\times10^{3}$ Pa, which is much larger than the equilibrium plateau modulus measured at $t_{\mathrm{r}} = 308$ min (where the gelation was almost completed), $G_{\mathrm{e}} = 450$ Pa; cf. Fig.3-1. Thus, the off-stoichiometry does not seem to be the main factor leading to the formation of the very scarce effective strands. Instead, the two-step gelation illustrated in Fig.3-6 is quite possibly responsible for the scarce strand formation.

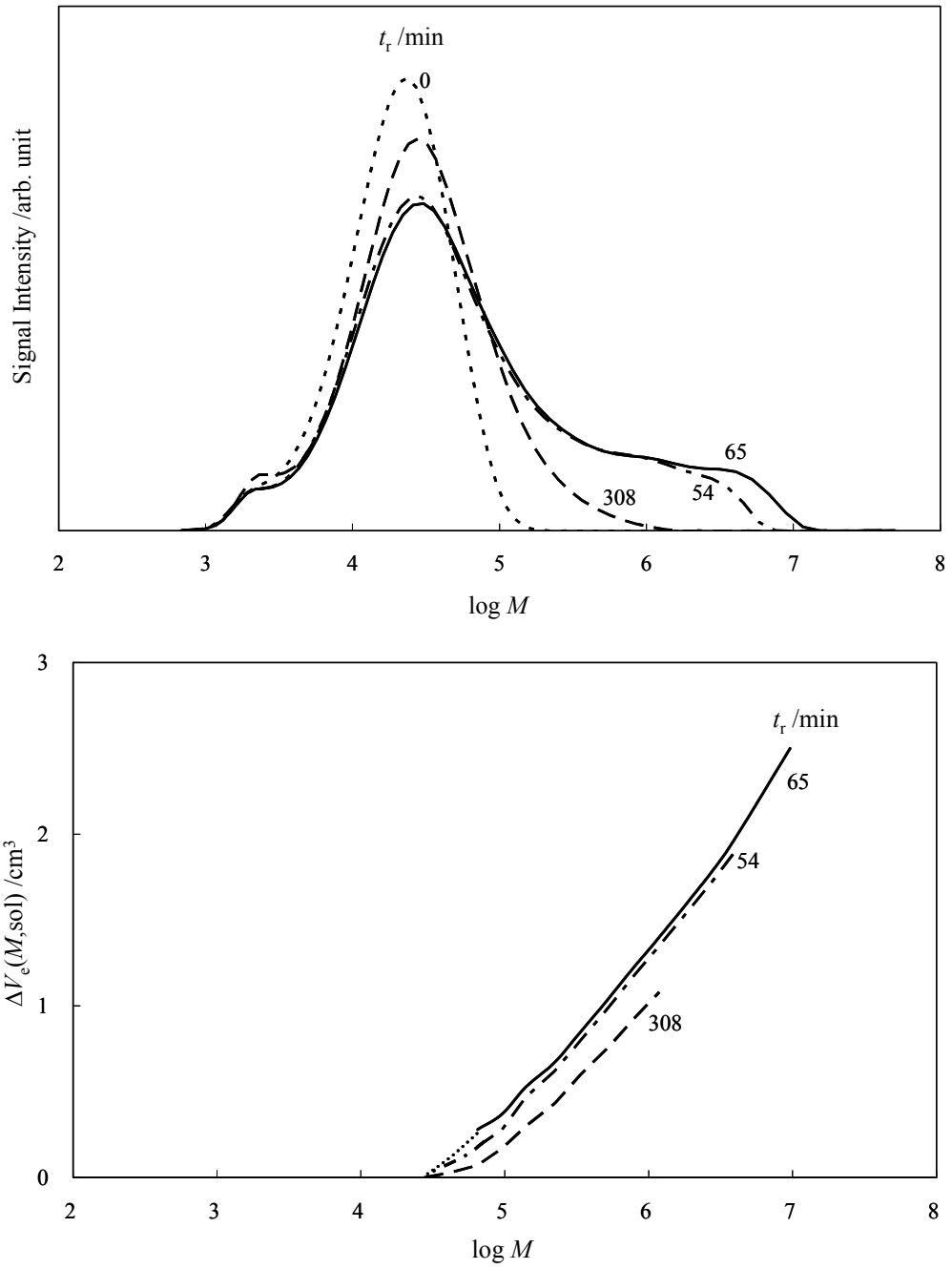

Figure 3-3 Molecular weight distribution (top panel) and elution volume difference $\Delta V_e(M,\mathrm{sol})$ (bottom panel) of toluene-soluble sol component collected at the reaction times t_r as indicated. For comparison, the molecular weight distribution of the prepolymer A is also shown (t_r = 0 in the top panel). The molecular weight M utilized in the abscissa axis was determined from the relative index and light scattering signals and thus the absolute molecular weight.

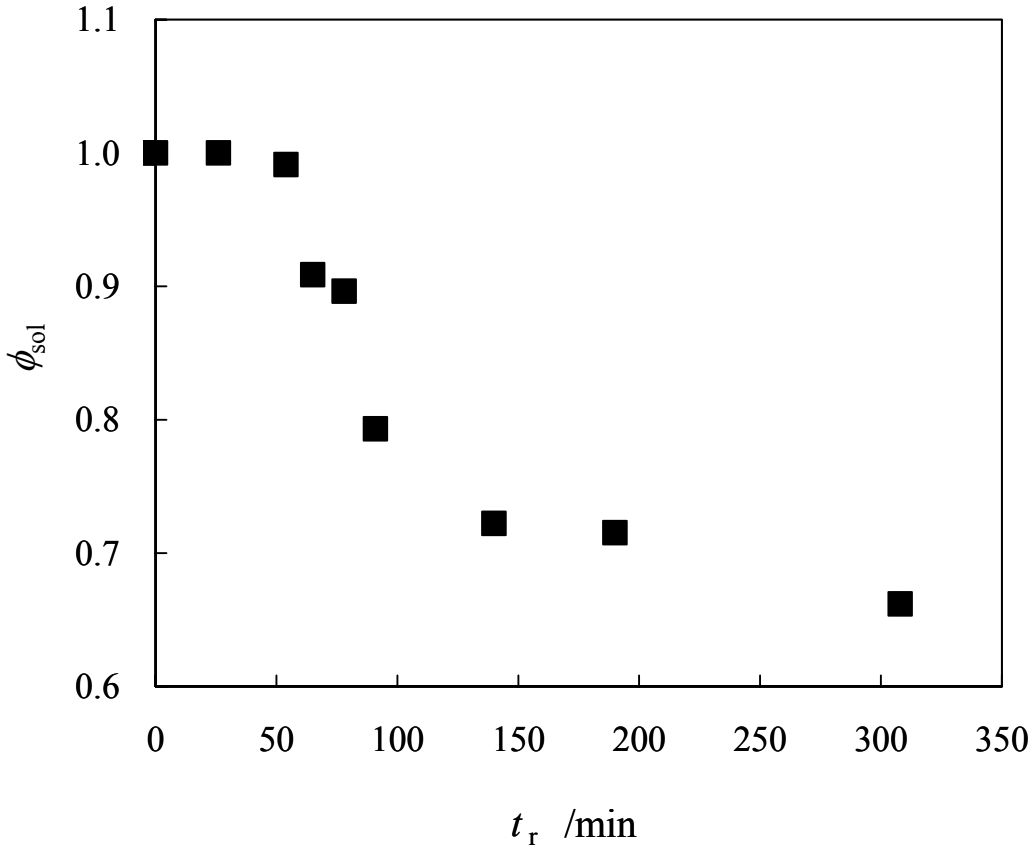

Figure 3-4 Changes of the weight fraction ϕ_{sol} of the sol component in the collected reaction mixture with the reaction time, t_r.

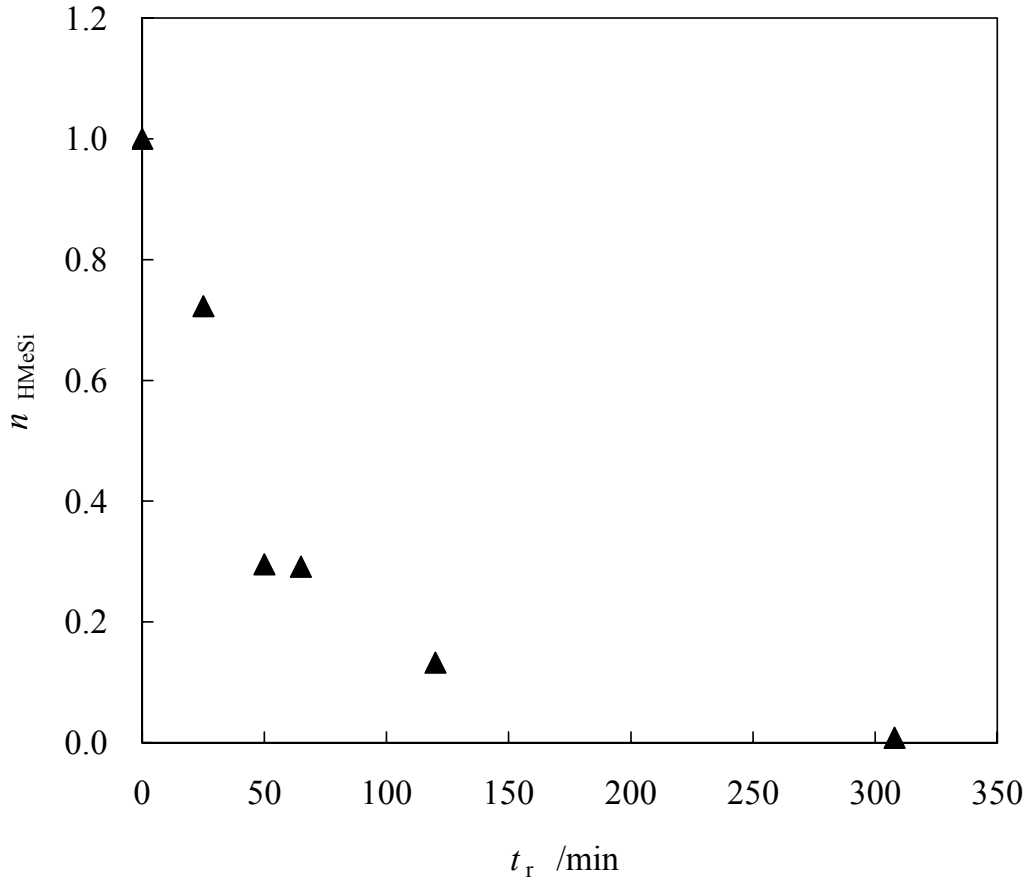

Figure 3-5 Changes of the number fraction n_{HMeSi} of unreacted HMeSi group in of the sol component in the collected reaction mixture with the reaction time, t_r.

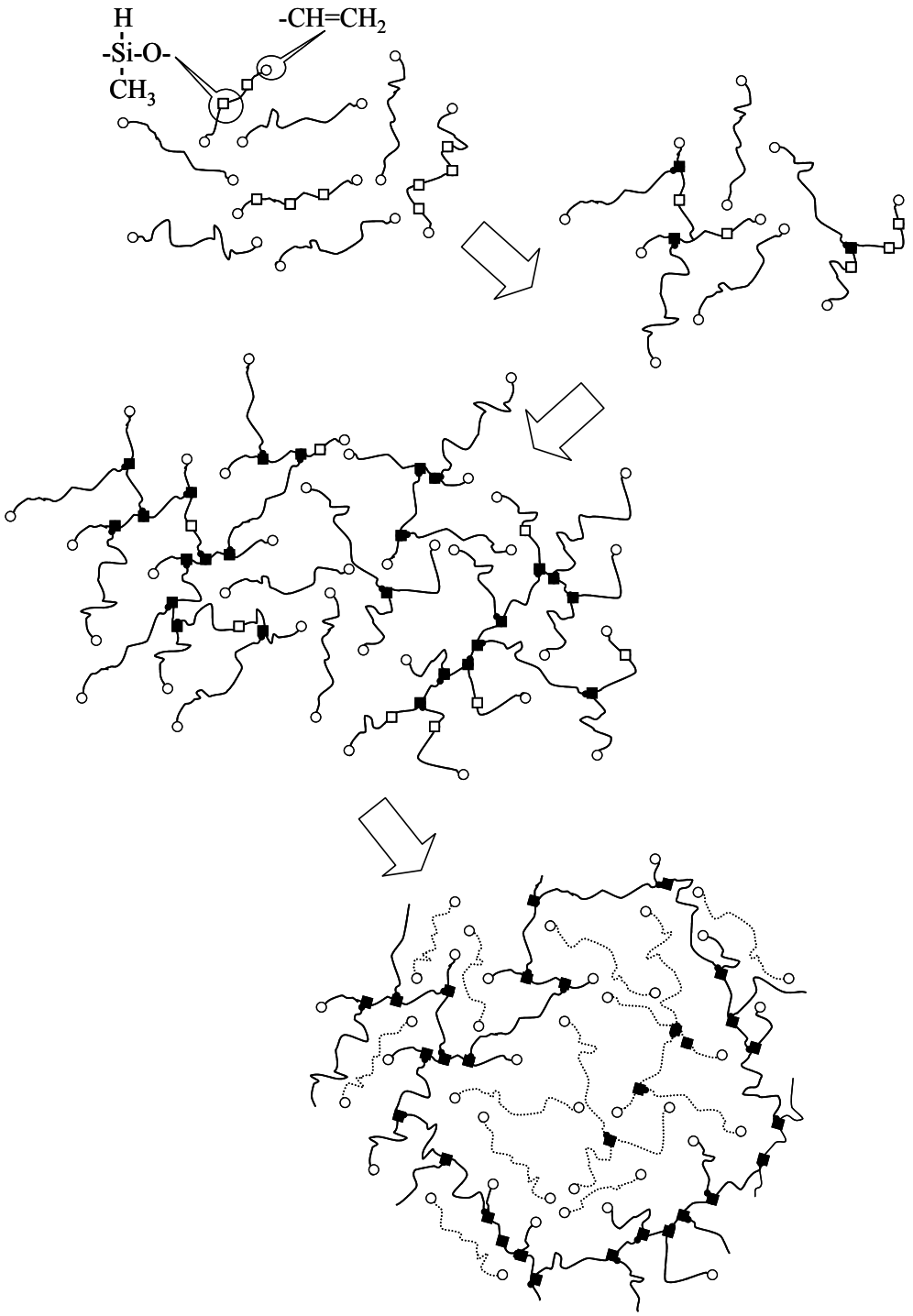

Figure 3-6 Schematic illustration of gelation process for Gel-1. Unfilled squares and circles denote unreacted vinyl and HMeSi groups, respectively, and the filled square and circles, the reacted groups. In the bottom part, the dotted curves indicate sol chains (that include the unreacted prepolymer chains), and the solid curves indicate the chains involved in the gel network.

3-4. Concluding Remarks

For a 1/1 (wt/wt) mixture of two PDMS prepolymers A and B ($M_{w,pre} = 3.5 \times 10^4$), the linear viscoelastic behavior was examined during the gelation process at 50˚C. The gelation occurred mainly through a reaction of monomethylsilyl groups (0.7 mol% in the prepolymer B backbone) and vinyl groups at the chain ends of A and B, giving a scarcely crosslinked gel containing a large sol fraction (ϕ_{sol} = 0.58 on completion of gelation) and exhibiting the equilibrium modulus G_e much smaller than the nominal modulus, $G_e^o = (1-\phi_{sol})\rho RT/M_{n,pre}$. It turned out that the critical gelation behavior characterized with the power-law relationship, $G''(\omega) = G'(\omega)tan\delta \propto \omega^{n_g}$ $(0 < n_g < 1)$, was *not* observed during the gelation process, suggesting that the gelation did not occur through formation of a huge, self-similarly hyper-branched critical gel chains. For further examination of this gelation process, the prepolymer mixture was collected at several reaction times t_r and the molecular characteristics of the sol component therein and a number fraction of the unreacted monomethylsilyl group n_{HMeSi} in this component were examined. It turned out that the high-M tail of the sol became enriched with densely branched pre-gel chains with the molecular weight almost reaching $M = 1 \times 10^7$ ($\cong 300M_{w,pre}$) and n_{HMeSi} rapidly decreased to $\cong 0.3$ with increasing t_r up to 65 min and then the branch content/molecular weight of the sol decreased and n_{HMeSi} gradually approached 0 on a further increase of t_r. These results suggested the gelation mechanism that the densely branched pre-gel chains (involving up to 300 prepolymer chains) were first formed on consumption of the majority of the monomethylsilyl groups at $t_r \leq 65$ min and then these pre-gel chains were scarcely linked trough a small amount of remaining monomethylsilyl groups to form the 3-dimensional gel at $t_r > 65$ min. This mechanism is consistent with the observation, the lack of critical gelation behavior as well as the small equilibrium modulus ($<< (1-\phi_{sol})\rho RT/M_{n,pre}$) on completion of gelation.

References

1) Flory PJ, *Principles of Polymer Chemistry*, Cornell University Press, Ithaca, New York, 1953.

2) Stockmayer WH, *J Chem Phys*, **11**, 45 (1943).

3) Stauffer D, Coniglio A, Adam A, *Adv Polym Sci* , **44**, 103 (1982).

4) de Gennes PG, *Scaling Concepts in Polymer Physics*, Cornell University Press, Ithaca, New York, 1979.

5) Martin JE, Adolf D, *Annu Rev Phys Chem*, **42**, 311 (1991).

6) Muthukumar M, Winter HH, *Macromolecules*, **19**, 1284 (1986).

7) Hess W, Vilgis TA, Winter HH, *Macromolecules*, **21**, 2536 (1988).

8) Muthukumar M, *Macromolecules*, **22**, 4656 (1989).

9) Adolf D, Martin JE, Wilcoxon JP, *Macromolecules*, **23**, 527 (1990).

10) Adolf D, Martin JE, *Macromolecules*, **23**, 3700 (1990).

11) Matjeka L, *Polym Bull*, **26**, 109 (1991).

12) Ishida H, Smith ME, *Rheol Acta*, **30**, 184 (1991).

13) Lairez D, Adam M, Emery JR, Durand D, *Macromolecules*, **25**, 286 (1992).

14) Miaoling LH, Williams JG, *Macromolecules*, **27**, 7423 (1994).

15) Eloundou JP, Feve M, Gerard JF, Harran D, Pascault JP, *Macromolecules*, **29**, 6907 (1996).

16) Eloundou JP, Gerard JF, Harran D, Pascault JP, *Macromolecules*, **29**, 6917 (1996).

17) Kuroki M, Takahashi H, Ishimuro Y, *Nihon Reoroji Gakkaishi (J Soc Rheol Japan)*, **27**, 235 (1999).

18) Smith ME, Ishida H, *J Appl Polym Sci*, **73**, 593 (1999).

19) Valentova H, Nedbal J, Ilavsky M, Bouchal K, *J Macromol Sci Phys*, **B38**, 51 (1999).

20) Valentova H, Nedbal J, Ilavsky M, Sedlacova Z, *Euro Polym J*, **37**, 1511 (2001).

21) Dimier F, Vergnes B, Vincent M, Sbirrazzuorin N, *Polym Eng Sci*, **44**, 518 (2004).

22) Calvet D, Giasson S, Wong JY, *Macromolecules*, **37**, 7762 (2004).

23) Chambon F, Winter HH, *Polym Bull*, **13**,449 (1985).

24) Winter HH, Chambon F, *J Rheol*, **30**, 367 (1986).

25) Chambon F, Winter HH, *J Rheol*, **31**,683 (1987).

26) Tordjeman P, Fargette C, Mutin PH, *J Rheol*, **45**, 995 (2001).

27) Tixer T, Tordjeman P, Cohen-Solal G, Mutin PH, *J Rheol*, **39** (2004).

28) Braun JL, Mark JE, Eichinger BE, *Macromolecules*, **35**, 5273 (2002).

29) Winter HH, Mours M, *Adv Polym Sci*, **134**, 165 (1997).

30) Graessley WW, *Adv. Polym. Sci.*, **47**, 68 (1982).

31) Mori S, Barth G, *Size Exclusion Chromatography*, Springer, Berlin, 1999, Chapter 2.

32) Yamakawa H, *Modern Theory of Polymer Solutions*, Harper & Row, New York, 1971, Chapter VI.

CHAPTER 4

Linear Viscoelastic Behavior of Scarcely Crosslinked Poly(dimethyl siloxane) Gel

4-1. Introduction

So-called "silicone gels" and "silicone rubbers", composed of polymer networks containing siloxane backbone, have been widely utilized in the industrial fields of electronics and automobile because of their excellent electrical property (high resistance) and chemical stability at high temperatures. The use of the "silicone gels" in the field of cosmetics is also being planned, because these gels are soft and serve as an excellent barrier against water.

These "silicone gels" and "silicone rubbers" are mostly prepared through a crosslinking reaction of poly(dimethyl siloxane) (PDMS) prepolymers. The network structure in these materials can be tuned fairly easily through a control of the molecular weight and a chemical modification of the prepolymers. Thus, the PDMS gels/rubbers serve as important model network systems free from a strain-induced crystallization that often disturbs studies of natural rubbers. For example, the critical gelation behavior[1)] and the fractal structure on this gelation[2,3)] have been investigated for PDMS gels, and the swelling dynamics[4)] and the length scale between the crosslinks[5)] have been examined with dynamic/static scattering methods. Studies have been also made for an effect of molecular weight distribution of the PDMS prepolymer on the rubber elasticity after crosslinking,[6)] an effect of dangling chains on the elasticity and swelling behavior,[7)] a relationships of the nonlinear viscoelastic property and the network structure,[8,9)] and the scattering behavior under large deformation.[10)] As described in Chapter 1, Urayama *et al.* made a series of studies for well characterized PDMS rubbers/gels to demonstrate interesting features of these rubbers/gels.[11-15)]

With this background, this Chapter focuses on the linear viscoelastic behavior of a PDMS gel network prepared with a double-liquid crosslinking reaction of two types of

vinyl-terminated prepolymers in bulk. Analysis of the viscoelastic data suggested a very soft gel network having a surprisingly small mechanical loss was prepared with this reaction. (The reaction utilized neither solvents nor multi-functional crosslinkers and thus differed from those in the previous studies explained in Chapter 1.) In addition, the soft gel exhibited weak but very slow relaxation modes that may be related to the gel network dynamics. Details of these results are presented/discussed below.

4-2. Experimental

4-2-1. Material

Commercially available two vinyl-terminated PDMS prepolymers (SE1886; Dow Corning-Toray Co. Ltd) were used, as explained in section 2-2. The number- and weight-average molecular weights of the prepolymer A (neat PDMS having vinyl groups at the ends) were $M_{n,pre} = 13.2 \times 10^3$ and $M_{w,pre} = 34.7 \times 10^3$, respectively. The other prepolymer B (chemically modified prepolymer), with a small fraction (0.7 mol%) of dimethylsilyl units being replaced by monomethylsilyl units, had $M_{n,pre} = 11.5 \times 10^3$ and $M_{w,pre} = 35.1 \times 10^3$.

The two prepolymers were mixed at 1/1 wt/wt ratio and cast in a metal mold of an inner diameter of ~20 mm and height of ~2 mm. This mixture was allowed to react at 120˚C for 3 h to prepare a PDMS gel. Some details of this *double-liquid crosslinking reaction* (catalyzed with a trace amount of Pt complex included in the neat PDMS prepolymer) are shown in Scheme 2-1: The vinyl group at a prepolymer end reacts with the monomethylsilyl units in the chemically modified prepolymer[16] as well as with the end vinyl group of the other prepolymer. The former route of the reaction, possibly occurring more frequently than the latter,[16] gives a dangling prepolymer grafted onto a middle of the other prepolymer if the reaction efficiency is low, which was the case for the gel examined in this Chapter.

A large fraction of a sol component was left after the reaction. This sol component effectively behaved as a solvent for the PDMS network, as discussed later.

4-2-2. Measurements

For the PDMS gel specimen prepared as above as well as for the prepolymers, dynamic oscillatory measurements were made with a laboratory rheometer (MR-500 Soliquid-meter; Reoroji Co. Ltd) to determine the storage and loss moduli, $G'(\omega)$ and $G''(\omega)$, in the condition described in section 2-4-5. The linearity of the G' and G'' data was confirmed by varying the oscillatory strain amplitude.

For the PDMS gel specimen, a creep test was also conducted with a laboratory stress rheometer (RS600; Haake Co. Ltd) to determine the creep compliance $J(t)$ at 20˚C; cf. section 2-4-5. The $J(t)$ data were converted to $G'(\omega)$ and $G''(\omega)$ data on the basis of the linear viscoelastic relationship explained in Appendix 4A.

For convenience of construction of master curves of the G' and G'' data of the PDMS gel, changes of its density with T were determined at various temperatures (between -40˚C and 100˚C) from a measurement of the linear thermal expansion coefficient made with a thermal equipment (CN8098D1; Rigaku Denki Co. Ltd). The measurement was conducted at a heating rate of 2K min^{-1} under a constant load of 0.5 g wt.

The as-prepared PDMS gel was also subjected to a swelling experiment. After the viscoelastic tests, the gel was soaked in a good solvent, toluene, at room temperature for 48 h, with the solvent being exchanged once in every 12 h. The sol component was thoroughly extracted in the toluene phase after this soaking procedure. The mass of the remaining gel was determined after full removal of toluene through vacuum evacuation. The mass of the sol component extracted in the supernatant toluene phase was determined from a concentration-calibration of this phase made with a GPC equipment (Model510; Waters Co.

Ltd) connected with a differential refractive index detector (RI-8020; Tosoh Co. Ltd).

In addition, for the extracted sol component, the molecular weight and its distribution were determined with GPC and low-angle light scattering (LALS) measurements; cf. section 2-3-3.

4-3. Results and Discussion

4-3-1. Relaxation behavior of PDMS prepolymers

Fig. 4-1 shows the G' and G'' data at 20˚C obtained for the neat PDMS prepolymer A. For the other, chemically modified prepolymer B (having a few monomethylsilyl groups in the backbone), the data were close to those shown here because the two prepolymers had nearly the same molecular weight and molecular weight distribution (MWD). Clearly, the prepolymers exhibit the terminal flow behavior characterized with the power-law dependencies, $G' \propto \omega^2$ and $G'' \propto \omega$.

The terminal relaxation time τ_w of these prepolymers was determined from those G' and G'' data as

$$\tau_w \equiv J_e \eta_0 = \left(\frac{G'}{\omega G''} \right)_{\omega \to 0} \tag{4.1}$$

Here, J_e and η_0 are the steady state compliance and zero-shear viscosity, respectively. Figs. 4-2a and 4-2b, respectively, compare the τ_w and η_0 data of the prepolymers with those of high-M, narrow-MWD PDMS ($M_w > 10^5$ and $M_w/M_n < 1.2$), the latter being evaluated from the G' and G'' data reported in literature.[17] Since the prepolymers A and B have a broad MWD ($M_{w,pre}/M_{n,pre}$ = 2.6 and 3.1), their τ_w should be considerably longer than that of narrow-MWD PDMS having the same M_w.[18,19] Thus, in Fig.4-2a, the τ_w data of the prepolymers have been

corrected for their MWD with a method explained in Appendix 4B. The τ_w values after this correction were:

$$\tau_w = 4.2 \times 10^{-5} \text{ s} \quad \text{for neat PDMS prepolymer} \tag{4.2a}$$

$$\tau_w = 2.1 \times 10^{-5} \text{ s} \quad \text{for chemically modified PDMS prepolymer} \tag{4.2b}$$

In contrast, the η_0 data are insensitive to MWD and essentially determined by M_w.[18,19] Thus, no correction of MWD has been made for the η_0 data of prepolymers shown in Fig.4-2b.

For PDMS homopolymers, the characteristic molecular weights for the onset of the entanglement effect on η_0 and J_e are reported to be $M_\eta = 24.4 \times 10^3$ and $M_J = 61.0 \times 10^3$, respectively.[18] Thus, the high-M PDMS chains examined in Fig.4-2 (circles) are in the well entangled state ($M_w > M_J$) and exhibit typical power-law relationships[18, 19] shown with the solid lines:

$$\tau_w = 1.0 \times 10^{-21} M_w^{3.6} \text{ (in s) at } 20^\circ\text{C} \tag{4.3a}$$

$$\eta_0 = 5.0 \times 10^{-17} M_w^{3.6} \text{ (in Pa s) at } 20^\circ\text{C} \tag{4.3b}$$

The τ_w and η_0 data of the prepolymers A and B (square and diamond), the former being subjected to the MWD correction, are well described by Eqs.(4.3a) and (4.3b). This result suggests that the vinyl groups at the prepolymer ends (and a few monomethylsilyl groups in the prepolymer B backbone) do not significantly affect the relaxation behavior.

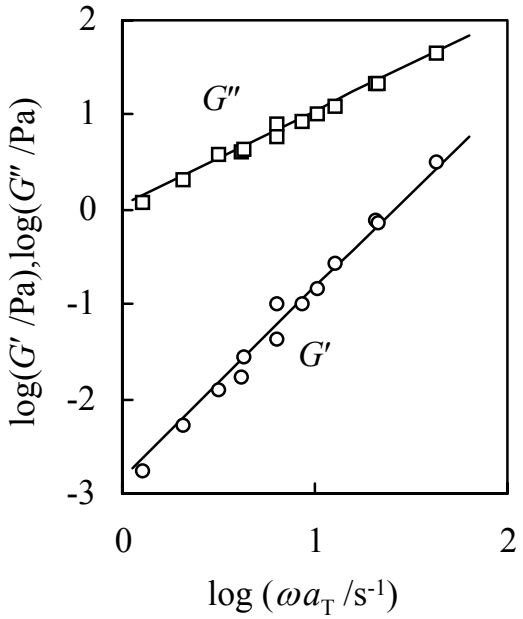

Figure 4-1 Dependence of storage modulus (G') and loss modulus (G'') on angular frequency (ω) measured for neat PDMS prepolymer A at 20℃.

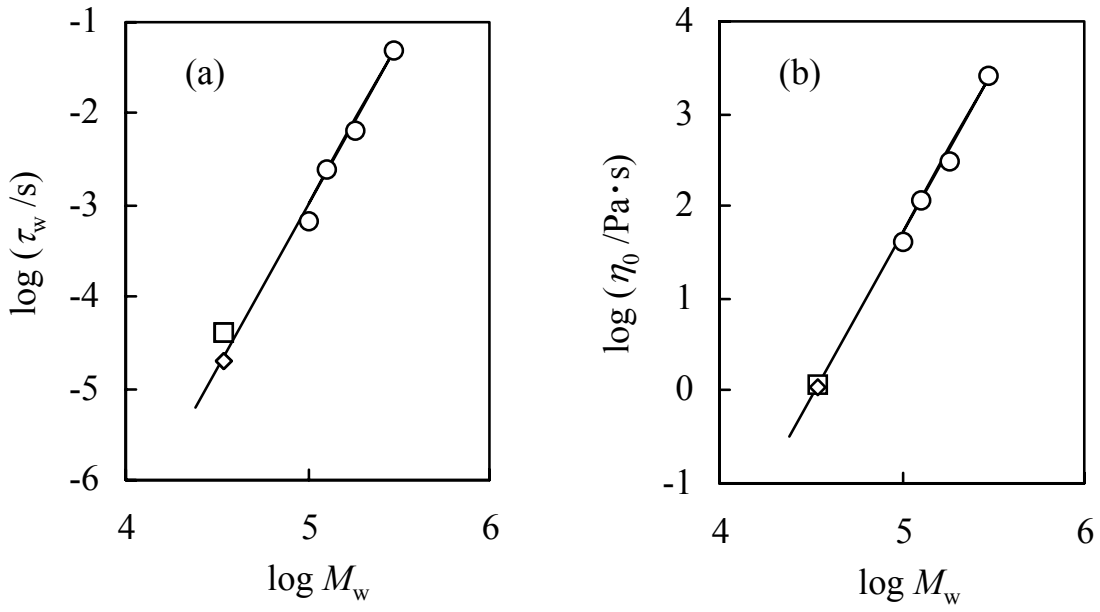

Figure 4-2 Molecular weight dependence of (a) terminal relaxation time τ_w and (b) zero-shear viscosity η_0 of well entangled linear PDMS chains at 20˚C reported in literature (circles).[17] Squares and diamonds indicate the τ_w and η_0 data of the prepolymers A and B, respectively. For these prepolymers, the τ_w data have been corrected for the molecular weight distribution, while no correction has been made for the η_0 data.

4-3-2. Relaxation behavior of PDMS gel

For the as-prepared PDMS gel (containing the sol component), Fig.4-3 shows the master curves of the G' and G'' data obtained from the dynamic oscillatory measurement (circles). The reference temperature is $T_r = 20^\circ C$. The intensity reduction factor utilized in Fig.4-3, $b_T = T_r\rho_r/T\rho$ with ρ being the density and T in the absolute temperature unit, was evaluated from the separately measured linear thermal expansion coefficient α_L: $\rho = \rho_r\{1+\alpha_L (T-T_r)\}^{-3}$. In the range of ω examined, G' decreases to the equilibrium plateau but G'' has not exhibited its terminal behavior characterized with the proportionality, $G'' \propto \omega$. Thus, a creep test was conducted to detect the behavior at lower ω.

The creep compliance data measured at $t < 10^4$ s are shown in Fig.4-4. These data were converted to a retardation spectrum (through a fit shown with the solid curve) and further to the G' and G'' data with a method described in Appendix 4A. The resulting G' and G'' data are shown in Fig.4-3 with squares. These data are in good agreement with those directly obtained from the dynamic measurements (circles) in the range of ω where the two sets of data are available.

In Fig.4-3, the PDMS gel exhibits a plateau of G' in a wide range of $\omega < 10^0$ s^{-1}. The equilibrium modulus, G_e = 2800 Pa, is about two orders of magnitude smaller than that of usual "silicone rubbers", meaning that the double-liquid crosslinking reaction gave a very soft material. In addition, the PDMS gel exhibits a surprisingly small mechanical loss, $\tan\delta = G''/G' \leq 10^{-2}$ at $\omega < 10^{-1}$ s^{-1}, which is hardly observed for usual rubbers (except for a few cases[7]). These features are discussed later in relation to gel network structure.

Now, the ω dependence of G'' that characterizes the relaxation mode distribution of the PDMS gel is examined. (This distribution is less clearly resolved for G' because the equilibrium plateau of G' masks changes of G' due to those relaxation modes.) G'' exhibits a characteristic power-law decrease with decreasing ω to 10^{-1} s^{-1},

$$G'' \propto \omega^{n_f} \quad \text{with } n_f \cong 0.6 \text{ at } \omega = 10^3 - 10^{-1} \text{ s}^{-1} \tag{4.4}$$

On a further decrease of ω, G'' becomes less dependent on ω and this behavior can be approximately described by the other form of power-law,

$$G'' \propto \omega^{n_s} \quad \text{with } n_s \cong 0.3 \text{ at } \omega = 10^{-1} - 10^{-4} \text{ s}^{-1} \tag{4.5}$$

Thus, the PDMS gel exhibits fast and slow relaxation processes that govern the behavior of G'' at respective ranges of ω.

Here, a comment needs to be made for the G'' data converted from the $J(t)$ data (squares in Fig.4-3). The G'' data in a range of $\omega > 10^{-4}$ s^{-1} (large squares) were accurately obtained and their power-law behavior (Eq.(4.5)) was detected with little uncertainties, because the $J(t)$ data were measured in the corresponding range of t (< 10^4 s). However, as explained in Appendix 4A, the real ω dependence of G'' at $\omega < 10^{-4}$ s^{-1} (small squares) may be somewhat weaker than that shown in Fig.4-3 because the $J(t)$ data at $t > 10^4$ s determining this dependence were not obtained in the creep test in this Chapter. This point is considered in the estimation of the terminal relaxation time described below.

In Fig.4-3, G'' decreases in proportion to ω and the terminal behavior of a viscoelastic solid (gel) prevails at very low ω (< 10^{-4} s^{-1}). From these G'' data, the terminal relaxation time of the slow process is estimated to be ≅ 5000 s. However, at $\omega < 10^{-4}$ s^{-1}, the real ω dependence of G'' *may* be somewhat weaker than that shown in Fig.4-3, as mentioned above. Thus, this estimate is to be regarded as the minimum and the real terminal relaxation time τ_w is specified as

$$\tau_w \geq 5000 \text{ s} \tag{4.6}$$

Finally, it is noted that G' decreases to its equilibrium (terminal) plateau at $\omega \cong 10^0$ s^{-1} while the terminal relaxation behavior of G'', if any, is observed at much lower ω ($< 10^{-4}$ s). This superficial inconsistency of the ω ranges for respective terminal behavior is related to an intensity of the slow relaxation process: This process should have the intensity negligibly smaller than the equilibrium plateau of G' ($G_e = 2800$ Pa), thereby allowing G' to practically approach its equilibrium plateau at $\omega \cong 10^0$ s^{-1} where the terminal relaxation has not been attained. Accordingly, G'' (not contributed from this equilibrium elasticity) is orders of magnitudes smaller than G' at low ω; see Fig.4-3.

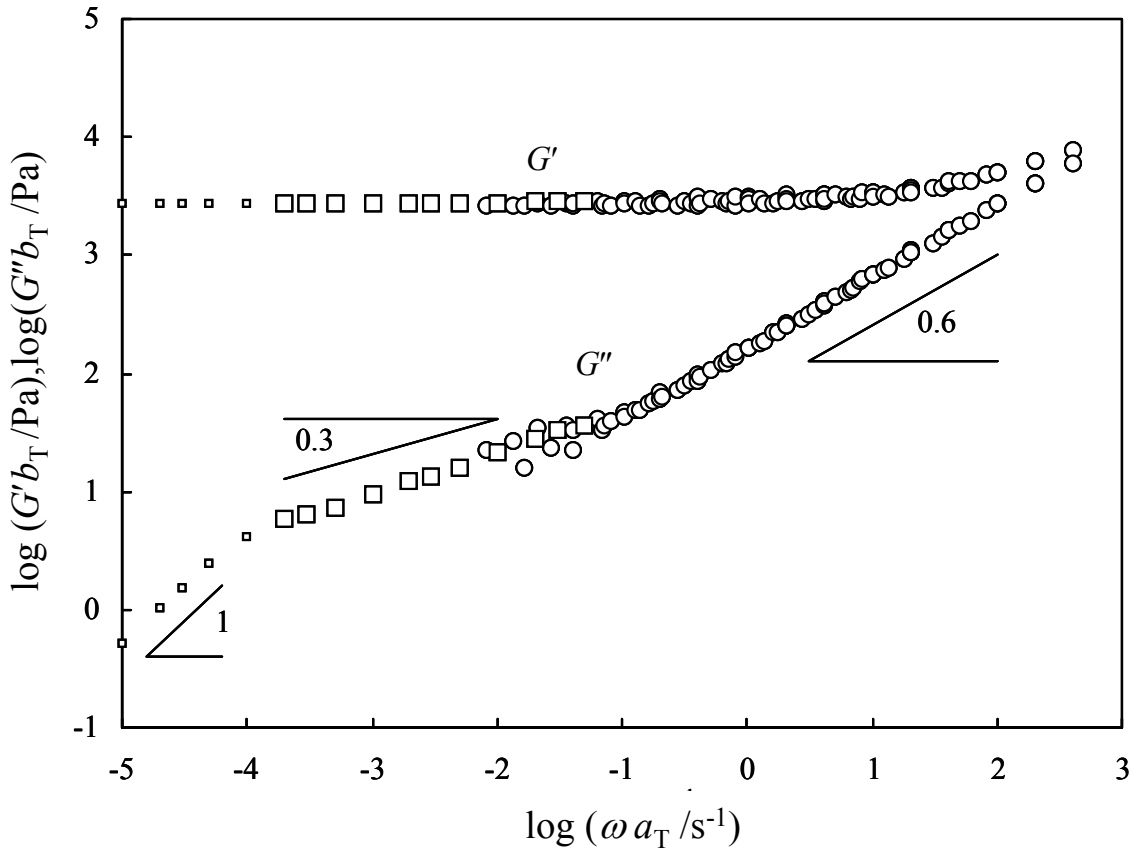

Figure 4-3 Dependence of storage modulus (G') and loss modulus (G'') on the angular frequency (ω) measured for the as-prepared PDMS gel at 20℃. Circles indicate the data directly obtained from dynamic oscillatory tests, and squares show the data converted from the creep compliance data.

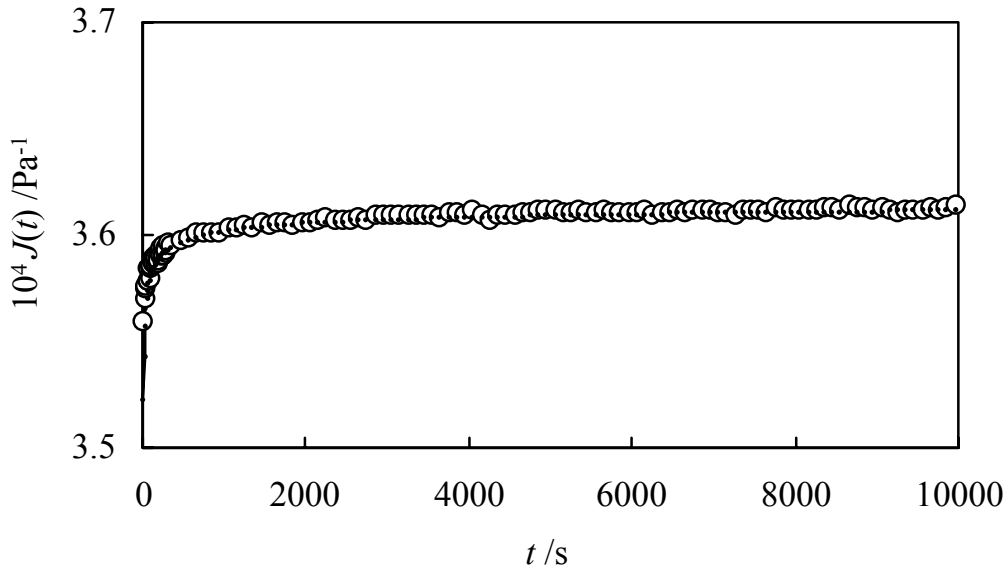

Figure 4-4 Creep compliance of the as-prepared PDMS gel at 20˚C. Solid curve indicates the fit with a set of four retardation times and intensities. Details of this fit are explained in Appendix 4A.

4-3-3. Characterization of gel network structure

For characterization of Gel-1's network, the swelling experiment in toluene with the method explained earlier was conducted. The sol component was fully extracted from the gel, and the sol fraction in the as-prepared gel (before the extraction) was determined to be

$$\phi_{\mathrm{sol}} = 0.58 \tag{4.7}$$

Fig.4-5 shows the GPC profile obtained for the sol component (solid curve) and the neat PDMS prepolymer A. The average molecular weight of the sol component was

$$M_{\mathrm{n,sol}} = 11.9\times10^{3} \quad \text{and} \quad M_{\mathrm{w,sol}} = 50.3\times10^{3} \tag{4.8}$$

This $M_{\mathrm{w,sol}}$ value is larger than $M_{\mathrm{w,pre}}$ of the prepolymer only by a factor ≅ 2, indicating that a large amount of the prepolymer was left unreacted in the as-prepared gel and the reaction efficiency was considerably low. The sol also has a high-M tail almost reaching to $M = 10^6$ but such high-M component is very minor in the sol; cf. Fig.4-5.

For the Gel-1 after the full extraction of the sol, the volumes V and V_0 were determined as a mass/density ratio in the swollen equilibrium state and the fully dried state, respectively. From the equilibrium swelling ratio defined by $Q_{\mathrm{eq}} = V/V_0$ (= 21.0), the (average) molecular weight between the crosslinks M_{c} can be estimated on the basis of the Flory-Rehner theory.[20,21] Since Gel-1 was crosslinked in the presence of a sol (unreacted diluent), the dry gel network after the full extraction of the sol collapsed compared to its natural state by a factor of $f_{\mathrm{gel}} = 1-\phi_{\mathrm{sol}} = 0.42$ (gel fraction in the as-prepared gel). Correspondingly, for this dry gel, a change in the elastic free energy on swelling to a magnitude Q can be expressed as

$\Delta F_{el} = (RTn_e/2)[3(Qf_{gel})^{2/3} - 3 - \ln(Qf_{gel})]$ with R and n_e being the gas constant and the number density of active gel strands (in mole unit), respectively.[20,21] With this expression, the Flory-Rehner theory gave (cf. Eqs.(2.25) and (2.26))

$$M_c = \frac{\upsilon_s}{\upsilon_{gel}} Q_{eq}^{5/3} \phi_{gel}^{2/3} \left(\frac{1}{2} - \chi_{PDMS/Tol} \right)^{-1} \cong 260 \times 10^3 \qquad (4.9)$$

Here, υ_s and υ_{gel} represent the molar volume of toluene (solvent) and the specific volume of the PDMS gel, respectively, and $\chi_{PDMS/Tol}$ is the interaction parameter between PDMS and toluene. The $\chi_{PDMS/Tol}$ value (= 0.463) was evaluated by extrapolating the concentration dependent $\chi_{PDMS/Tol}$ data in literature[25] to the PDMS concentration in swollen Gel-1.

The conventional expression of plateau modulus G_e[19,20] (cf. Eq.(2.23)) was also utilized to estimate M_c as

$$M_c = \frac{\rho \phi_{gel} RT}{G_e} \cong 340 \times 10^3 \times (G_e = 2800 \text{ Pa}) \qquad (4.10)$$

(The factor $\rho\phi_{gel}$ represents the concentration of the network strands in the as-prepared gel; the sol chains behave as a diluent for these strands at $\omega \to 0$.) This M_c value is satisfactorily close to that obtained from the swelling experiment (Eq.(4.9)).

The above estimate of M_c include some uncertainty because it does not account for the effects of the crosslinking point fluctuation,[20,22] trapped entanglements,[23,24] and dangling chains. The M_c values given in Eqs.(4.9) and (4.10) are an order of magnitude larger than the molecular weight of the PDMS prepolymers ($M_{n,pre} \cong 11 \times 10^3$). However as considered in section 3-3-2, the strands between crosslinks would be composed of the densely branched chains. Since the *nominal* M_c value obtained from Eqs.(4.9) and (4.10) is contributed from not only the mutually linked (percolated) strands but also the dangling chains, the real M_c

value for the former would be smaller than 340×10^3.

The upper route of the crosslinking reaction shown in Scheme 2-1 (grafting reaction) occurs more frequently than the lower route,[16] and the efficiency of reaction is considerably low (as noted from the large ϕ_{sol} value; Eq.(4.7)). Thus, the gel strand would be a *scarce comb-like* strand that is composed of linearly linked prepolymers and dangling chains grafted thereto. (The number of prepolymers per strand, $M_c/M_{n,pre} \cong 30$, includes those dangling chains). Because of the low efficiency of the reaction, the majority of the dangling chains would be the prepolymers that reacted only at one end. These dangling prepolymers could have an important effect on the viscoelastic properties of Gel-1, as discussed below.

The crosslinking reaction in bulk phase usually leads to formation of many trapped entanglements, and these entanglements effectively decreases M_c (thereby giving $M_c < M_{pre}$) and enhance the mechanical loss at low ω. Gel-1 was crosslinked in the bulk phase but still has $M_c >> M_{n,pre}$ and a surprisingly small mechanical loss, $\tan\delta = G''/G' \leq 10^{-2}$ at $\omega < 10^{-1}$ s^{-1}. These unexpected features can be related to the fairy short sol chains and dangling prepolymers existing in the as-prepared gel. The sol fraction during the reaction should have been larger than that after the reaction ($\phi_{sol} = 0.58$; Eq.(4.7)), and such concentrated sol chains could have significantly diluted the trapped entanglements during the reaction, as similar to the situation for the solution-crosslinked rubbers.[11] The steric repulsion between the dangling prepolymers would further suppress the formation of the trapped entanglements. In addition, the fairly short sol chains and dangling prepolymers (having $M_{w,sol} \cong 2M_\eta$ and $M_{w,pre} \cong 1.4M_\eta$) would have relaxed quickly and hardly enhanced the mechanical loss at low ω. The unexpectedly large M_c value and small tan δ value of Gel-1 can be attributed to these effects of the short sol chains and dangling prepolymers.

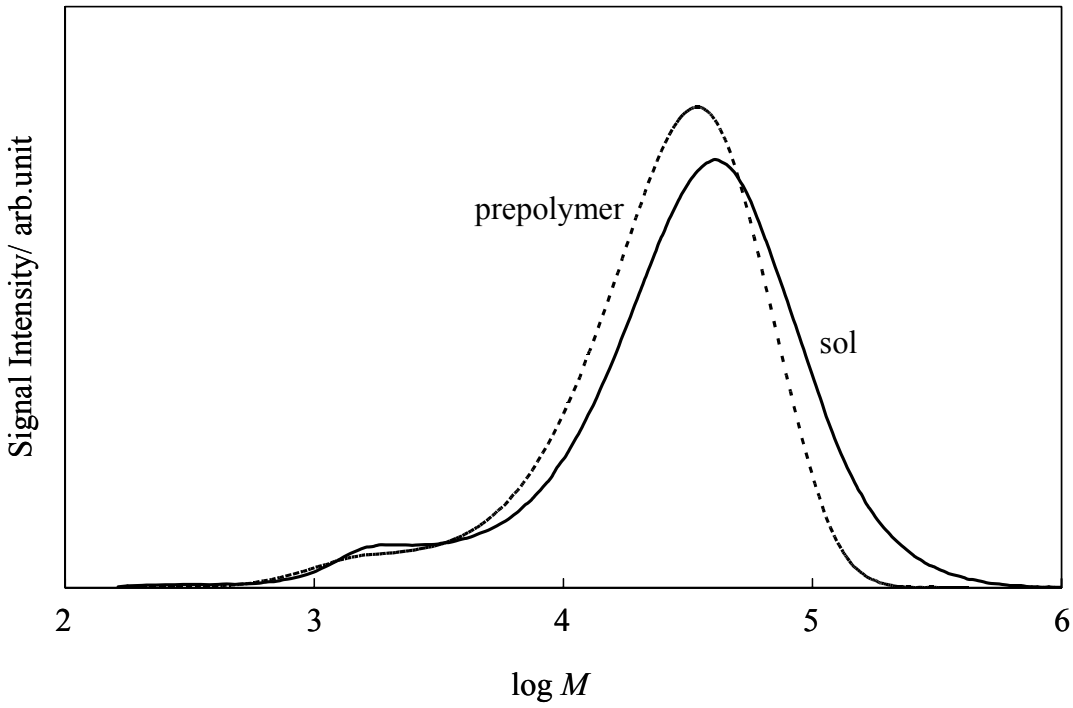

Figure 4-5 Molecular weight distributions of the PDMS prepolymer A (dotted curve) and sol fraction in the as-prepared PDMS Gel-1 (solid curve).

4-3-4. Relaxation mechanisms in PDMS gel

The as-prepared Gel-1 exhibits the fast and slow relaxation processes at $\omega > 10^{-1}$ s^{-1} and $\omega < 10^{-1}$ s^{-1}, respectively; cf. Fig.4-3 and Eqs.(4.4) and (4.5). In the followings, several molecular mechanisms are considered and the responsibility of these mechanisms for the fast and slow processes is examined.

4-3-4-1. Role of sol chains and dangling chains in the fast process

For the fast process occurring at $\omega > 10^{-1}$ s^{-1}, the mechanism to be considered first is the motion of the gel strands and sol/dangling chains *within* the entanglement segment of the molecular weight M_e (= 8.1×10^3 for PDMS[18]). This motion is free from any entanglement effect, and its characteristic time $\tau^{\circ}(M_e)$ can be estimated in the following way.

In general, the zero-shear viscosity η_0 and steady state compliance of monodisperse linear polymers scale with M as[18,19]

$$\eta_0 \propto M \text{ for } M < M_\eta, \quad \eta_0 \propto M^{3.5\pm0.2} \text{ for } M > M_\eta \tag{4.11}$$

$$J_e \propto M \text{ for } M < M_J, \quad J_e \propto M^0 \text{ for } M > M_J \tag{4.12}$$

Here, M_η and M_J are the characteristic molecular weights for the onset of the entanglement effect on η_0 and J_e: $M_\eta = 24.4 \times 10^3$ and $M_J = 61.0 \times 10^3$ for PDMS.[18] From Eqs.(4.11) and (4.12), the terminal relaxation time $\tau_w = J_e \eta_0$ scales with M as

$$\tau_w \propto M^2 \text{ for } M < M_\eta \tag{4.13a}$$

$$\tau_w \propto M^{4.5\pm0.2} \text{ for } M_\eta < M < M_J \tag{4.13b}$$

$$\tau_w \propto M^{3.5\pm0.2} \text{ for } M_J < M \tag{4.13c}$$

The empirical Eq.(4.3a), obtained for $M > M_J$, gives $\tau_w(M_J) = 1.0\times10^{-21} M_J^{3.6} \cong 1.7\times10^{-4}$ s. This $\tau_w(M_J)$ value is combined with Eq.(4.13b) to obtain $\tau_w(M_\eta) = \{M_\eta/M_J\}^{4.6}\tau_w(M_J) \cong 2.5\times10^{-6}$ s. From Eq.(4.13a) and this $\tau_w(M_\eta)$ value, $\tau^\circ(M_e)$ for the entanglement can be estimated as

$$\tau^\circ(M_e) = \left(\frac{M_e}{M_\eta}\right)^2 \tau_w(M_\eta) \cong 2.8\times10^{-7} \text{ s} \tag{4.14}$$

Literature data[26] suggest that G' of well entangled homo-PDMS chains at 20°C levels off at the entanglement plateau at $\omega \sim 10^6$ -10^7 s^{-1}, i.e., at $t \sim 10^{-7}$-10^{-6} s, lending support to this estimate.

For Gel-1, the fast relaxation process ends at $\omega \sim 10^{-1}$ s^{-1} << $1/\tau^\circ(M_e)$; cf. Fig.4-3. Thus, this process should involve motion of a portion of PDMS chains much larger than the entanglement segment, although the motion within the entanglement segment should have certainly occurred at high ω (> 10^6 s^{-1}) not covered in Fig.4-3.

The characteristic time τ_{sol} for the global motion of the PDMS sol chains can be estimated similarly. The majority of the sol chains have $M_{w,sol} = 50.3\times10^3$ (Eq.(4.8)), which is between M_η and M_J. Thus, τ_{sol} can be estimated as

$$\tau_{sol} \cong 3\times\left(\frac{M_{w,sol}}{M_J}\right)^{4.6} \tau_w(M_J) \cong 2.1\times10^{-4} \text{ s} \tag{4.15}$$

Here, the front factor of 3 accounts for the retardation of the motion of entangled linear chains in a matrix of much longer chains and/or gel network.[27] The corresponding frequency, $1/\tau_{sol} \cong 5\times10^3$ s^{-1}, is too large compared to the terminal frequency of the fast relaxation process, $\omega \cong 10^{-1}$ s^{-1}. The sol has the high-M tail up to 10^6 (cf. Fig.4-5), and $1/\tau_{sol} \cong 10^{-1}$ s^{-1} for linear sol

chains of $M = 10^6$. Scheme 2-1 suggests that the crosslinking reaction could have also produced star-branched high-M sol chains (or a fragment of network), and these star chains would have even smaller $1/\tau_{sol}$. However, such high-M chains are very minor in the sol (cf. Fig.4-5) and could have just a secondary contribution, at best, to fast process characterized with the power-law behavior, Eq.(4.4). Thus, the dominant part of this process cannot be attributed to the motion of the sol chains, although the majority of these chains should have significantly contributed to G'' at $\omega \geq 1/\tau_{sol}(\text{majority}) \cong 5 \times 10^3$ s^{-1}.

A contribution from dangling chains, which would have formed mainly through the upper route of the reaction shown in Scheme 2-1, also needs to be examined. For high-M dangling chains (with $M >> M_\eta$), the relaxation mode distribution should be close to that of highly entangled star-branched chains. Such star chains exhibit a broad terminal relaxation mode distribution, and their G'' data reported in literature [28,29] can be approximately cast in a power low form,

$$G_{star}'' \propto \omega^{n''} \text{ with } n'' = 0.15\text{-}0.2 \text{ for } \omega_t < \omega < \omega_R \tag{4.16}$$

with ω_t and ω_R being the terminal relaxation frequency and Rouse frequency of the star arm, respectively. This power-law behavior is quite different from that seen for the fast relaxation process of the PDMS gel (Eq.(4.4)). In addition, Scheme 2-1 suggests that the molecular weight distribution is not significantly different for the sol chains and dangling chains. As judged from the GPC trace of the sol (Fig.4-5), the high-M (highly entangled) dangling chains would have been a minor component in the gel. For these reasons, the fast process of Gel-1 does not seem to be related to the high-M dangling chains.

On the other hand, a considerable amount of the dangling prepolymers should have been formed in Gel-1, as explained earlier. Since the dangling prepolymers (with $M_{w,pre} \cong 1.4M_\eta$)

are just moderately entangled, their relaxation frequency would not be significantly different from that of the majority of the sol component, $\tau_{sol} \cong 2.1 \times 10^{-4}$ s; Eq.(4.15). Thus, the dangling prepolymers hardly contribute to the dominant part of the fast process seen at ω = 10^3-10^{-1} s^{-1}, although they would have contributed to G'' at higher ω, as similar to the situation for the majority of the sol chains.

4-3-4-2. Role of gel strands in the fast process

The Gel-1's strand would be a scarce comb-like strand having some grafts, and the majority of the grafts would be the dangling prepolymers, as discussed earlier. The dangling prepolymers should have fully relaxed at ω = 10^3-10^{-1} s^{-1}, as discussed above. Thus, the motion of the strand considered here is the motion of the backbone of the comb-like strand. Hereafter, this backbone is simply referred to as the strand.

Since the power-law behavior of G'' (Eq.(4.4)) is not identical but close to the behavior expected for a Rouse chain with fixed ends[27,30] ($G'' \propto \omega^{1/2}$), it is tempting to assign the fast process to the Rouse motion of the strand. However, for a gel network composed of *monodisperse* strands, the terminal behavior of G'' ($\propto \omega^{1/2}$) emerges immediately after G' reaches the equilibrium plateau on a decrease of ω, as explained later in more details. Thus, the gel network having the strand length distribution has to be considered. For the Rouse network with this distribution, G' and G'' are described by[30]

$$G'(\omega) = \sum_i \frac{C_{st} w_i RT}{M_i} \left[1 + \sum_{p \geq 1} \frac{\omega^2 \{\tau_R(M_i)\}^2 p^{-4}}{1 + \omega^2 \{\tau_R(M_i)\}^2 p^{-4}} \right] \tag{4.17}$$

$$G''(\omega) = \sum_i \frac{C_{st} w_i RT}{M_i} \left[\sum_{p \geq 1} \frac{\omega \tau_R(M_i) p^{-2}}{1 + \omega^2 \{\tau_R(M_i)\}^2 p^{-4}} \right] \tag{4.18}$$

with

$$\tau_R(M_i) = \tau^* M_i^2 \tag{4.19}$$

Here, C_{st} is the total concentration of the gel strands, w_i is the weight fraction of the i-th strand having the molecular weight M_i, and $\tau_R(M_i)$ is the longest Rouse relaxation time of the i-th strand. In Eq.(4.19), the front factor τ^* is regarded as an adjustable parameter representing a local time constant.

With an assumption that Gel-1 contains four components of strands with their $\{w_i, M_i\}$ distribution being summarized in Table 4.1, G' and G'' were calculated according to Eqs. (4.17) and (4.18). In this calculation, C_{st} was replaced by the actual concentration of the gel strand, $\rho\phi_{gel}$ (cf. Eq.(4.10)), and the $\{w_i, M_i\}$ distribution was chosen in a way that the calculated equilibrium modulus agreed with the data. As shown in Fig.4-6, the G' and G'' calculated for $\tau^* = 8.7\times10^{-14}$ s (solid curves) agree well with the data in the dominant part of the fast relaxation process. This result suggests that the fast process is attributable to the Rouse motion of the Gel-1's strands having a considerably broad length distribution, although the actual distribution in the PDMS gel would not necessarily agree with that in the calculation (M_w/M_n = 4.38 for $\{w_i, M_i\}$ shown in Table 4.1), as suggested from the two-step gelation mechanism discussed in Chapter 3.

For examination of the effect of polydispersity on the G' and G'' curves, the same τ^* value was utilized to conduct the calculation for the monodisperse strand with $M = M_c = 340\times10^3$. The results are shown in Fig.4-6 with the dotted curves. The G' calculated for the monodisperse strands is almost the same as that for the polydisperse strands and close to the data. However, for the monodisperse strands, G'' begins to decrease in proportion to ω as soon as G' reaches the equilibrium plateau and the power-law behavior seen at $\omega > 10^{-1}$ s^{-1}, $G''\propto\omega^n$ with $n \cong 0.6$, cannot be reproduced. Thus, the polydispersity of the gel strands, naturally expected from Scheme 2-1, is essential for this power-law behavior to be observed in the plateau regime for G'. (The high-M component of the strands has a very small number

fraction ($\propto w_i / M_i$) and negligibly contributes to the equilibrium plateau of G'. However, this component has a long relaxation time and thus significantly contribute to G'' at low ω where the lower-M components have relaxed. This contribution of the high-M component of the strands results in the power-law-like behavior seen for the solid curve in Fig.4-6.

Further details of the Rouse motion of the polydisperse strands can be examined for their relaxation time τ_R. The front factor τ^* utilized in the above calculation gives the Rouse time for the entanglement segment ($M_e = 8.1 \times 10^3$):

$$\tau_R(M_e) = 5.7 \times 10^{-6}\,\mathrm{s} \tag{4.20}$$

This τ_R value is significantly longer than the *intrinsic* (*entanglement-free*) relaxation time of this segment, $\tau(M_e) = 2.8 \times 10^{-7}$ s (Eq.(4.14)). Thus, the Rouse motion giving the power-law behavior in the fast relaxation process cannot be the intrinsic Rouse motion. Instead, the Rouse motion in the fast process is attributable to the *constraint release* (CR) Rouse motion of the polydisperse gel strands, as discussed below.

The strands in Gel-1 do not significantly form the trapped entanglement (permanent knots) among themselves, as discussed earlier. However, the large-scale motion of a gel strand (over a distance comparable to their dimension R_{st}) should be still constrained, in a short time scale, by the surrounding sol/dangling chains and other gel strands, both having $M > M_\eta$. In this sense, the strand is entangled with the sol/dangling chains and the other strands, as schematically shown in Fig.4-7, where the branched dangling chains are not shown for simplicity.

Since the gel strand has no freedom of translational diffusion, the entanglement segment of this strand is allowed to achieve a local hopping motion and partially relax only when the entangling sol/dangling chains and/or other strands exhibit large scale motion. Accumulation

of this local CR hopping results in the global relaxation over the distance close to the dimension of the gel strand, and this global CR relaxation has the Rouse-like character as established from extensive studies for blends of linear homopolymer chains.[27] Thus, the Rouse-like power-law behavior observed in the fast relaxation process is attributable to the global CR relaxation of individual strands (having a considerable polydispersity), although the sol chains and dangling prepolymers may have secondary contributions to this process.

Within this molecular scenario, the Rouse time $\tau_R(M_e)$ obtained for the entanglement segment (Eq.(4.20)) is regarded to be the time required for the local CR-hopping of this segment. In the as-prepared PDMS gel, this time should be determined by the sol chains as well as the gel strands/dangling prepolymers. A contribution of the sol chains to this local CR time can be viscoelastically tested for the dry gel after full extraction of the sol chains. This test is made in Chapter 5.

Table 4.1 Parameters utilized in Rouse calculation shown in Figure 4-6

i	w_i	$10^{-3}M_i$	$10^2\,\tau_R(M_i)$/s
1	0.14	85.0	0.0625
2	0.35	340	1
3	0.35	1360	16
4	0.16	5440	256

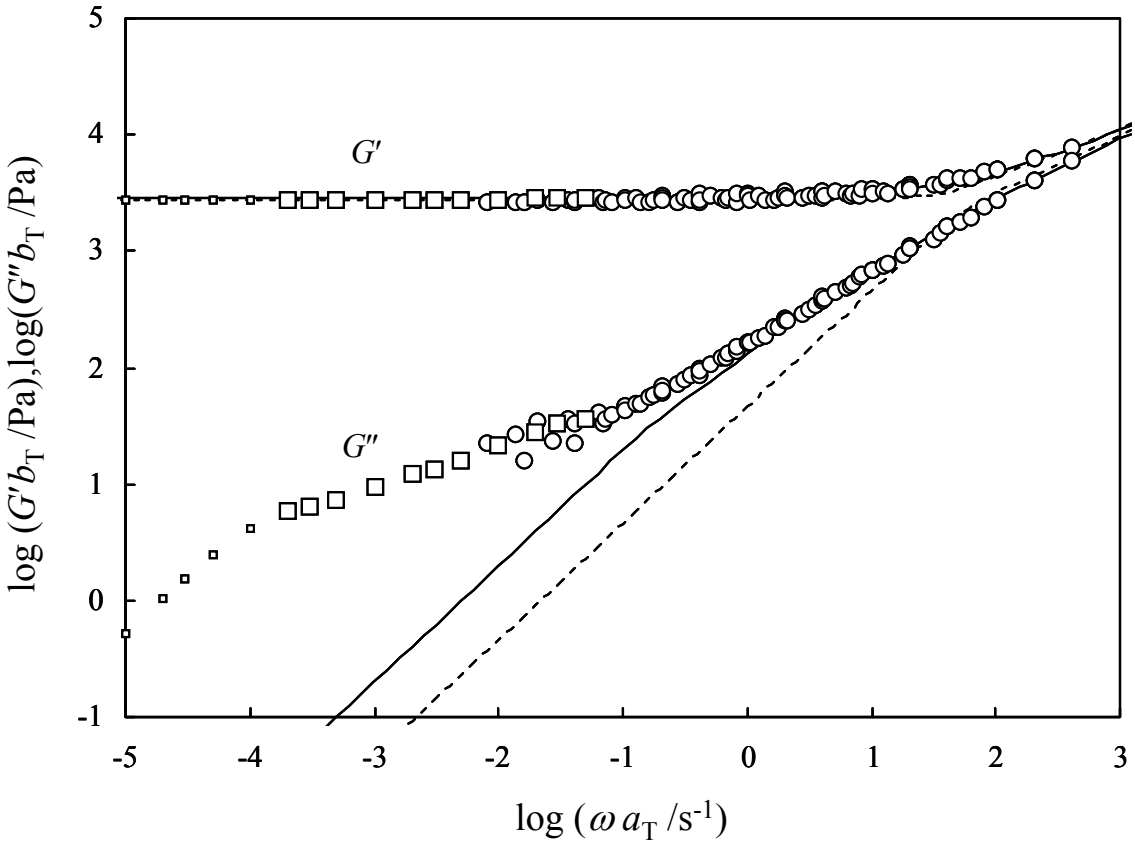

Figure 4-6 Comparison of the Rouse calculation for polydisperse gel strands (solid curves) and the G' and G'' data (symbols). The dotted curves indicate the calculation for monodisperse strands.

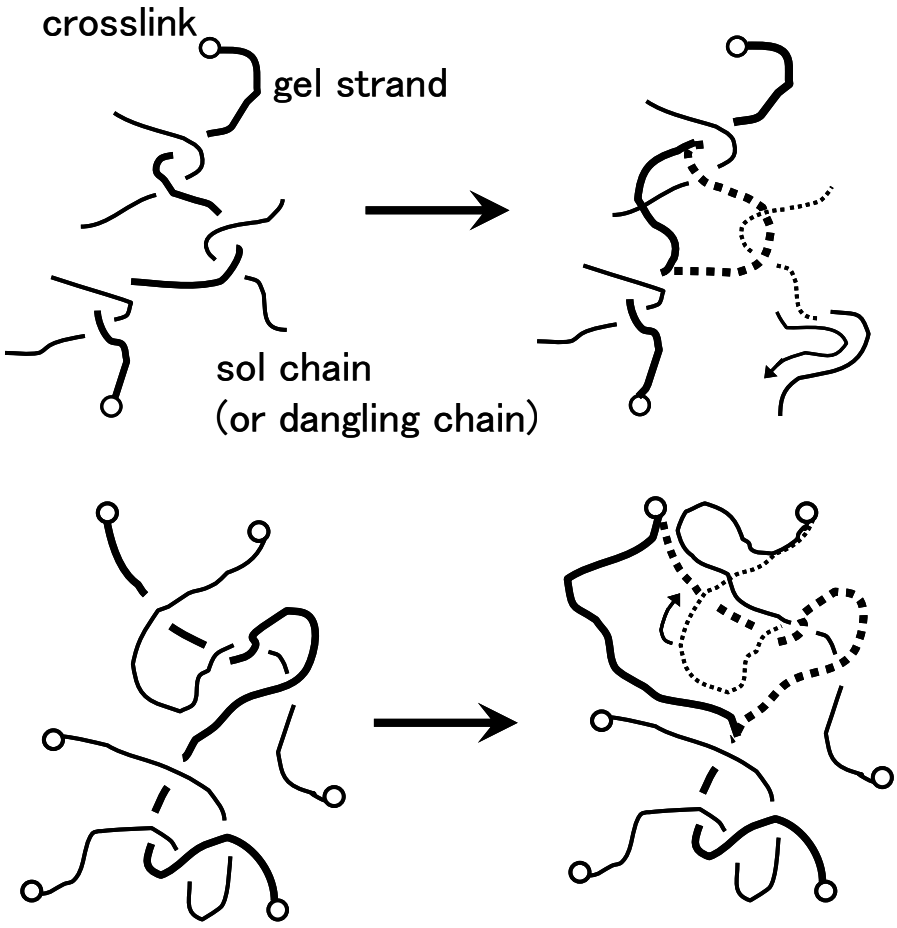

Figure 4-7 Schematic illustration of constraint release (CR) process for a gel strand. The branched dangling chains grafted on the strand are not shown for simplicity. In the top panel, motion of the sol chain or dangling chain (thin curve) activates the local CR hopping of a focused gel strand (backbone of the scarce comb-like strand; thick curve). In the bottom panel, the local CR hopping of the focused strand (thick curve) is activated by motion of a surrounding gel strand (thin curve) that is entangled, without forming a permanent knot, with the focused strand.

4-3-4-3. slow process

The slow relaxation process of Gel-1 is characterized with the power-law behavior (Eq.(4.5)) and the terminal relaxation frequency $\omega_r = 1/\tau_w \leq 2\times10^{-4}\,s^{-1}$ (Eq.(4.6)). If linear sol chains are to have this ω_r, their molecular weight should be of the order of 10^7 or mores, as judged from Eq.(4.3). Because no such high-*M* chains are seen in the GPC profile (Fig.4-5), the slow relaxation cannot be attributed to the sol chains. Similarly, ω_r appears to be too small for dangling chains/star-like sol chains of reasonable molecular weights. In addition, the power-law behavior observed for the slow process (Eq.(4.5)) is somewhat different from that expected for these chains (Eq.(4.16)). Thus, the dangling chains/star-like sol chains appear to have just a secondary contribution, at best, to the slow relaxation process of Gel-1.

From this argument, the slow process should be mainly related to the gel strands themselves (backbone of the scarce comb-like strand having a few grafts). Since this process is orders of magnitude slower than the fast process assigned as the Rouse-CR relaxation of individual gel strands, the slow process may be attributed to thermal fluctuation of the crosslinking points (*CP*) that is equivalent to cooperative CR motion of many gel strands connected at *CP*: The viscoelastic mode distribution associated to this fluctuation should changes with the distribution of the strand length in the 3-dimensional network as a whole, as analogous to the normal-mode vibration of a jungle-gym-like cage. Although this 3-D length distribution has not been accurately determined, the corresponding viscoelastic mode distribution should be surely different from the Rouse mode distribution (giving $G''\propto\omega^{1/2}$) characteristic to an end-fixed linear strand.

4-4. Concluding Remarks

Linear viscoelastic behavior of a PDMS gel (Gel-1) prepared with the double-liquid

crosslinking reaction of vinyl-terminated linear PDMS prepolymers in bulk has been examined. Gel-1, having the sol fraction $\phi_{sol} = 0.58$, behaved as a very soft viscoelastic solid. Analysis of the equilibrium modulus and swelling ratio suggested that the gel strand had $M_c \cong 340 \times 10^3$. Thus, the double-liquid crosslinking reaction gave a very scarce gel structure that hardly contained trapped entanglements, possibly because the sol chains/dangling prepolymers effectively diluted the trapped entanglements during the reaction.

Gel-1 exhibited fast and slow relaxation processes. The fast process was associated with the power-law behavior, $G'' \propto \omega^{n_f}$ with $n_f \cong 0.6$. This process is attributable to the Rouse-like constraint release (CR) motion of polydisperse gel strands being activated by the motion of the surrounding sol chains/dangling chains/ gel strands. (The polydispersity is essential for the gel to exhibit this power-law behavior of G'' in the plateau regime of G'.) The slow process was associated with the other type of power-law behavior, $G'' \propto \omega^{n_s}$ with $n_s \cong 0.3$. This process may be related to thermal fluctuation of the crosslinking points that is equivalent to cooperative CR motion of many gel strands connected at these points.

Appendix 4A. Evaluation of G' and G'' from $J(t)$ data

For a viscoelastic solid, the creep compliance $J(t)$ is expressed in terms of the equilibrium compliance J_e (= $1/G_e$) and the retardation spectrum $\{J_p, \lambda_p\}$ as

$$J(t) = J_e - \sum_{p=1}^{N} J_p \exp(-\frac{t}{\lambda_p}) \tag{4.A1}$$

(Here, a discrete spectrum composed of N retardation modes is assumed.) Thus, the retardation times λ_p and retardation intensities J_p (p = 1-N) can be evaluated by fitting the $J(t)$ data with Eq.(4.A1).

In the actual fitting procedure for the $J(t)$ data of Gel-1 (Fig.4-4), J_e (=$[J(t)]_{t\to\infty}$) was first determined: Since the $J(t)$ data were constant within experimental scatter at t > 8000 s (cf. Fig.4-4), the $J(t)$ value at those t was utilized as the best estimate of J_e (= 3.61×10^{-4} Pa^{-1}). Then, a difference, $J_e - J(t)$, was fitted with a sum of exponential decay terms, $J_p\exp(-t/\lambda_p)$ with p = 1-N. (This fitting was made from long t to short t with Tobolsky's Procedure X method.[19]) The fit for N = 4 excellently reproduced the $J(t)$ data, as shown in Fig.4-4 with the solid curve. The longest retardation time in this fitting was $\lambda_1 = 5.4\times10^3$ s. Equally good fit was achieved for N = 6 and 8, suggesting that the fitting for N = 4 was made with satisfactory accuracy.

From the J_e value and the retardation spectrum $\{J_p, \lambda_p\}$ for N = 4, the real and imaginary components of the complex compliance, $J'(\omega)$ and $J''(\omega)$, are straightforwardly obtained as

$$J'(\omega) = J_g + \sum_{p=1}^{4} J_p \frac{1}{1+(\omega\lambda_p)^2} \quad \text{with } J_g = J_e - \sum_{p=1}^{4} J_p \tag{4.A2}$$

$$J''(\omega) = \sum_{p=1}^{4} J_p \frac{\omega\lambda_p}{1+(\omega\lambda_p)^2} \tag{4.A3}$$

These components are simply converted to $G'(\omega)$ and $G''(\omega)$ as

$$G'(\omega) = \frac{J'(\omega)}{J'(\omega)^2 + J''(\omega)^2}, G''(\omega) = \frac{J''(\omega)}{J'(\omega)^2 + J''(\omega)^2} \tag{4.A4}$$

These $G'(\omega)$ and $G''(\omega)$ data are shown in Fig.4-3 with the squares.

Here a comment needs to be made for changes of $J(t)$ that *might* occur in a range of t > 10^4 s not covered in the creep test in this Chapter. Although the above fitting (with λ_1 = 5400 s) satisfactorily described the data at $t \le 10^4$ s and thus the $G'(\omega)$ and $G''(\omega)$ are accurately obtained in the corresponding range of $\omega > 10^{-4}$ s, the ω dependence of $G''(\omega)$ at $\omega < 10^{-4}$ s^{-1}

might be weaker than that shown in Fig.4-3 (small squares) *if* the PDMS gel had undetectably slow retardation modes (with $\lambda_1 >> 5400$ s) and its $J(t)$ increases with $t > 10^4$ s. For this case, the terminal relaxation time is longer than the time, ≅ 5000 s, obtained from the data in Fig.4-3. In other words, 5000 s is to be interpreted as the minimum for the actual terminal relaxation time. (From the $G'(\omega)$ and $G''(\omega)$ data reliably obtained at $\omega > 10^{-4}$ s^{-1}, it can be unequivocally concluded that the terminal relaxation time is not shorter than 5000 s.)

Appendix 4B. Correction of molecular weight distribution for the relaxation time

For entangled linear polymers with a unimodal molecular weight distribution, the zero-shear viscosity η_0 is essentially determined by the weight-average molecular weight M_w and hardly depends on the molecular weight distribution (MWD) while the steady state compliance J_e is quite sensitive to MWD.[19] Thus, the terminal relaxation time $\tau_w = J_e\eta_0$ is also sensitive to MWD. This should be the case also for the PDMS prepolymers A and B examined in this Chapter.

For a correction of this MWD effect, an empirical equation reported by Agarwal[31] was utilized

$$J_e \propto \frac{M_z M_{z+1}}{M_w M_n} = \left(\frac{M_{z+1}}{M_z}\right)\left(\frac{M_z}{M_w}\right)^2\left(\frac{M_w}{M_n}\right) \tag{4.B1}$$

Here, M_{z+1}, M_z, and M_n are the z+1, z, and number-averaged molecular weights, respectively. Linear polymers of unimodal MWD often have $M_{z+1}/M_z \cong M_z/M_w \cong M_w/M_n$. For such polymers, Eq.(4.B1) is reduced to $J_e \propto (M_w/M_n)^4$. Thus, a factor $(M_w/M_n)^{-4}$ was multiplied to the measured τ_w of the PDMS prepolymers to make the correction for the MWD effect. These corrected τ_w data are shown in Fig.4-2a with the square and diamond symbols. (The

empirical equation by Mills,[32] $J_e \propto (M_z/M_w)^{3.7}$, gave nearly the same magnitude of correction.)

References

1) Chambon F, Winter HH, *J Rheol*, **31**, 683 (1987).

2) Tixier T, Tordjeman Ph, Cohen-Solal G, Mutin PH, *J Rheol*, **48**, 39 (2004).

3) Adolf D, Martin JE, *Macromolecules*, **24**, 6721 (1991).

4) Oikawa H, Murakami K, *Macromolecules*, **24**, 1117 (1991).

5) Horkay F, Hecht AM, Zrínyi M, Geisslar E, *Polymer Gels and Networks*, **4**, 451 (1996).

6) Schimmel KH, Heinrich G, *Colloid Polym Sci*, **269**, 1003 (1991).

7) Patel SK, Malone S, Cohen C, Gillmor JR, Colby RH, *Macromolecules*, **25**, 5241 (1992).

8) Mark JE, *Acc Chem Res*, **27**, 271 (1994).

9) Larsen AL, Hansen K, Sommer-Larsen P, Hassager O, Bach A, Ndoni S, Jφrgensen M, *Macromolecules*, **36**, 10063 (2003).

10) Soni VK, Stein RS, *Macromolecules*, **23**, 5257 (1990).

11) Urayama K, Kohjiya S, *Eur Phys J B*, **2**, 75 (1998).

12) Urayama K, Kawamura T, Hirata Y, Kohjiya S, *Polymer*, **39**, 3827 (1998).

13) Urayama K, Kawamura T, Kohjiya S, *Macromolecules*, **34**, 8252 (2001).

14) Urayama K, Kawamura T, Kohjiya S, *Macromolecules*, **34**, 8261 (2001).

15) Urayama K, Miki T, Takigawa T, Kohjiya S, *Chem Mater*, **16**, 173 (2004).

16) Macosko CW, Benjamin GS, *Pure Appl Chem*, **53**, 1505 (1981).

17) Ressia JA, Villar MA, Vallés EM, *Polymer*, **41**, 6885 (2000).

18) Graessley WW, *Adv Polym Sci*, **16**, 1 (1974).

19) Ferry JD, *Viscoelastic Properties of Polymers*, *3rd Ed*, Wiley, New York, 1980.

20) Flory PJ, *Principles of Polymer Chemistry*, Cornell Univ Press, Ithaca, New York, 1953.

21) Flory PJ, Rehner J, *J Chem Phys*, **11**, 521 (1943).

22) James HM, Guth EJ, *J Chem Phys*, **15**, 669 (1947).

23) Langley NR, *Macromolecules*, **1**, 348 (1968).

24) Dossin LM, Graesrrey WW, *Macromolecules*, **12**, 123 (1979).

25) Schuld N, Wolf BA, in *Polymer Handbook*, 4th Ed., edited by Brandrup J, Immergut EH, Grulke EA, Wiley, New York, Volume2,1999, chapterⅦ, p.253

26) Rahalkar RR, Lamb J, Harrison G, Barlow AJ, *Faraday Symp Chem Soc*, **18**, 103 (1983).

27) Watanabe H, *Prog Polym Sci*, **24**, 1253 (1999).

28) Fetters LJ, Kiss AD, Pearson DS, Quack GF, Vitus FJ, *Macromolecules*, **26**, 647 (1993).

29) Watanabe H, Matsumiya Y, Inoue T, *Macromolecules*, **35**, 2339 (2002).

30) Doi M and Edwards SF, *The Theory of Polymer Dynamics*, Clarendon, Oxford, 1986.

31) Agarwal PK, *Macromolecules*, **12**, 342 (1979).

32) Mills NJ, *Nature (London)*, **219**, 1249 (1968).

CHAPTER 5

Linear Viscoelastic Behavior of Scarcely Crosslinked Poly(dimethyl siloxane) Gels: Effects of Sol component and Network Strand Length

5-1. Introduction

So-called "silicone gels", composed of poly(dimethyl siloxane) (PDMS) networks, are widely utilized in industries because of their excellent properties.[1)] Chapter 4 examined linear viscoelastic properties of a "silicone gel", Gel-1, prepared through the double-liquid reaction of two PDMS prepolymers, with its focus being placed on the structure-property relationship of this gel. It turned out that gel had an enormously scarce network structure containing many sol chains (sol fraction $\phi_{sol} = 0.58$) and exhibited a very small mechanical loss ($\tan \delta \sim 0.01$ at angular frequency $\omega < 0.1$ s^{-1} at room temperature), despite a fact that the gel was prepared in bulk state without any low molecular weight diluent. This scarce structure was formed possibly through the two-step gelation discussed in Chapter 3, and the concentrated sol chains (having $\phi_{sol} > 0.58$ during the gelation process) appeared to behave as a dilutent to suppress formation of the densely trapped entanglements thereby providing the gel with the very small mechanical loss. In addition, the gel exhibited weak but characteristic relaxation processes at high and low ω. The high-ω relaxation was attributable to the constraint release (CR)-Rouse relaxation of individual gel strands having a broad length distribution, while the low-ω relaxation could be related to cooperative CR process involving several gel strands.

The scarce PDMS gel examined in Chapter 4 was an as-prepared gel containing concentrated sol chains ($\phi_{sol} = 0.58$). Full viscoelastic characterization of the gel requires a test of the mechanical behavior of the gel strands themselves in the absence of the sol chains.

It is also desired to test the behavior for a series of (as prepared) gels having different length of the gel strands. The results of these tests are described in this Chapter.

5-2. Experimental

5-2-1. Material

Commercially available two vinyl-terminated PDMS prepolymers (SE1886; Toray-Dow Corning Silicone Co., Ltd) were used, as explained in Chapter 2. These prepolymers are the same as those utilized in previous chapters. The prepolymer A, a neat PDMS having vinyl groups at the ends, had the number- and weight-average molecular weights of $M_{n,pre}$ = 13.2×10^3 and $M_{w,pre}$ = 34.7×10^3. The prepolymer B, a chemically modified PDMS with a small fraction (0.7 mol%) of the dimethylsilyl units being replaced by monomethylsilyl units, had $M_{n,pre}$ = 11.5×10^3 and $M_{w,pre}$ = 35.1×10^3.

The prepolymers A and B were mixed at compositions w_A/w_B = 1/2 and 2/1 (wt/wt ratio) and allowed to react at 120˚C for 3 h in metal molds (of height = 2-3 mm) to give as-prepared gel sheet samples. The vinyl groups at the ends of prepolymers A and B react with the monomethylsilyl units in the prepolymer B to give the gel with dangling prepolymer B (main reaction), and the reaction between two vinyl groups could occur though less frequently, as explained in section 2-2. The as-prepared gels with w_A/w_B = 1/2 and 2/1 are coded as Gel-2 and Gel-3, respectively, and the gel with w_A/w_B = 1/1 prepared/examined in the previous chapters is coded as Gel-1.

A part of the Gel-2 and Gel-3 sheet samples was soaked in a good solvent, toluene, at room temperature for 72 h, with the solvent being exchanged once in every 12 h, to thoroughly extract the sol chains. These sol chains were subjected to GPC analysis to determine their weight-average molecular weight, $M_{w,sol}$. The sol fraction ϕ_{sol} was determined from the total

weight of the sol chains and the weight of the gel thoroughly dried in vacuum after the extraction. For the as-prepared Gel-2 and Gel-3 samples, the characteristics thus determined and the average molecular weight between the crosslinks M_c (evaluated from the equilibrium modulus) are summarized in Table 2-2. The Gel-1 sample was similarly subjected to the sol extraction procedure, as explained in Chapter 4. The sample after the sol extraction, coded as Gel-1E, was subjected to the dynamic viscoelastic test in this chapter. Table 2.2 also includes the characteristics of the Gel-1 and Gel-1E samples.

5-2-2. Measurements

For the as-prepared Gel-2 and Gel-3 samples as well as the Gel-1E sample after the sol extraction, the storage and loss moduli $G'(\omega)$ and $G''(\omega)$ were obtained from dynamic oscillatory tests conducted with MR-500 Soliquid-meter (Reoroji Co., Ltd) in the condition shown in Table 2.2. (The test for the as-prepared Gel-1 sample was made in Chapter 4.)

The time-temperature superposition was valid for the G' and G'' data thus obtained at temperatures between –40˚C and 100˚C. The master curves of these data at a reference temperature of T_r = 20˚C were successfully constructed with the method described in Chapter 4.

For the gel samples, the creep compliance $J(t)$ was also measured with RS600 (Haake Co., Ltd) in the condition described in section 2-4-5. The $J(t)$ data at $t < 10^4$ s was converted into the $G'(\omega)$ and $G''(\omega)$ data at ω between 10^{-4} s^{-1} and 10^{-1} s^{-1} with the method described in Appendix 4A.

For determination of ϕ_{sol} and $M_{w,sol}$ of the sol chains extracted from the as-prepared Gel-2 and Gel-3 samples, GPC measurements were conducted in the condition described in section 2-3-3. The sol chains from the Gel-1 sample were characterized in Chapter 4.

5-3. Results and Discussion

5-3-1. Viscoelastic behavior and structure of the gels with and without sol component

5-3-1-1. Overview

Fig.5-1 compares the G' and G'' master curves for the as-prepared Gel-1 sample (top panel; obtained in Chapter 4) and the Gel-1E sample after the sol extraction (bottom panel). Fig.5-2 compares the loss tangent, tan δ, of these samples.

In Fig.5-1, the filled symbols indicate the data directly obtained from the dynamic oscillatory test, and the unfilled symbols represent those converted from the creep compliance $J(t)$ measured at $t < 10^4$ s. This conversion was made with no ambiguity in the range of ω between 10^{-4} s^{-1} and 10^{-1} s^{-1} (where the corresponding $J(t)$ data were available; cf. Appendix 4A). The superposition of the data were successfully made with the aid of the intensity shift factor b_T (= $T_r\rho_r/T\rho$).

As noted in the top panel of Fig.5-1, the Gel-1 sample with the sol fraction ϕ_{sol} = 0.58 exhibits the equilibrium plateau modulus, $G_e = G'(\omega < 1\ s^{-1})$ = 2800 Pa. As described in Chapter 4, the Gel-1 sample was crosslinked in the presence of the sol chains. Since these sol chains behaved as a simple diluent (not a good solvent) during the crosslinking reaction, the network strands in the Gel-1 sample would have had a conformation close to the Gaussian conformation, not the highly expanded conformation[2)] seen for gels prepared through crosslinking of fairly dilute prepolymers in a good solvent. Thus, to a good approximation, the Gel-1E sample obtained by extracting the sol chains from the Gel-1 sample is expected to have the equilibrium modulus $(1-\phi_{sol})^{-1}G_e \cong 6700$ Pa, where G_e is the equilibrium modulus of Gel-1 and the factor of $(1-\phi_{sol})^{-1}$ simply represents an increase of the number density of the gel strands on the sol extraction. The equilibrium modulus measured for the Gel-1E sample, G_e = 7200 Pa (bottom panel of Fig.5-1), agrees well with this expectation, indicating that the gel network connectivity was not affected/destroyed by the sol extraction procedure. The

average molecular weight between the crosslinks M_c, evaluated on the basis of the classical theory of rubber elasticity (cf. Chapter 2),[3,4] is given by

$$M_c = \frac{\rho RT}{G_e} \cong 340 \times 10^3 \tag{5.1}$$

where ρ, R, and T represent the density of the Gel-1E sample, gas constant, and absolute temperature, respectively. Thus, the Gel-1E and Gel-1 samples have scarce gel strands each being composed of ≅ 10 prepolymers on average (cf. $M_{w,pre} \cong 35 \times 10^3$). This scarce structure was formed possibly because the sol chains behaved as the diluent during the crosslinking reaction, as fully discussed in Chapter 4.

As seen in Fig.5-1, the ω dependencies of G' and G'' are qualitatively similar for the Gel-1 and Gel-1E samples with and without the sol chains. Both samples exhibit very small mechanical loss, $\tan\delta \leq 0.01$ at $\omega < 0.1$ s^{-1} (cf. Fig.5-2), indicating that the dominant part of the relaxation has been completed at $\omega < 0.1$ s^{-1}. Such a small loss is never observed for usual gels/rubbers (except for a very special case[5]) because of the trapped entanglements[3, 4] densely formed in those rubbers/gels. In contrast, in the PDMS gel (Gel-1), the sol chains behaved as the diluent during the crosslinking reaction to suppress formation of the trapped entanglements, thereby giving the very small mechanical loss.

As noted in Fig.5-1, the Gel-1 and Gel-1E samples clearly exhibit the relaxation processes characterized by power-law relationship for G'' ($\propto \omega^n$). The power-law exponents n_f and n_s for the fast and slow relaxation processes are evaluated as

For Gel-1: $n_f \cong 0.6$ at $\omega/\text{s}^{-1} = 10^3 - 10^{-1}$, $n_s \cong 0.3$ at $\omega/\text{s}^{-1} = 10^{-1} - 10^{-4}$ (5.2)

For Gel-1E: $n_f \cong 0.5$ at $\omega/\text{s}^{-1} = 10^3 - 10^{-2}$, $n_s \cong 0.8$ at $\omega/\text{s}^{-1} = 10^{-2} - 10^{-4}$ (5.3)

The fast relaxation exponent n_f is a little smaller while the slow relaxation exponent n_s is

considerably larger for Gel-1E than for Gel-1. Correspondingly, the tan δ value is a little larger for Gel-1E than for Gel-1 at high-to-middle ω while the opposite is observed at low ω; cf. Fig.5-2. These differences are discussed below in relation to the relaxation mechanisms for the fast and slow processes.

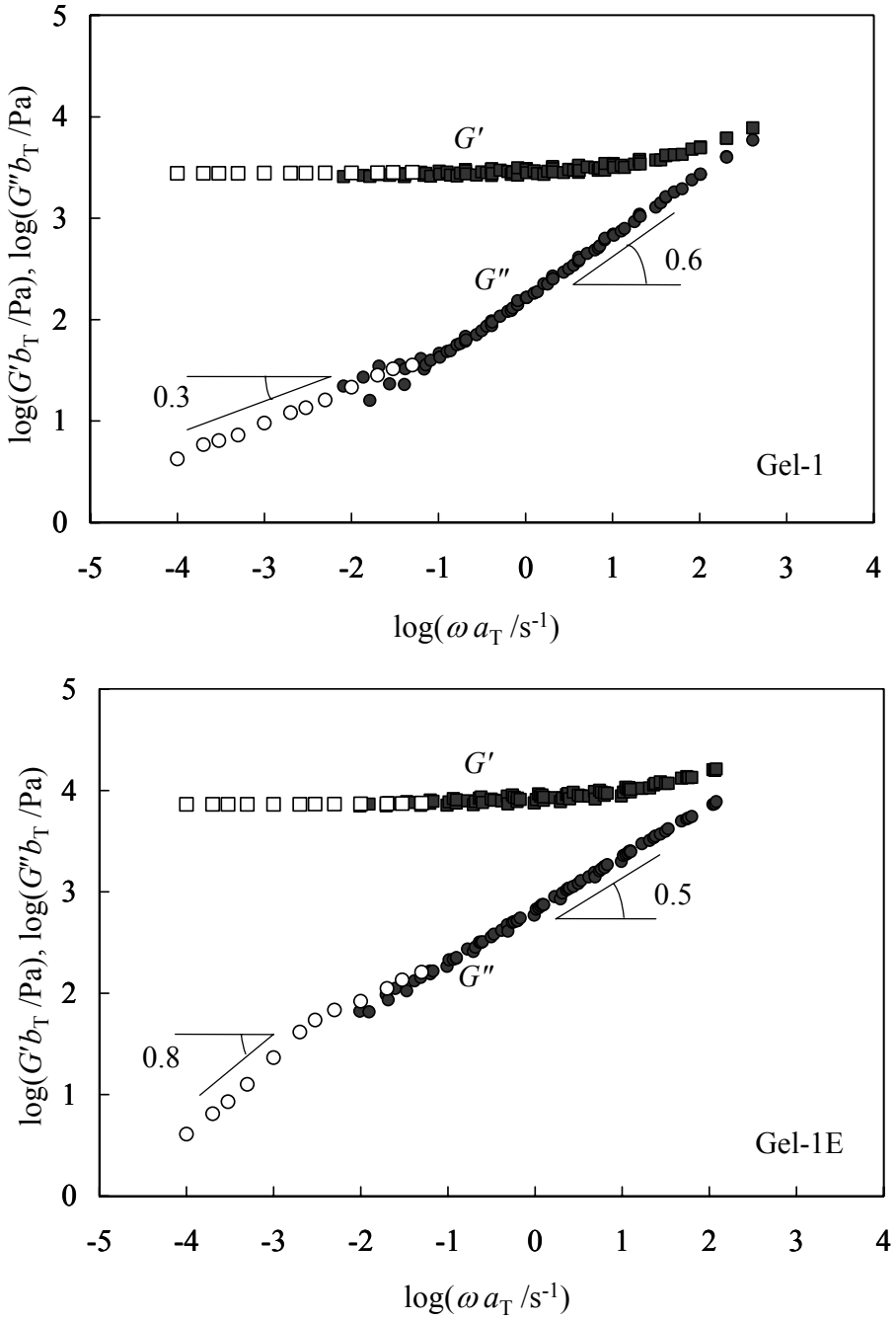

Figure 5-1 Dependence of storage modulus (G') and loss modulus (G'') on the angular frequency (ω) at 20℃ measured for the as-prepared PDMS gel (Gel-1; top panel) and the PDMS gel after sol-extraction (Gel-1E; bottom panel). Filled symbols indicate the data directly obtained from dynamic oscillatory tests, and unfilled symbols show the data converted from the creep compliance data.

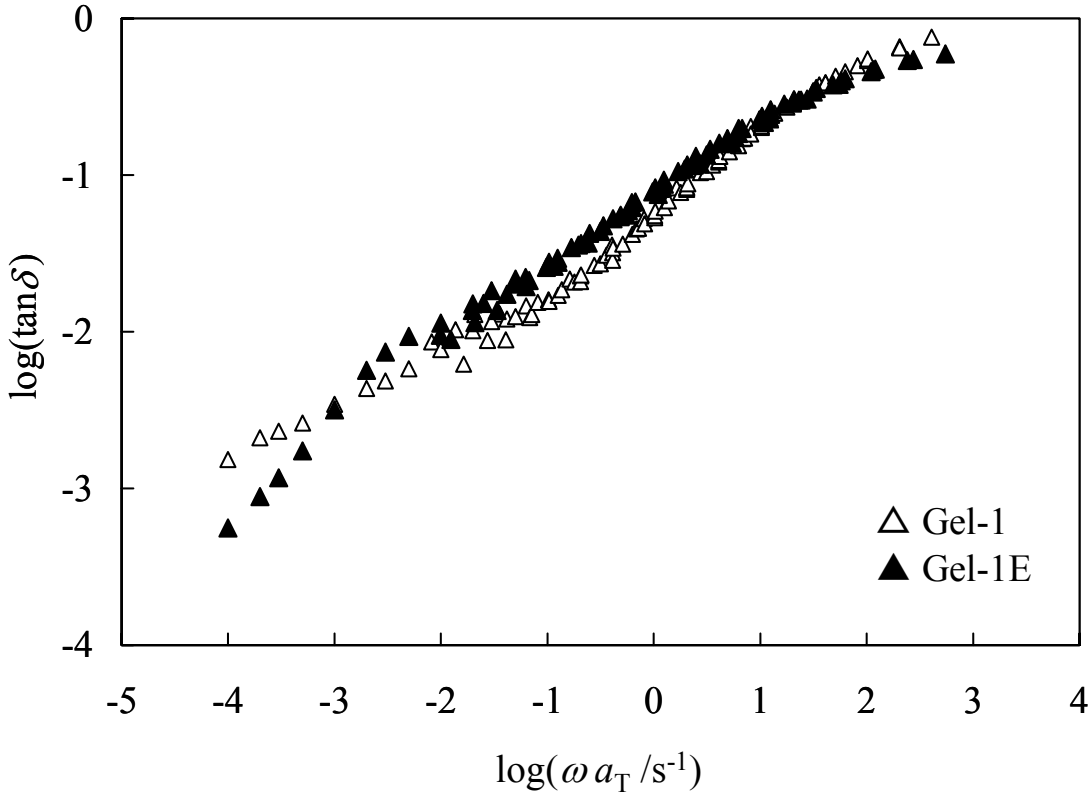

Figure 5-2 Comparison of the loss tangent of the Gel-1 and Gel-1E samples at 20˚C. Filled and unfilled symbols indicate loss tangent of Gel-1E and Gel-1, respectively

5-3-1-2. Fast relaxation mechanism

The network strand in the Gel-1 and Gel-1E samples would have dangling prepolymer chains (as suggested from the low crosslinking efficiency; cf. Chapter 4). However, these dangling prepolymers should have relaxed in the experimental window ($\omega < 10^3$ s^{-1}), as concluded in Chapter 4 on the basis of the relaxation time data for linear PDMS chains. Similarly, the sol chains in the Gel-1 sample should have mostly relaxed at those ω, as judged from their average molecular weight ($M_{w,sol} = 50.3\times10^3$; cf. Table 2.2) and the molecular weight distribution (negligibly small content of high-M chains with $M > 300\times10^3$); cf. Chapter 4. Thus, the power-law type fast relaxation of G'' seen for the Gel-1 and Gel-1E samples (Fig.5-1) can be primarily attributed to the motion of the backbone of the strand, and the terminal relaxation tail of G'' ($\propto \omega$) of the sol/dangling chains has just minor contributions to the measured G''.

In relation to this point, it is noted that the power-law behavior of the Gel-1E sample in the fast relaxation regime, $G'' \propto \omega^{0.5}$ (Eq.(5.3)), coincides with the behavior expected for the Rouse relaxation of the gel strands. Nevertheless, this power-law behavior is not attributed to the *intrinsic* (entanglement-free) Rouse relaxation of the backbone of the gel strands, as concluded in Chapter 4 and confirmed below.

The dynamic modulus for the intrinsic Rouse relaxation can be unequivocally calculated with the method explained in section 4-3-4-2. This intrinsic relaxation of Gel-1E, shown with the dotted curves in the bottom panel of Fig.5-3, is significantly faster than the observed relaxation (symbols). Instead, the observed relaxation at ω/s^{-1} = 10^3 - 10^{-2} (fast relaxation) is close to the *non-intrinsic*, constraint release (CR) Rouse relaxation of *polydisperse* stands shown with the solid curves: These curves were calculated with the method explained in section 4-3-4-2 for the component molecular weights and weight fractions $\{M_{c,i}, w_i\}$ specified in Table 5.1 and the component CR-Rouse times τ_i ($\propto M_{c,i}^2$) set as

$$\tau_i/\mathrm{s} = 1.1\times10^{-13}\times M_{\mathrm{c},i}^{2} \quad (i = 1, 2, \ldots) \quad \text{for Gel-1E} \tag{5.4}$$

(This τ_i is determined by the entanglement for the strands and is significantly longer than the intrinsic Rouse time described in section 4-3-4-2, $\tau_{\mathrm{R},i} = 4.3\times10^{-15}\times M_{\mathrm{c},i}^{2}$.)

Table 5.1 Strand length distribution utilized in the Rouse calculation for Gel-1E and Gel-1.

i	w_i	$10^{-3}M_{\mathrm{c},i}$
1	0.009	10
2	0.18	100
3	0.25	1000
4	0.26	10000
5	0.30	100000

Here, a consistency of the fast relaxation processes of the Gel-1E and Gel-1 samples is examined, the latter having the same gel network structure as Gel-1E but being swollen with the sol chains. For this purpose, the contribution of the sol chains to the measured G'' is evaluated in the following way. Linear PDMS chains of the molecular weight $M_{\mathrm{w}} = 50.3\times10^{3}$ (= $M_{\mathrm{w,sol}}$) have the zero shear viscosity of $\eta_0^{[\mathrm{b}]} = 4.6$ Pa s in the bulk state at 20˚C, as evaluated from the viscosity data compiled in section 4-3-1. Since the sol chains have relaxed at ω examined, only their terminal tail should contribute to the measured G'' of Gel-1. Thus, this contribution is estimated to be $\phi_{\mathrm{sol}}\eta_0^{[\mathrm{b}]}\omega = 2.7\omega$ with $\phi_{\mathrm{sol}} = 0.58$ (sol fraction in Gel-1) *if the sol chain motion is not affected by the gel strands*. However, in general, the chain motion is retarded by a factor of ≅ 2 in the presence of almost equal amount of slowly moving chains[6] (= gel strands in Gel-1). With this retardation effect, the sol contribution to

G'' is estimated to be $2\phi_{sol}\eta_0{}^{[b]}\omega = 5.4\omega$ (in Pa). Correspondingly, the G' and G'' expected for Gel-1 can be written as

$$G'(\omega) = (1-\phi_{sol})G_{1E}'(\omega\lambda_r), \quad G''(\omega) = (1-\phi_{sol})G_{1E}''(\omega\lambda_r) + 5.4\omega \qquad (5.5)$$

Here, G_{1E}' and G_{1E}'' indicate the CR-Rouse moduli calculated for Gel-1E (cf. solid curves in the bottom panel of Fig.5-3), and the factor λ_r represents a possible change of the CR relaxation time of the gel strands due to the sol chains in the Gel-1 sample. (The terminal tail of G' ($\propto\omega^2$) of the sol chains should hardly contribute to the measured G' of Gel-1 and is neglected in Eq.(5.5))

In the top panel of Fig.5-3, the G' and G'' thus expected for Gel-1 with $\lambda_r = 0.5$ are shown with the solid curves. These curves are close to the data for Gel-1, suggesting that fast relaxation processes of the Gel-1 and Gel-1E samples are consistently described as the CR-Rouse relaxation of polydisperse strands (plus a minor contribution of the terminal tail of the sol chains for the case of Gel-1).

Equally good fit was achieved without incorporating the contribution of the terminal tail of the sol chains but utilizing a strand length distribution narrower than that given in Table 5-1, thereby leading to the same conclusion of the consistency for Gel-1 and Gel-1E. (The fit in the top panel of Fig.5-3 is conceptually more accurate than this fit, but a numerical difference is not significant.)

The above result, consistent description of the fast relaxation processes of the Gel-1E and Gel-1 on the basis of the CR-Rouse molecular picture, lends support to this picture. In this picture, the large-scale motion of a strand is constrained by the surrounding strands (as illustrated in the bottom panel of Fig.4-7) as well as by the sol/dangling chains if any, as discussed in section 4-3-4-2. The strand is entangled in this sense, and its CR-Rouse relaxation is activated by the motion of the surrounding gel strands and sol/dangling chains.

In relation to this point, it is informative to examine the λ_r value (= 0.5) utilized for the fit for Gel-1; cf. solid curves in the top panel of Fig.5-3. This λ_r value is smaller than unity, indicating that the fast relaxation of Gel-1 is accelerated by the sol chains compared to that of Gel-1E. Since the sol chains are more mobile and activate the CR process more quickly compared to the gel strands, this acceleration effect is in harmony with the CR-Rouse molecular picture explained above.

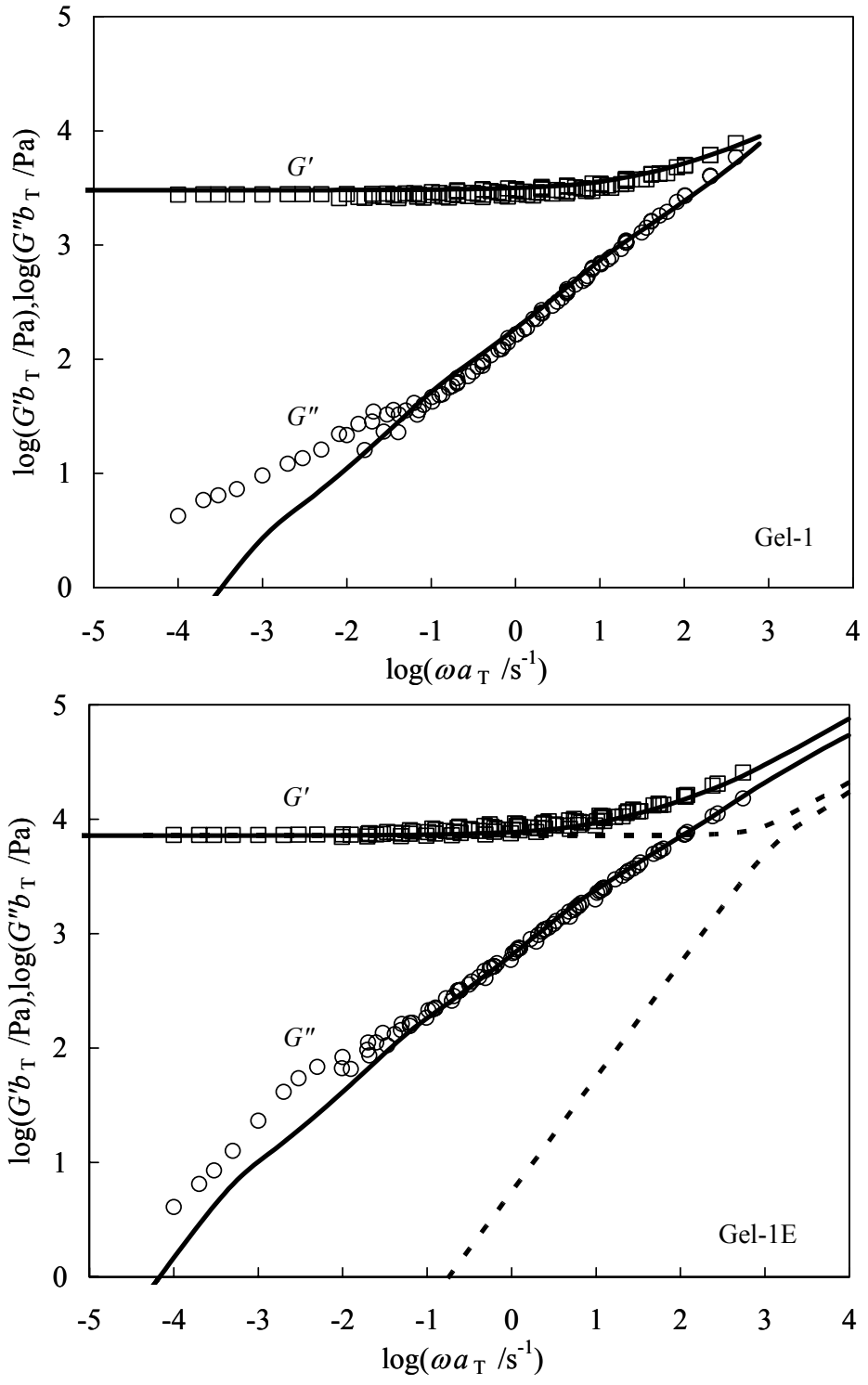

Figure 5-3 Comparison of the viscoelastic behavior of the Gel-1 and Gel-1E samples (symbols) with the intrinsic (entanglement free) Rouse behavior of monodisperse gel stand having $M_c = 340 \times 10^3$ (dotted curve) and entanglement-affected, CR-Rouse behavior of polydisperse stands having the length distribution given in Table 5.1 (solid curves).

5-3-1-3. Slow relaxation mechanism

For both of Gel-1 and Gel-1E samples, the slow relaxation occurs after the CR-Rouse relaxation (fast process) of *individual* gel strands having the length distribution. Thus, the slow relaxation can be related to cooperative CR motion involving *several* neighboring gel strands. (The dangling chains/sol chains have fully relaxed before/during the fast relaxation process and thus possess a secondary contribution, at best, to the G'' data in the slow relaxation regime, as concluded in section 4-3-4-1.)

In relation to this point, it is noted that the power-law exponent n_s characterizing the slow relaxation is considerably larger for Gel-1E than for Gel-1; cf. Eqs.(5.2) and (5.3). This result suggests that the intensive (dominant) part of the slow process occurs more quickly for Gel-1E containing no sol chains than for Gel-1. At first sight, this difference is rather puzzling because the cooperative CR is expected to be slower for the case of slower CR of individual strands, i.e., for Gel-1E. However, this difference of n_s may reflect a spatial heterogeneity of the gel network (illustrated in Fig.3-6), as hypothesized below.

In the absence of the sol chains, the strands in a densely crosslinked region may move much slowly compared to those in the scarcely crosslinked region, in particular in long time scales after the CR-Rouse process of individual strands. Then, the cooperative CR motion involving the former type of strands could be too slow to be detected in the experimental window and thus the detected process may just involve the mobile strands in the coarsely crosslinked region. In contrast, in the presence of the sol chains, the strands in the densely crosslinked region would be more mobile due to the sol chains and may be also involved in the detectably fast cooperative CR process. For this case, the cooperative CR process seen in the experimental window can be *superficially* slower for Gel-1 than for Gel-1E.

5-3-2. Viscoelastic behavior of gels having different prepolymer composition

In the double-liquid reaction, the crosslinks are formed mainly through the reaction of vinyl groups at the ends of prepolymers A and B with the monomethylsilyl group in the prepolymer B, as explained in section 2-2. Thus, the crosslinking density increases on an increase of the w_A/w_B mixing ratio. For the as-prepared Gel-2 and Gel-3 samples with w_A/w_B = 1/2 and 2/1, respectively, the master curves of G' and G'' are shown in the top and bottom panels of Fig.5-5. The sol fraction is ϕ_{sol} = 0.34 and 0.92 for Gel-2 and Gel-3, respectively.

The Gel-3 sample contained just a small amount of the gel network (ϕ_{gel} = 1− ϕ_{sol} = 0.08) and exhibited no clear plateau of G'. No continuous network appears to be well developed at the mixing ratio of w_A/w_B = 2/1 in this sample.

In contrast, the Gel-2 sample clearly exhibits the plateau of G' at $\omega < 1$ s^{-1} because a sufficient number of crosslinking sites (monomethyl siloxane group in the prepolymer B) exists at the mixing ratio of w_A/w_B = 1/2. The average molecular weight between crosslinks, M_c, is evaluated from the equilibrium plateau modulus $G_e = G'$ ($\omega < 1$ s^{-1}) = 23000 Pa as

$$M_c = \frac{\rho(1-\phi_{sol})RT}{G_e} = 64\times10^3 \tag{5.6}$$

This M_c value is smaller than that for Gel-1, reflecting the increase of the number of the crosslinking sites with increasing w_A/w_B ratio. At the same time, it should be also noted that the Gel-2 sample exhibits an enormously small mechanical loss that is comparable with the loss of the Gel-1 sample (cf. Figs.5-1 and 5-4). The sol chains in the Gel-2 sample (ϕ_{sol} = 0.34) appear to be still sufficient to suppress formation of the trapped entanglements during the crosslinking reaction and provide the sample with such a small loss.

It is also noted that the Gel-2 sample exhibits the power-law relaxation of G'' ($\propto \omega^n$), as similar to the behavior of Gel-1. The fast relaxation, seen in a quite wide range of ω (=

10^3-$10^{-2.5}$ s^{-1}), is characterized with the power-law exponent

$$n_f \cong 0.5 \quad \text{(for Gel-2)} \tag{5.7}$$

The power-law feature of the slow relaxation is not clearly resolved for Gel-2 because the fast relaxation extends down to a vicinity of the low-ω end of the experimental window.

The power-law exponent for the fast relaxation of Gel-2 is a little larger than that for Gel-1 (and close to that for Gel-1E); cf. Eqs.(5.2), (5.3), and (5.7). This result possibly reflects a fact that the as-prepared Gel-2 contains a smaller amount of the sol chains (ϕ_{sol} = 0.34) compared to Gel-1, and the sol contribution to G'' of Gel-2 is negligible compared to the contribution from the gel strands.

The Rouse-like power-law behavior observed for Gel-2 is not attributed to the intrinsic (entanglement-free) Rouse relaxation of respective strands, as confirmed from a comparison of the intrinsic Rouse curve and G'' data being similar to that in the bottom panel of in Fig.5-3. Instead, the observed behavior can be again attributed to the CR-Rouse relaxation of polydisperse gel strands. In fact, the data (symbols in the top panel of Fig.5-4) are close to the CR-Rouse modulus (solid curves) calculated with the method explained in Chapter 4 for the strand length distribution $\{w_i , M_{c,i}\}$ specified in Table 5.2 and the CR-Rouse time of the components τ_i set as

$$\tau_i \text{/s} = 2.5\times10^{-13}\times M_{c,i}^2 \quad (i = 1, 2, \ldots) \qquad \text{for Gel-2} \tag{5.8}$$

This τ_i for Gel-2 is a little longer than τ_i for Gel-1E (Eq.(5.4)), despite a fact that Gel-2 contains the sol chains while Gel-1E does not. This difference between Gel-2 and Gel-1E suggests that the CR motion of the strands is more strongly affected by the crosslinks than by the sol chains.

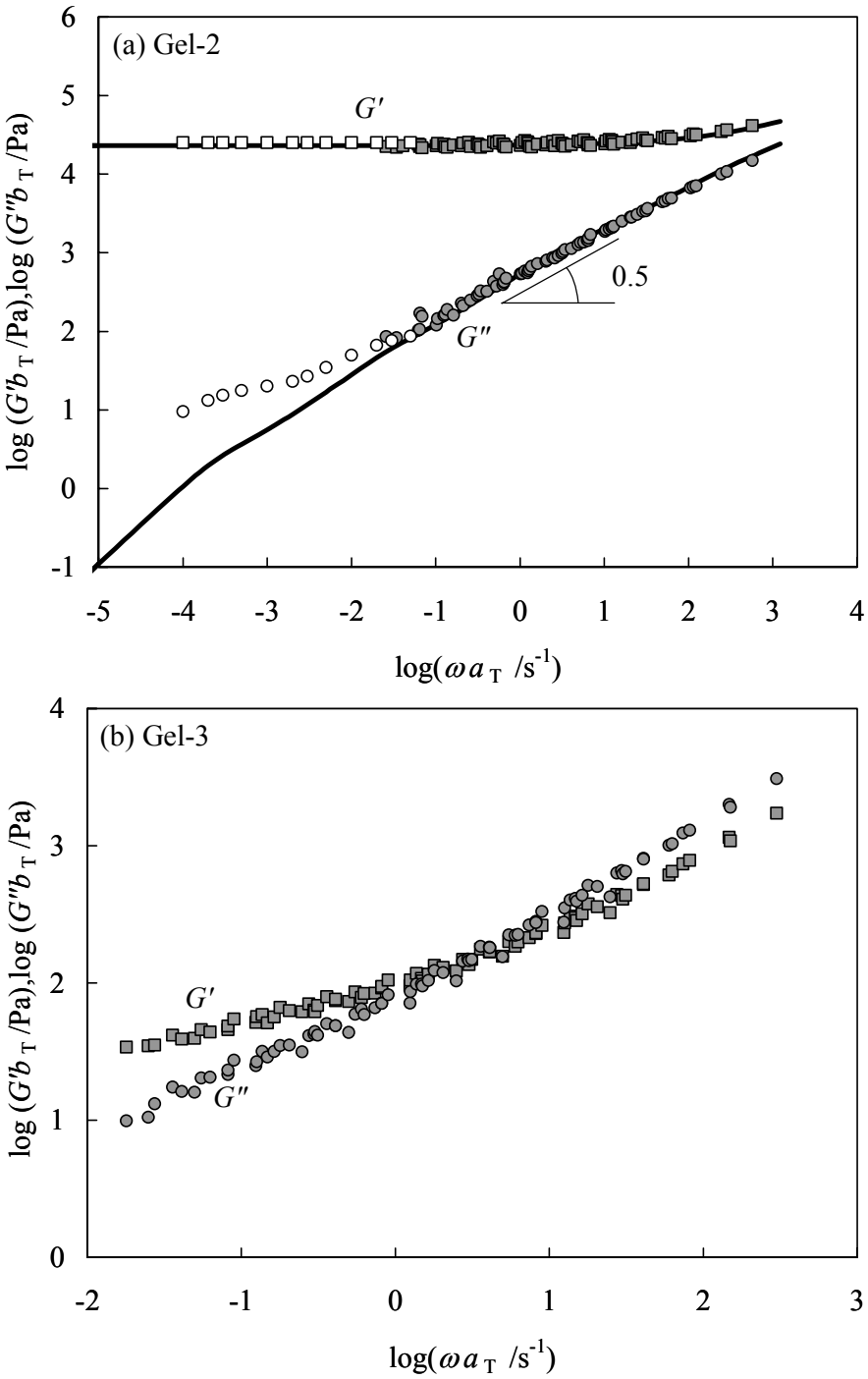

Figure 5-4 Dependence of storage modulus (G') and loss modulus (G'') on the angular frequency (ω) at 20℃ measured for Gel-2 (top panel) and Gel-3 (bottom panel). Filled symbols indicate the data directly obtained from dynamic oscillatory tests, and unfilled symbols show the data converted from the creep compliance data. The solid curves in the top panel indicate the CR-Rouse relaxation of gel strands having the length distribution given in Table 5.2.

Table 5.2 Strand length distribution utilized in the Rouse calculation for Gel-2.

i	w_i	$10^{-3}M_{c,i}$
1	0.12	10
2	0.22	100
3	0.33	1000
4	0.19	10000
5	0.14	100000

5-4. Concluding Remarks

The linear viscoelastic behavior of the PDMS gels scarcely crosslinked through the double-liquid reaction has been examined. The gel sample after the sol extraction, Gel-1E, exhibited the fast and slow relaxation processes characterized with two types of power-law behavior, $G'' \propto \omega^{0.5}$ and $G'' \propto \omega^{0.8}$, respectively. The fast relaxation was attributed to the constraint release (CR)-Rouse relaxation of individual gel strands having a considerable length distribution; this relaxation was essentially the same as that in the Gel-1 sample before the sol extraction. In contrast, the slow relaxation attributable to cooperative CR involving several neighboring strands appeared to be faster for Gel-1E (after the sol extraction) than for Gel-1 (before the extraction). This puzzling result may have reflected a spatial heterogeneity of the crosslinking density.

The linear viscoelastic behavior of as-prepared (sol-containing) PDMS gels of different crosslinking densities has been also examined. An increase of the crosslinking density resulted in an extension of the fast CR-Rouse relaxation tail to low frequencies compared to that in the Gel-1E sample containing no sol chains. Thus, the CR motion of the strands appeared to be more strongly affected by the crosslinks than by the sol chains.

References

1) Kobayashi R, Yabe S, Nomura T, *Polym Adv Tech*, **8**, 351 (1997).

2) Flory PJ , "*Principles of Polymer Chemistry*", Cornell Univ Press, Ithaca, New York, 1953.

3) Graessley WW, *Adv Polym Sci*, **16**, 1 (1974).

4) Ferry JD, *Viscoelastic Properties of Polymers*, *3rd Ed*, Wiley, New York, 1980.

5) Patel SK, Malone S, Cohen C, Gillmor JR, Colby RH, *Macromolecules*, **25**, 5241 (1992).

6) Watanabe H, *Prog Polym Sci*, **24**, 1253 (1999).

CHAPTER 6

Nonlinear Mechanical Behavior of Scarcely Crosslinked Poly (dimethyl siloxane) Gel :Effect of Strand Length Polydispersity

6-1. Introduction

As described in Chapter 1, the rubber elasticity has been one of the most important subjects in the field of polymer physics, and the relationship(s) between the mechanical properties and the network structure of rubbers/gels has been studied over several decades. In Chapters 4 and 5, a model PDMS gel (Gel-1) was prepared through the double-liquid reaction of two types of PDMS prepolymers having vinyl groups at the chain ends. The Gel-1 sample had a large fraction ϕ_{sol} of sol chains (ϕ_{sol} = 0.58; mostly unreacted prepolymers), and the sol chains appeared to have suppressed formation of densely trapped entanglements during the crosslinking reaction. Thus, a very scarcely crosslinked network structure was formed in Gel-1. In a linear viscoelastic test, this gel behaved as a soft elastomer and exhibited a surprisingly small mechanical loss tangent (< 0.01) because of the lack of densely trapped entanglements. Analysis of the linear viscoelastic modulus suggested that the strands in Gel-1 had a very broad distribution in their molecular weight. Consequently, Gel-1 serves as a good model system for investigation of the effect of the gel strand length distribution on the mechanical properties without being disturbed by the trapped entanglements. The effect on the linear viscoelastic properties was fully examined in Chapters 4 and 5. Thus, this chapter is devoted for a study of nonlinear properties.

For this purpose, the scarce PDMS gel (referred to as Gel-1/1) was re-prepared and its behavior under constant-rate elongation and large step shear strains was examined. In the elongational test, Gel-1/1 exhibited strain hardening followed by a macroscopic rupture. The elongational ratio at rupture was significantly smaller than that expected for a gel composed of

monodisperse strands, suggesting that the low molecular weight (M) fraction of the gel strands was highly stretched and broken under rather small elongation thereby governing the strain-hardening/rupture of the Gel-1/1 system. In the step shear tests, Gel-1/1 showed significant stress decay with time that was also related to the scission of those low-M strands. Details of these results are described below.

6-2. Experimental

6-2-1. Materials

Commercially available two vinyl-terminated PDMS prepolymers (SE1886; Toray-Dow Corning Co., Ltd) were used. These prepolymers were from the same batches as those utilized in Chapters 3-5, and their molecular characteristics were explained in Chapter 2.

The prepolymers A and B were mixed at a weight ratio of w_A/w_B = 1/1 and allowed to react at 120˚C for 3 h to give the as-prepared gel referred to as Gel-1/1. As shown in the top part of Scheme 2-1, the heat (at 120˚C) and a Pt catalyst (contained in the prepolymer B) allowed the vinyl groups at the ends of prepolymers A and B to react with the monomethylsilyl group in the prepolymer B to form the crosslinks. In addition to this major reaction, two vinyl groups can also react with each other to give the crosslinks (bottom part of Scheme 2-1), though this minor reaction occurred less frequently.

The Gel-1/1 thus prepared contained a large amount of sol chains. The sol fraction ϕ_{sol} therein was determined from a sol extraction test, as done in section 4-3-3. In this test, a small sheet specimen of Gel-1/1 was soaked in fresh toluene (good solvent for PDMS) for 48 h, with toluene being replaced in every 12 h. All sol chains were extracted with this procedure, and the sol fraction in the as-prepared Gel-1/1, ϕ_{sol} = 0.53, was evaluated from the weights of the dry specimen before and after the sol extraction. This ϕ_{sol} value was a little

smaller than the value of Gel-1(= 0.58).

The sol chains extracted from the Gel-1/1 specimen were characterized with low-angle laser light scattering (LALS) and gel permeation chromatography (GPC) utilizing a LALS photometer (KMX-6, Chromatrix Co. Ltd) and a GPC unit (Model510, Waters Co. Ltd) connected to a differential refractive index detector (RI-8020, Tosoh Co. Ltd). The solvent was toluene, and commercially available monodisperse polystyrenes (TSK, Tosoh Co. Ltd) were utilized as the elution/LALS standards. The weight-average molecular weight and the polydispersity index of the sol chains, $M_{w,sol} = 45.8 \times 10^3$ (determined from LALS) and $M_{w,sol}/M_{n,sol} = 4.1$ (evaluated from GPC calibration), were not significantly different from those of the prepolymers. Thus, quite a large fraction of the prepolymers was left unreacted during the preparation of Gel-1/1, as was the case also for Gel-1 examined in Chapters 3-5.

These results indicated that the gel network in the Gel-1/1 sample was very scarce ($\phi_{gel} = 1-\phi_{sol} = 0.47$). This scarce network structure of Gel-1/1 (hardly having the trapped entanglement, as discussed in Chapters 4,5) was composed of highly polydisperse strands, as revealed from analysis of its linear viscoelastic moduli (cf. Fig.6-1 shown later).

The Gel-1/1 sample was subjected to constant-rate elongational tests and step shear tests. The specimens for the elongational test were prepared through the above reaction made in a small metal mold of thickness ≅ 1.0 mm. The resulting Gel-1/1 sheet was cut with a razor into rectangular specimens of length ≅ 20 mm and width ≅ 10 mm to be utilized in the test. The step shear test was made in a cone-plate (CP) geometry. Since the flat sheet sample could not fit in this geometry, the specimens for the step shear test were prepared through the reaction directly made in the CP fixture mounted in a rheometer chamber. (An extra material squeezed out of the fixture was carefully removed with a razor after the reaction.)

A PDMS gel composed of monodisperse strands was utilized as a reference material for the elongational test. This gel, identical to the NL-138 sample in Ref.25 and referred to as

Gel-U in this chapter, was generously supplied from Prof. Urayama at Kyoto University. He synthesized the gel through tetrafunctional end-linking of monodisperse PDMS prepolymer ($M_n = 84\times10^3$) in bulk in the presence of unreactive, guest homo-PDMS chains ($M_g = 138\times10^3$; ϕ_{guest} = 15 vol% in the system).[1] Gel-U had the equilibrium shear modulus of $G_e \cong 1.4\times10^5$ Pa at 30˚C (cf. Fig.1 of Ref.1). The corresponding molecular weight of the effective gel strands, $M_c = \rho(1-\phi_{guest})RT/G_e \cong 15\times10^3$ (ρ = PDMS density, R = gas constant, and T = absolute temperature), was considerably smaller than the prepolymer molecular weight (84×10^3) and rather close to the entanglement molecular weight ($M_e \cong 8.1\times10^3$ for PDMS[2]), indicating that Gel-U prepared through the end-linking reaction in bulk contained densely trapped entanglements.[1] This Gel-U sample, supplied in a form of thick disk of the thickness ≅ 5 mm, was carefully sliced with a razor into rectangular specimens of the thickness ≅ 1 mm, length ≅ 20 mm, and width ≅ 10 mm, and these specimens were utilized in the elongational test.

6-2-2. Measurements

For the Gel-1/1 and Gel-U rectangular specimens, the true elongational stress σ_E (not the engineering stress reduced to unit cross-sectional area before the elongation) at 20˚C was measured with an extensional viscosity fixture (EVF) attached to a laboratory rheometer (ARES, Rheometrics Co. Ltd; currently TA Instruments). The elongational strain rate was set at 0.01 and 0.1 s^{-1}. For Gel-1/1, step shear tests were also conducted at 20˚C with a cone-plate (CP) fixture of diameter = 20 mm and gap angle = 2 deg mounted on a laboratory rheometer (Soliquid-meter, Reoroji Co. Ltd). Further details of experimental conditions were explained in Chapter 2.

6-3. Results and Discussion

6-3-1. Linear viscoelastic behavior of as-prepared Gel-1/1

For the as-prepared Gel-1/1 sample that experienced no large strain, Fig.6-1 shows the angular frequency (ω) dependence of the storage and loss moduli, G' and G'', measured at 20˚C (room temperature). G' is quite insensitive to ω, while G'' is much smaller than G' at low ω and exhibits the Rouse-like power-law behavior, $G'' \propto \omega^{n_{1/1}}$ with $n_{1/1} \cong 0.5$. These features are characteristic to a gel network hardly having trapped entanglements. A large fraction of the sol chains ($\phi_{sol} = 0.53$; mostly prepolymers) remained in Ge1-1/1, and these sol chains possibly suppressed the trapped entanglement formation during the gelation process, as fully discussed in Chapters 4,5.

The elasticity of the as-prepared Gel-1/1 sample is characterized with the equilibrium shear modulus G_e ($= G'(\omega \to 0)$) and the average molecular weight M_c of the gel strands: $M_c = C_{gel} RT/G_e = \rho(1-\phi_{sol})RT/G_e$ where C_{gel} is the mass concentration of the gel strands in Gel-1/1, ρ is the density of Gel-1/1 as a whole, R is the gas constant, and T is the absolute temperature. From the G' data shown in Fig.6-1, G_e and M_c are evaluated as

$$G_e = 6.0 \times 10^3 \text{ Pa}, \quad M_c = 190 \times 10^3 \tag{6.1}$$

This M_c is much larger than the molecular weights of the prepolymers A and B, confirming the scarce network structure in the Gel-1/1 sample.

A comment needs to be added for the above G_e and M_c values. In Chapters 4 and 5, the Gel-1 specimen was made from the same batches of the prepolymers A and B as utilized in this Chapter. Nevertheless, Gel-1 had $G_e = 2.8 \times 10^3$ Pa and $M_c = 340 \times 10^3$ and was softer than Gel-1/1 prepared in this Chapter. This difference could be partly due to an uncontrolled thermal history in the gel preparation process. The Gel-1/1 specimens for the shear and elongational tests, respectively, were prepared in the small cone-plate (CP) fixture and the thin

metal mold (of thickness ≅ 1 mm), as explained earlier. In both cases, the prepolymer mixture was rapidly heated to the set temperature (120˚C) to start the crosslinking reaction quickly, because the CP fixture and thin mold had small heat capacities (and the reaction in the CP fixture was made under forced convection in the rheometer chamber). In contrast, the Gel-1 specimen was prepared in a thicker metal mold (of thickness = 2-3 mm) having a larger thermal capacity, and the reaction started rather slowly. Despite this difference, the Gel-1/1 specimens utilized in this Chapter were reproducibly prepared in the small fixture/thin mold (as confirmed from the reproducibility of their linear viscoelastic moduli shown in Fig.6-1). Thus, the properties of the network in Gel-1/1 could be unequivocally examined.

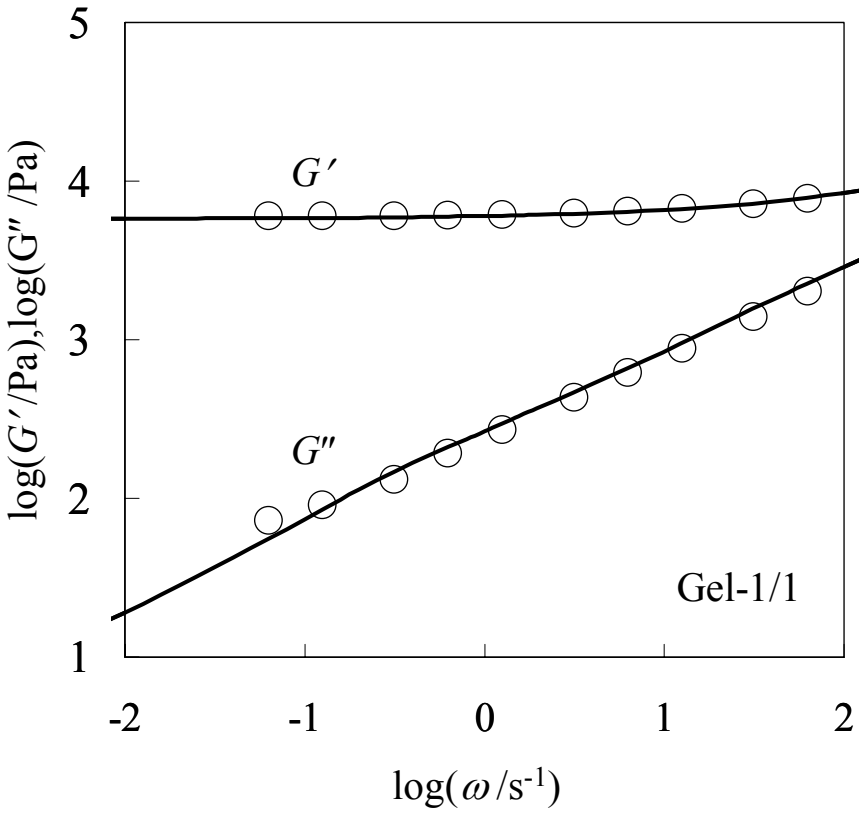

Figure 6-1 Linear viscoelastic moduli of as-prepared (neat) Gel-1/1 system at 20˚C. The solid curves indicate the results of fitting with the Rouse network model. The strand molecular weight distribution utilized in the fit is summarized in Table 6.1.

6-3-2. Molecular weight distribution of as-prepared Gel-1/1 strands

For the gel network composed of *monodisperse* strands, all strands relax at the same rates. Thus, for such gels, G'' exhibits its terminal tail ($G'' \propto \omega$) at low ω where G' becomes independent of ω, as described in Chapter 4. However, Fig.6-1 demonstrates that the Gel-1/1 system shows the non-terminal power-law behavior ($G'' \propto \omega^{n_{1/1}}$ with $n_{1/1} \cong 0.5$) at $\omega < 1$ s^{-1} where G' is quite insensitive to ω. This result unequivocally indicates that the gel strands therein have a broad molecular weight distribution, as fully discussed in Chapters 4 and 5.

The width of this distribution can be estimated by fitting the G' and G'' data shown in Fig.6-1 with a Rouse network model discussed in Chapters 4 and 5:

$$G'(\omega) = \sum_i \left[\frac{C_i RT}{M_i} \left\{ 1 + \sum_{p \geq 1} \frac{\omega^2 (\tau_i / p^2)^2}{1 + \omega^2 (\tau_i / p^2)^2} \right\} \right] \tag{6.2a}$$

$$G''(\omega) = \eta_{\mathrm{sol}} \omega + \sum_i \left[\frac{C_i RT}{M_i} \sum_{p \geq 1} \frac{\omega (\tau_i / p^2)}{1 + \omega^2 (\tau_i / p^2)^2} \right] \tag{6.2b}$$

Here, C_i is the mass concentration of the i-th component of the strands having the molecular weight M_i, $\tau_R(M_i)$ is the longest relaxation time of this component. The set of C_i satisfies a relationship, $\Sigma_i C_i = \rho(1-\phi_{\mathrm{sol}})$ with ρ being the density of the Gel-1/1 system as a whole. (In Eqs.(4.17) and (4.18), C_i was represented as $C_{\mathrm{st}} w_i$ with C_{st} and w_i being the total concentration of the gel strands and the weight fraction of the i-th strand having the molecular weight M_i, respectively.) In Eq.(6.2b), η_{sol} is the viscosity of the sol chains in Gel-1/1. (At the frequencies examined in Fig.6-1, the sol chains of $M_{\mathrm{w,sol}} = 45.8 \times 10^3$ have fully relaxed and contributed only to G'' as a viscous component, as discussed in section 5-3-1-2). The relaxation time of the strands is expressed in the Rouse form,

$$\tau_R(M_i) = \tau^* M_i^2 \quad (\tau^* = \text{reference time}) \tag{6.3}$$

Since $M_{w,sol}$ ($=45.8\times10^3$) of the sol chains is larger than the entanglement molecular weight for PDMS, $M_e=8.1\times10^3$,[2] η_{sol} of the sol chains is affected by the entanglement with the gel strands as well as the entanglement among the sol chains. From the bulk viscosity data of entangled linear PDMS chains, η_{sol} of those sol chains was estimated to be 3 Pa s with the method explained in section 5-3-1-2. With this η_{sol} value, the fit of the G' and G'' data of Gel-1/1 with Eq.(6.2) was attempted to estimate the molecular weight distribution of the strands. In Fig.6-1, the solid curves indicate the best fit results obtained for the reference time $\tau^*=8.7\times10^{-14}$ s and the M_i and C_i values specified in Table 6.1. (This set of $\{M_i, C_i\}$ is later shown in Fig.6-6 as the C_i *vs* M_i plots.) The corresponding polydispersity index of the Gel-1/1 strands is

$$\frac{M_w}{M_n}=\frac{\left\{\sum_i C_i M_i\right\}\left\{\sum_i C_i M_i^{-1}\right\}}{\left\{\sum_i C_i\right\}^2}\cong 600 \tag{6.4}$$

Thus, the strands in Gel-1/1 should have a very broad molecular weight distribution, which corresponds to the scarce network structure having the average strand molecular weight $M_c >> M_{w,pre}$ (cf. Eq.(6.1)).

Here, a comment needs to be made for the above fitting process where M_i was chosen rather arbitrary and C_i was determined to achieve the best fit of the G' and G'' data. This choice was not unique. Namely, equally good fitting was achieved for different sets of $\{M_i, C_i\}$ with M_i being chosen in a range similar to that of Table 6-1. However, the polydispersity index of the gel strands was not significantly different for those sets of $\{M_i, C_i\}$, suggesting a reliability of this index given in Eq.(6.4). In this sense, the set of M_i chosen with an interval of one decade (Table 6.1) is to be regarded as a representative, coarsened set of M_i for the actual Gel-1/1 strands. This set of M_i is later utilized in the characterization of Gel-1/1 after

the imposition of large step strains.

An additional comment is to be made for the reference time τ^* appearing in Eq.(6.3). In section 4-3-4-2, the entanglement-free, intrinsic Rouse relaxation time for $M_e = 8.1\times10^3$ was estimated from the viscoelastic data of linear homo-PDMS as $\tau_e = 2.8\times10^{-7}$ s. From this τ_e value, the reference time for the intrinsic Rouse motion is obtained as $\tau_{int}^* = \tau_e/M_e^2 = 4.3\times10^{-15}$ s. This τ_{int}^* is considerably smaller than τ^* (= 8.7×10^{-14} s) giving the good fit in Fig.6-1. Namely, the Rouse-like relaxation seen in Fig.6-1 is attributable to the constraint release (CR) Rouse motion of *temporarily* (non-permanently) entangled gel strands. Further discussion of this CR-Rouse motion has been given in Chapters 4 and 5.

Table 6.1 Molecular Weight Distribution of Gel Strands Utilized for the Fit in Fig. 6-1.

$10^{-3}M_i$	C_i /g·cm^{-3}
5	0.00376
50	0.0705
500	0.0893
5000	0.108
50000	0.103
500000	0.0987

6-3-3. Elongational behavior of Gel-1/1

For the as-prepared Gel-1/1 sample having significantly polydisperse strands, the true elongational stress σ_E was measured at 20˚C (room temperature) at constant Hencky strain rate, $\dot{\varepsilon}$ = 0.01 and 0.1 s^{-1}. In Fig.6-2, the σ_E data normalized by the equilibrium tensile modulus

in the linear viscoelastic regime, $3G_e$ (with G_e given in Eq.(6.1)), are double-logarithmically plotted against the Hencky strain ε (= ln λ with λ being the elongational ratio). The σ_E data are insensitive to the strain rate $\dot{\varepsilon}$ (≤ 0.1 s^{-1}). This behavior is consistent with the almost purely elastic behavior seen at angular frequencies $\omega < 1$ s^{-1} (cf. Fig.6-1). The weak relaxation process characterized by the power-law behavior of $G'' \propto \omega^{n_{1/1}}$; $n_{1/1} \cong 0.5$) has a very minor contribution to the stress of the system at those low ω. Thus, the σ_E data measured at similarly low $\dot{\varepsilon}$ (Fig.6-2) are hardly contributed from this relaxation process. These data characterize the Gel-1/1 network structure under elongation.

As seen in Fig.6-2, Gel-1/1 exhibits the linear elastic behavior, $\sigma_E/3G_e\varepsilon = 1$ (solid line), under small elongation at $\varepsilon < 0.5$ ($\lambda < 1.7$). For larger ε and λ, σ_E becomes larger than that expected for this linear behavior, and the macroscopic rupture occurs at $\varepsilon_{max} = 1.5$ ($\lambda_{max} = 4.5$) after this hardening. This behavior is *qualitatively* similar to usual crosslinked rubbers/gels. For example, Fig.6-3 shows the σ_E data at 20˚C measured for the Gel-U sample having *monodisperse* strands with trapped entanglements (and containing 15 wt% of the guest sol chains of $M_n = 138 \times 10^3$) measured in this study at 20˚C. These data, normalized by the G_e data taken from literature ($\cong 1.4 \times 10^5$Pa)[1] and plotted against ε, clearly indicate the nonlinear hardening/rupture after the linear elastic behavior at small ε.

Thus, the strand length polydispersity in Gel-1/1 has no qualitative effect on the nonlinear elongational behavior. However, this distribution should have a *quantitative* effect. For an examination of this effect, the σ_E data can be compared with the Edward-Vilgis (EV) slip-link model.[3] This molecular model, formulated for a network of *monodisperse* strands, is known to describe the rubber elasticity most accurately.[4] In this model, the elongational stress σ_E was originally expressed in terms of the elongational ratio λ, the number densities N_C and N_S of chemically crosslinked network strands and slip-links (trapped entanglements), the link-slippage parameter η, and the extensibility parameter α.[3] This σ_E can be re-written as a

function of λ, the number density ratio $\theta = N_S/N_C$, η, α, and the equilibrium shear modulus G_e.[5] The explicit form of this function is shown in Appendix 6.

The parameter α is identical to the reciprocal of the maximum possible elongational ratio λ_{max}° defined for the sub-strand between trapped entanglement points (in the presence of these entanglements) and for the strand as a whole (in the absence of the entanglements). The Gel-1/1 system hardly includes the trapped entanglements while the Gel-U system has densely trapped entanglements, as explained earlier. For both systems, α can be given by $1/\lambda_{max}^{\circ}$, with λ_{max}° being evaluated from the strand molecular weight M_c evaluated from the plateau modulus G_e. (For Gel-U, M_c is the molecular weight of the trapped entanglement strands, not the neat strands equivalent to the PDMS prepolymer.) The λ_{max}° values thus calculated are:

$$\lambda_{max}^{\circ} \equiv \frac{\left\langle R_c^2 \right\rangle^{1/2}}{b_K} = 53 \text{ (for Gel-1/1), } 16 \text{ (for Gel-U)} \qquad (6.5)$$

Here, $\left\langle R_c^2 \right\rangle$ is the mean-square end-to-end distance of the strand of the molecular weight M_c under no external elongation ($\left\langle R_c^2 \right\rangle = 0.00422 M_c$ nm^2 for PDMS[6]), and b_K is the Kuhn step length (= 0.53 nm for PDMS[7]): b_K is identical to a ratio of $\left\langle R_c^2 \right\rangle$ to the full-stretch length of the strand.

A comment needs to be made for the λ_{max}° value for the Gel-1/1 system. The M_c value of this system (= 190×10^3; Eq.(6.1)) is an *average* over the polydisperse strands therein and thus the λ_{max}° obtained from M_c is also regarded as an average. Despite this polydispersity, the use of the average λ_{max}° seems to allow the application of the EV model (formulated for monodisperse strands) to the Gel-1/1 system with the highest consistency.

With the G_e data and the above λ_{max}° values (= $1/\alpha$) in the EV model, the σ_E of the Gel-1/1 and Gel-U systems were calculated as a function of ε (= ln λ). The results are shown in Figs.6-2 and 6-3 with the dashed curves. The vertical dotted lines indicate $\varepsilon_{max}^{\circ}$ = ln λ_{max}°.

For definiteness, η was chosen to be zero and θ was utilized as a fitting parameters to achieve the best fit of the data. The calculated σ_E was insensitive to the θ value given that θ was set below 0.2 (20% population of the slip-links compared to the chemical crosslinks). Thus, such treatment of the parameters θ and η introduced little uncertainty in the fitting. The curves shown in Figs.6-2 and 6-3 were calculated for $\eta = 0$ and $\theta = 0.05$.

As seen in Figs.6-2 and 6-3, the σ_E data of the Gel-1/1 and Gel-U systems are close to the EV calculation made for monodisperse strands. In this sense, the strand length polydispersity in the Gel-1/1 system appears to have little effect on the elongational behavior. However, a remarkable effect is noted for the maximum strain at rupture, ε_{max}, shown with the vertical solid lines. For the Gel-U system prepared by end-linking of monodisperse prepolymer chains (*neat strands*), ε_{max} is close to $\varepsilon_{max}^{\circ}$ defined for the trapped entanglement strands therein; $\varepsilon_{max} \cong 0.9\varepsilon_{max}^{\circ}$ and $\lambda_{max} \cong 0.8\lambda_{max}^{\circ}$ for Gel-U. This result indicates that most of the trapped entanglement strands therein are stretched but not broken until the macroscopic rupture occurs. (In fact, the rupture point is not very far even from the full-stretch point ($\lambda_{max,neat}^{\circ} \cong 36$) defined for the longer, neat strands with $M_n = 84 \times 10^3$; $\lambda_{max} \cong 0.4\lambda_{max,neat}^{\circ}$.)

In contrast, for the Gel-1/1 system, ε_{max} is considerably smaller than $\varepsilon_{max}^{\circ}$, giving $\lambda_{max} \cong 0.08\lambda_{max}^{\circ}$. This result suggests that low-M fractions of the polydisperse strands are highly stretched and broken at rather small $\lambda << \lambda_{max}$ because λ_{max}° decreases with decreasing M; $\lambda_{max}^{\circ} \propto M^{1/2}$ as seen from Eq.(6.5) . Thus, the hardening/rupture of Gel-1/1 appears to be governed by the short strands, demonstrating the important effect of the strand length polydispersity on the toughness of the gel: The toughness is reduced as the strands become polydisperse. This effect is further discussed below in relation the stress decay of Gel-1/1 under large step strains.

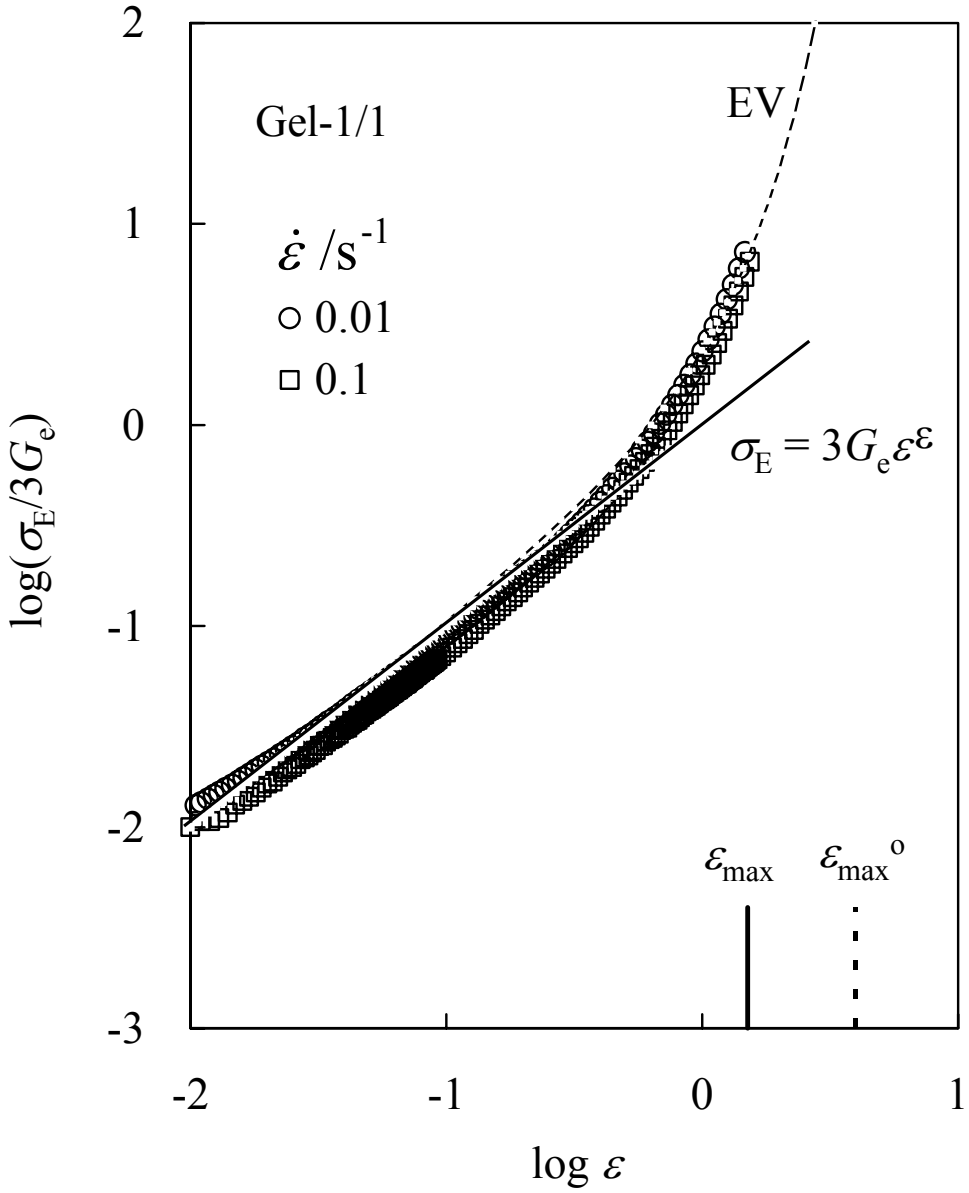

Figure 6-2 Elongational behavior of Gel-1/1 system at 20˚C. The solid curve indicates the elastic behavior expected from the linear viscoelastic moduli of as-prepared (neat) Gel-1/1. The dotted curve indicates the result of fitting with the Edward-Vilgis model.

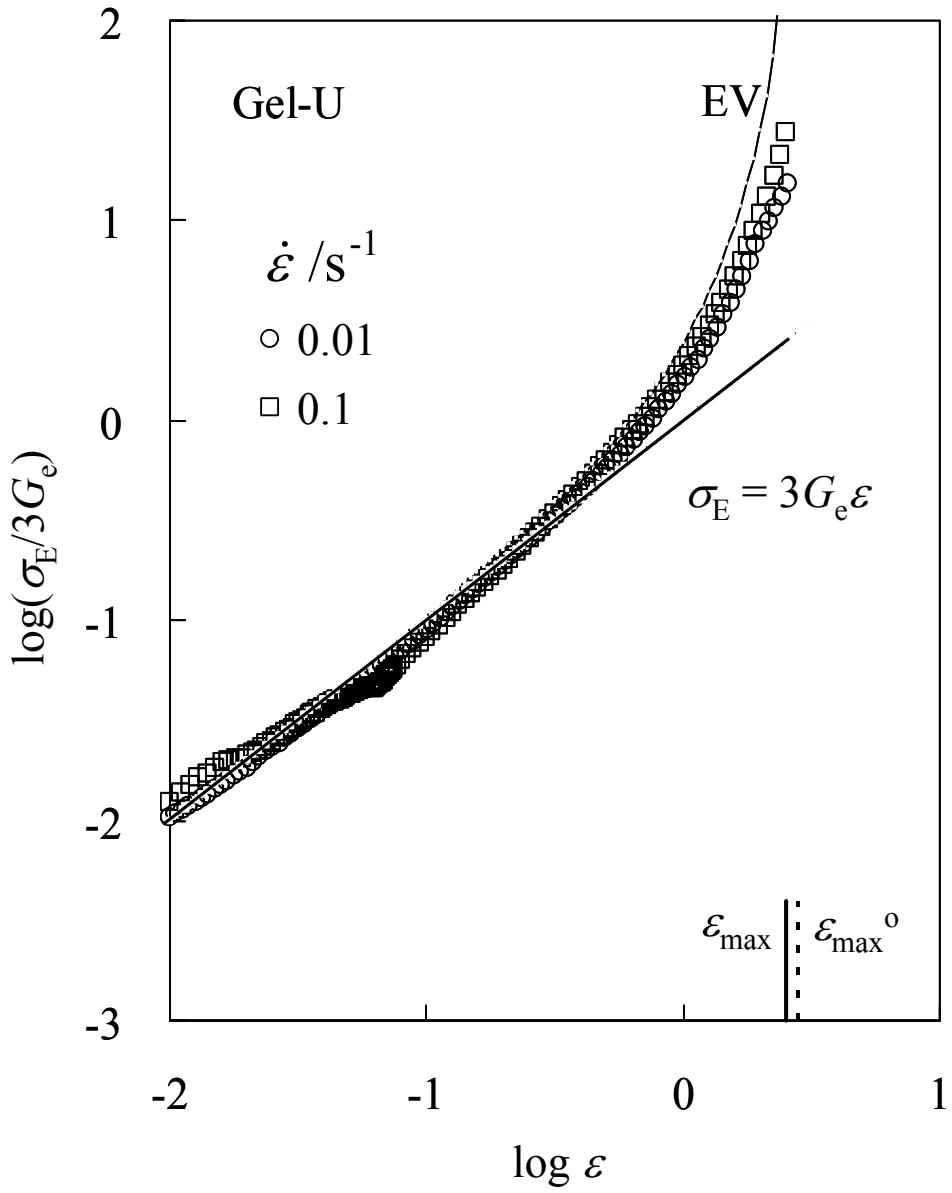

Figure 6-3 Elongational behavior of Gel-U system at 20˚C. The solid curve indicates the elastic behavior expected from the linear viscoelastic moduli of Gel-U, and the dotted curve indicates the result of fitting with the Edward-Vilgis model.

6-3-4. Stress decay of Gel-1/1 under large step shear

The Gel-1/1 specimens were subjected to step shear strains of various magnitudes γ ($\leq$ 5.1) at 20˚C (room temperature), and the shear stress $\sigma(t,\gamma)$ was measured with time t up 10000 s. Fig.6-4 shows changes of the *apparent* relaxation modulus $G(t,\gamma)$ (= $\sigma(t,\gamma)/\gamma$) with t. For $\gamma \leq 2$, $G(t,\gamma)$ remains independent of t and its value agrees with the equilibrium modulus in the linear viscoelastic regime, $G_e = 6.0 \times 10^3$ Pa (Eq.(6.1)). Thus, no shear-induced change (scission) occurred for the Gel-1/1 network at $t \leq 10000$ s and $\gamma \leq 2$. In contrast, for larger $\gamma \geq 2.6$, $G(t,\gamma)$ decays with t significantly, and the decay is faster and larger for larger γ. This nonlinear decay should be contributed not only from a molecular relaxation process (gel strand motion) but also from the strand cession, as discussed later for Figs.6-5 and 6-8. In this sense, $G(t,\gamma)$ of Gel-1/1 shown here is qualitatively different from the nonlinear relaxation modulus of uncrosslinked homopolymer chains that detects only the non-equilibrium chain motion.[8] (For this reason, $G(t,\gamma)$ of Gel-1/1 was referred as the *apparent* relaxation modulus.)

Fig.6-5 shows the linear viscoelastic moduli of the Gel-1/1 specimens measured after the imposition of step strains γ for 10000 s. For clarity of Figure, only the data for representative γ values are shown. The moduli after the imposition of strain $\gamma \leq 2$ were indistinguishable from those before the imposition, confirming that the gel network was not broken at those γ. For larger γ, the storage modulus G' still exhibits a low-ω plateau but the plateau height decreases with increasing γ. This decrease unequivocally indicates that the gel network sustaining the G' plateau was partly broken by the large step strains to decrease the number density of the elastically effective strands. (The network was not fully broken in the range of γ examined, as noted from the long-time plateau of $G(t,\gamma)$ and low-ω plateau of G'.)

Some details of this partially broken network structure can be examined for the loss modulus, G''. As noted in Fig.6-5, G'' at high ω decreases significantly while G'' at low ω hardly decreases (or even slightly increases) after the imposition of large step strains. Thus,

the disruption of the gel network is expected to have occurred from the short strands (governing the high-ω response of the system) to long strands on the increase of γ. This expectation can be tested by fitting the G' and G'' data with the Rouse network model (Eq.(6.2)). The strand molecular weights M_i (Table 6.1) and the strand relaxation times τ_i (Eq.(6.3)) identical to those for the as-prepared Gel-1/1 specimen (Fig.6-1) were utilized in Eq.(6.2) to estimate the mass concentrations of the strands C_i from the fit of the data after the large step shear. The solid curves in Fig.6-5 shows the best-fit results, and Fig.6-6 shows the corresponding set of C_i plotted against M_i. (The plot for $\gamma \leq 2$ represents the $\{M_i,C_i\}$ set summarized in Table 6.1.) Fig.6-6 demonstrates that the concentration decreases and increases, respectively, for the low-M and high-M strands with increasing γ. The set of M_i utilized here is to be regarded as a representative, coarsened set of M_i for the actual Gel-1/1 strands, as discussed earlier. However, the result seen in Fig.6-6 qualitatively confirms the above expectation without ambiguity.

Here, a comment needs to be made for the increase of the long strand concentration with increasing γ. The shear-induced disruption of the network might appear to just result in the decrease of the short strand concentration without enriching the long strands. If the short and long strands fully segregate in space, this type of network disruption could certainly occur. However, if the short and long strands are mixed in space (which seems to be the case for the Gel-1/1 system), some short strands bridge the long strands; see, for example, two short strands marked with asterisk in the top part of Fig.6-7 (where only the connected backbones of the comb-like strands are shown). The scission of such short strands converts these strands into short dangling chains and, at the same time, releases the bridging point between the long strands to convert these long strands into longer strands carrying the short dangling chains; see the middle part of Fig.6-7 (where the dangling chains are not shown for simplicity). In other words, the scission of the short strands tends to enrich the longer strands. The increase of the

long strand concentration seen in Fig.6-6 appears to reflect this mode of network disruption.

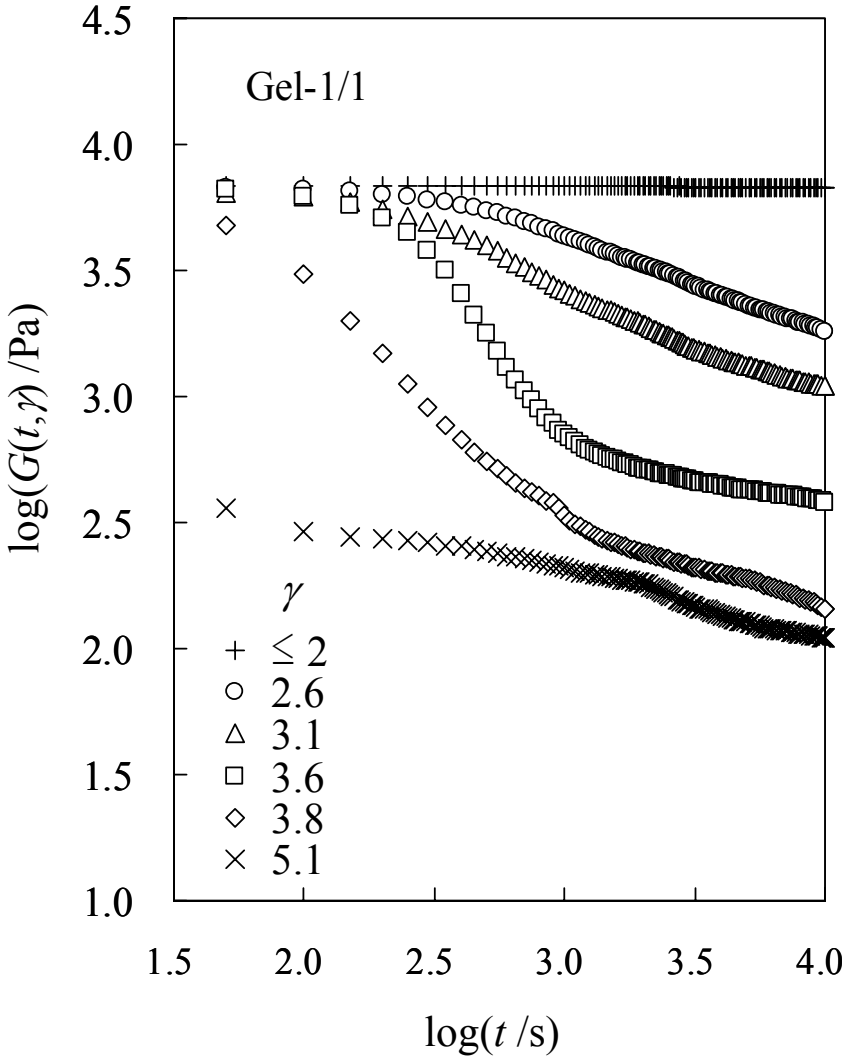

Figure 6-4 Nonlinear stress decay behavior of Gel-1/1 system subjected to step shear strains of various magnitudes γ.

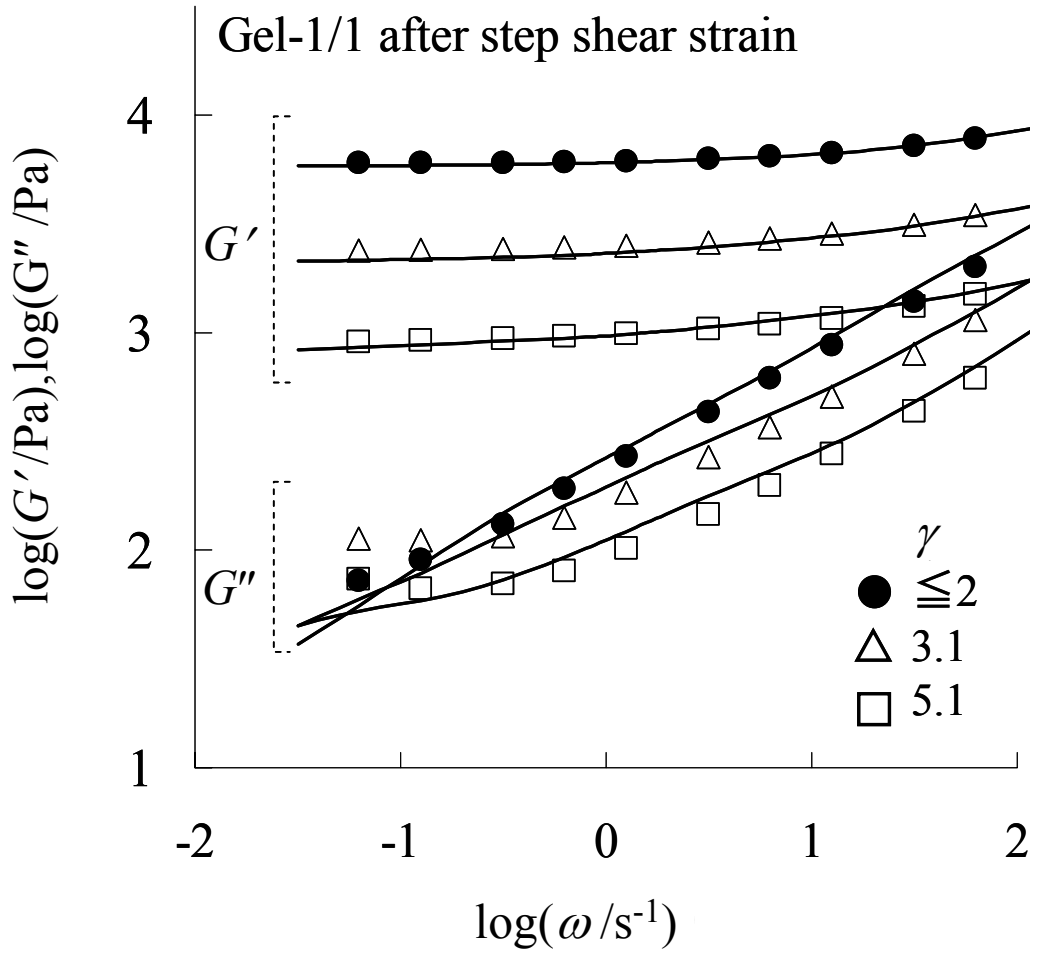

Figure 6-5 Linear viscoelastic moduli of Gel-1/1 system measured after imposition of step shear strains of various magnitudes γ. The solid curves indicate the results of fitting with the Rouse network model. The strand molecular weight distributions obtained from the fitting are shown in Fig.6-6.

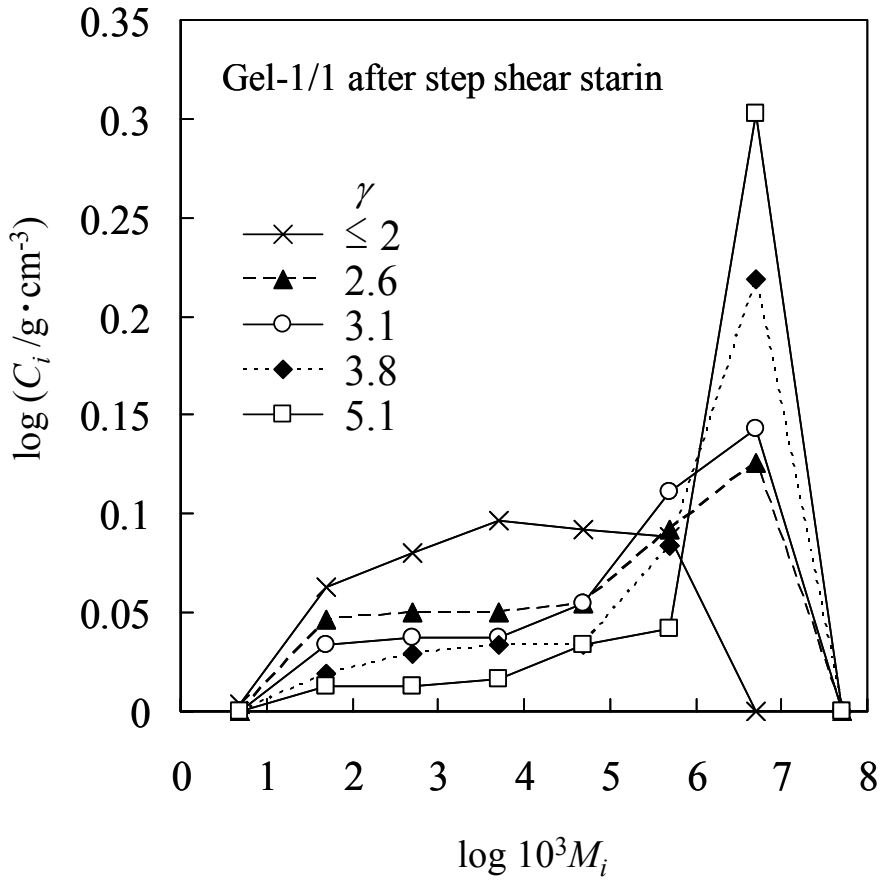

Figure 6-6 The strand molecular weight distribution of Gel-1/1 after imposition of shear strain. The distribution was obtained from the fitting with the Rouse network model (cf. Fig.6-5).

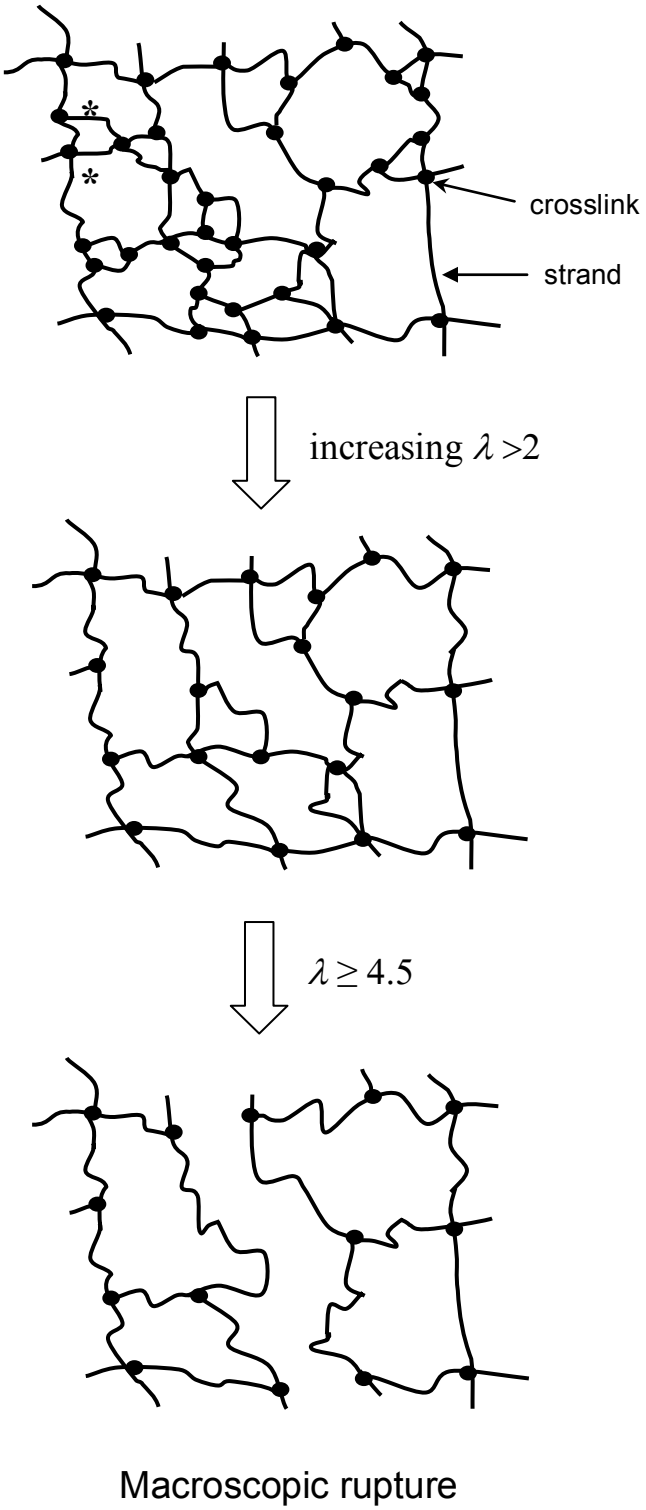

Figure 6-7 Schematic illustration of the mode of scission of the network in Gel-1/1.

6-3-5. Comparison of Gel-1/1 network disruption under elongation and shear

The nonlinear elongational and shear behavior of Gel-1/1 seen in Figs.6-2 and 6-4 commonly reflects the scission of the gel strands (that starts from short strands and propagates to long strands), as discussed earlier. This similarity of the elongational and shear behavior can be further examined for the elongational ratio λ_s under the step shear strain of the magnitude γ; $\lambda_s = (1+\gamma^2/3)^{1/2}$ for the affine deformation. For the maximum shear strain examined, $\gamma = 5.1$, the modulus $G(t,\gamma)$ at long times decayed by a factor of ~50 compared to $G(t,\gamma)$ before the shear imposition (cf. Fig.6-4) and the Gel-1/1 sample was *almost* macroscopically disrupted. The corresponding λ_s value (= 3.1) is fairly close to the λ_{max} value (= 4.5) at the elongational rupture point, demonstrating the similarity of the elongational and shear nonlinearities of Gel-1/1. However, a delicate difference between these nonlinearities is also noted, as discussed below.

As explained for Fig.6-7, the scission of short strands yields a long strand. This long strand would have a distorted conformation when it is formed, and its motion can result in relaxational decay of the stress. If this long strand has the maximum elongational ratio λ_{max}° (defined by Eq.(6.5)) comparable to/smaller than λ_s, its scission should also contribute to the stress decay. The very gradual decay of $G(t,\gamma)$ under the large step shear, occurring in a range of $t \geq 1000$ s (Fig.6-4), would have reflected both of the motion and scission of the scission-formed long strands.

In relation to this point, it is informative to compare the storage modulus measured after imposition of the step shear, $G'(\omega = 0.06\ s^{-1})$ with 0.06 s^{-1} being the lowest ω examined in Fig. 6-5, and the apparent relaxation modulus under step shear, $G(t = 10000\ s)$ with 10000 s being the longest t examined in Fig.6-4. $G'(\omega = 0.06\ s^{-1})$ and $G(t = 10000\ s)$ commonly exhibit the nonlinear decrease from the equilibrium modulus G_e of the as-prepared Gel-1/1 on the increase of γ (> 2), as shown in Fig.6-8. More importantly, $G(t = 10000\ s)$ is smaller than

$G'(\omega = 0.06\ s^{-1})$ in this nonlinear regime possibly because the slow motion of the scission-formed long strands leads to the relaxation at long t (= 10000 s) while this motion does not contribute the behavior at short t (= $1/\omega$ = 17 s corresponding to $\omega = 0.06\ s^{-1}$).

In relation to this time scale of the motion/relaxation of the scission-formed long strands, it is noted that the macroscopic rupture of the Gel-1/1 under elongation occurred in the time scale of $t = \varepsilon_{max}/\dot{\varepsilon} \leq 150$ s (ε_{max} = 1.5 and $\dot{\varepsilon}$ = 0.1 and 0.01 s^{-1}; cf. Fig.6-2). Thus, the motion/relaxation of the scission-formed long strands should have hardly occurred in the elongational test, as similar to the situation for the G' data measured after the step shear. In this sense, the disruption behavior of Gel-1/1 under the elongation and shear (Figs.6-2 and 6-4) is not identical. Nevertheless, the fundamental feature of disruption, the scission propagating from short to long strands, is common for the elongational and shear behavior of Gel-1/1 having highly polydisperse strands.

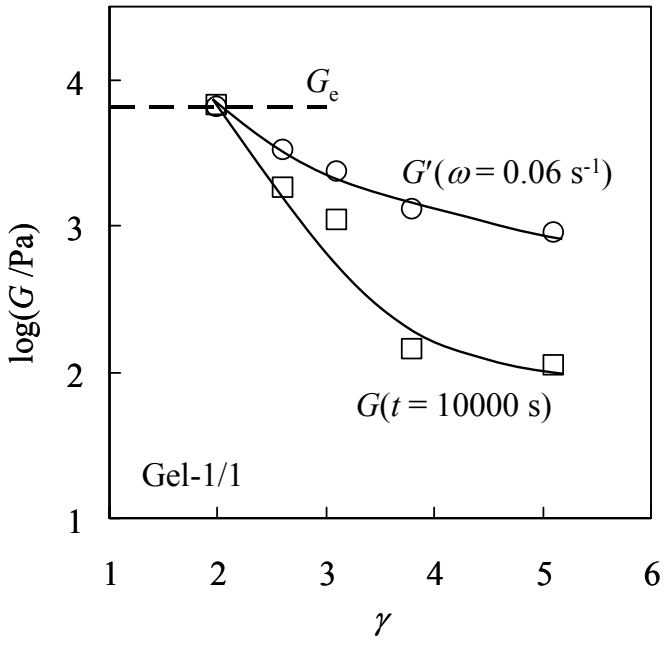

Figure 6-8 Comparison of the apparent relaxation modulus at long times measured under step shear strains, $G(t$ = 10000 s), and the linear storage modulus at low frequency measured after imposition of step shear strains, $G'(\omega = 0.06\ s^{-1})$.

6-4. Concluding Remarks

Nonlinear mechanical behavior was examined for a scarcely crosslinked poly(dimethyl siloxane) gel, Gel-1/1, under constant-rate elongation and large step shear. The gel strands in Gel-1/1 had an average molecular weight of $M_c = 190 \times 10^3$ and a very broad molecular weight distribution ($M_w/M_n \cong 600$), as noted from the fit of its linear viscoelastic moduli with the Rouse network model.

In the elongational test, Gel-1/1 sample exhibited the strain hardening followed by the macroscopic rupture at the elongational ratio of $\lambda_{max} = 4.5$. This λ_{max} was significantly smaller than the maximum elongational ratio (full-stretch ratio; $\lambda_{max}^{\circ} = 53$) nominally expected for a gel composed of monodisperse strands of $M_c = 190 \times 10^3$. This difference between λ_{max} and λ_{max}° is attributable to the polydispersity of the strand length. Namely, the scission of the low-M fractions of the strands in Gel-1/1 should have occurred at λ much smaller than λ_{max}°, thereby governing the nonlinear elongational behavior/rupture of Gel-1/1. The scission would have propagated from short to long strands to result in the rupture.

Under large step shear strains γ (> 2), Gel-1/1 exhibited nonlinear decay of the shear stress with time. Analysis of the linear viscoelastic moduli of Gel-1/1 after imposition of large strains indicated that the stress decay reflected scission of the low-M fractions of the gel strands (as well as the motion of scission-formed long strands) occurring with time. This behavior was similar to the nonlinear elongational behavior, although a delicate difference related to a time-dependent cessation/motion of the scission-formed long strands remained between the nonlinearities under the large step shear and elongation.

Appendix 6. Edwards-Vilgis Model

For rubbers containing no dangling loop/tail, Edwards and Vilgis [3] derived a theoretical relationship between the uniaxial tensile force f_E and the elongational ratio λ being expressed in terms of the link-slippage parameter η and the extensibility parameter α as well as the number densities of the network strands and trapped entanglements, N_C and N_S. This f_E–λ relationship can be rearranged into a relationship between the extensional stress σ_E and λ that includes the equilibrium shear modulus (plateau modulus) G_e as a parameter. The results are summarized as[5]

$$\frac{\sigma_E}{G_e} = \frac{f_c(\lambda;\alpha)}{g_c(\alpha)+\theta\, g_s(\alpha,\eta)} + \frac{f_{s1}(\lambda;\alpha,\eta)+f_{s2}(\lambda;\alpha)+f_{s3}(\lambda;\alpha,\eta)+f_{s4}(\lambda;\eta)}{\theta^{-1}g_c(\alpha)+g_s(\alpha,\eta)} \tag{6.A1}$$

with

$$G_e = N_C k_B T\{g_c(\alpha)+\theta\, g_s(\alpha,\eta)\},\ \theta = N_S/N_C \tag{6.A2}$$

The functions g's and f's appearing in Eqs.(6.A1) and (6.A2) are defined below.

$$g_c(\alpha) = \frac{1-2\alpha^2+3\alpha^4}{\left(1-3\alpha^2\right)^2},\ g_s(\alpha,\eta) = \frac{1-(2-2\eta-2\eta^2)\alpha^2+(3+6\eta)\alpha^4}{\left(1-3\alpha^2\right)^2(1+\eta)^2} \tag{6.A3}$$

$$f_c(\lambda;\alpha) = \frac{\left\{1-2\alpha^2+\alpha^4(\lambda^2+2\lambda^{-1})\right\}}{\left\{1-\alpha^2(\lambda^2+2\lambda^{-1})\right\}^2}(\lambda^2-\lambda^{-1}) \tag{6.A4}$$

$$f_{s1}(\lambda;\alpha,\eta) = \frac{(1-\alpha^2)\alpha^2(1+\eta)}{\left\{1-\alpha^2(\lambda^2+2\lambda^{-1})\right\}^2}\left(\frac{\lambda^2}{1+\eta\lambda^2}+\frac{2}{\eta+\lambda}\right)(\lambda^2-\lambda^{-1}) \tag{6.A5}$$

$$f_{s2}(\lambda;\alpha) = \frac{-\alpha^2}{\left\{1-\alpha^2(\lambda^2+2\lambda^{-1})\right\}}(\lambda^2-\lambda^{-1}) \tag{6.A6}$$

$$f_{S3}(\lambda;\alpha,\eta)=\frac{(1-\alpha^2)(1+\eta)}{\left\{1-\alpha^2(\lambda^2+2\lambda^{-1})\right\}}\left\{\frac{\lambda^2}{\left(1+\eta\lambda^2\right)^2}-\frac{\lambda}{(\eta+\lambda)^2}\right\} \tag{6.A7}$$

$$f_{S4}(\lambda;\eta)=\eta\left\{\frac{\lambda^2}{1+\eta\lambda^2}-\frac{1}{\eta+\lambda}\right\} \tag{6.A8}$$

For fitting the σ_E data of Gel-1/1 and Gel-U systems, the measured G_e data and maximum stretch ratio of the gel strands λ_{max}° (= $1/\alpha$) were utilized in Eqs.(6.A1) and (6.A2). For definiteness, η was chosen to be zero and θ was utilized as a fitting parameters to achieve the best fit of the data.

References

1) Urayama K, Yokoyama K, Kohjiya S, *Macromolecules*, **34**, 4513 (2001).

2) Graessley WW, *Adv Polym Sci*, **16**, 1 (1974).

3) Edwards SF, Vilgis TA, *Polymer*, **47**, 483 (1986).

4) Urayama K, Kawamura T, and Kohjiya S, *Macromolecules*, **34**, 8261 (2001).

5) Watanabe H, Matsumiya Y, Sawada T, Iwamoto T, *Macromolecules*, **40**, 6885 (2007).

6) Fetters LJ, Lohse DJ, Colby RH, *Chain Dimension and Entanglement Spacing, in Mark JE ed. Physical Properties of Polymers Handbook (2nd ed.)*, Springer, New York (2007).

7) Evmenenko G, Mo H, Kewalramani S, Dutta P, *Polymer*, **47**, 878 (2006).

8) Watanabe H, *Prog Polym Sci*, **24**, 1253 (1999).

CHAPTER 7

SUMMARY

This thesis attempts to add a new insight to a fairly established field of research on poly(dimethyl siloxane) (PDMS) gels through rheological, swelling, GPC, and ^{1}H-NMR measurements. The rheological measurements were conducted for scarcely crosslinked PDMS gels made through the double-liquid reaction of two prepolymers as well as for the prepolymers to detect the large-scale chain dynamics in these materials. The swelling measurements gave the molecular weight between crosslinks of the PDMS gels, and GPC/NMR measurements characterized the prepolymers and sol components included in the gels.

Following the general introduction (Chapter 1) and the explanation of material preparation as well as the principle/method of each measurement (Chapter 2), the results and discussion of the viscoelastic, swelling, GPC, and ^{1}H-NMR measurements are described in Chapters 3 to 6. The main points in these chapters are summarized below.

In Chapter 3, linear viscoelastic behavior was investigated during a gelation process of a 1/1 (wt/wt) mixture of two PDMS prepolymers A and B having the molecular weight $M_{w,pre} = 3.5\times10^3$. The gelation occurred mainly through a reaction of monomethylsilyl groups (0.7 mol% in the backbone of the prepolymer B) and vinyl groups at the chain ends of A and B, giving a scarcely crosslinked gel containing a large sol fraction ($\phi_{sol} = 0.58$ on completion of gelation) and exhibiting the equilibrium modulus much smaller than a nominal modulus, $(1-\phi_{sol})\rho RT/M_{n,pre}$ with ρ = density. The reaction was conducted at a relatively low temperature, 50℃, so that this reaction proceeded slowly and the viscoelastic changes during the gelation process were well resolved. The terminal flow behavior was observed at a

reaction time $t_r \leq 54$ min (pre-gel stage), while the elasticity at low angular frequencies ω became prominent at $t_r \geq 60$ min (post-gel stage). The critical gelation behavior characterized with a power-law relationship between the storage/loss moduli and the angular frequency ω, $G'' \propto G' \propto \omega^n$ $(0 < n < 1)$, was *not* observed at t_r between these stages, suggesting that the gelation did not occur through formation of a huge, self-similarly hyper-branched critical gel network. For further examination of this gelation process, the prepolymer mixture was collected at several reaction times t_r and the molecular characteristics of toluene-soluble sol chains therein and a number fraction of the remaining (unreacted) monomethylsilyl group ϕ_{HMeSi} were examined. It turned out that the high-M tail of the sol became enriched with densely branched chains of $M \cong 1\times10^7$ ($\cong 300M_{pre}$) and ϕ_{HMeSi} rapidly decreased to ~0.3 with increasing t_r up to 65 min while the branch content/molecular weight of the sol decreased and ϕ_{HMeSi} gradually approached 0 on a further increase of t_r. These results suggested a gelation mechanism that the densely branched pre-gel chains involving up to 300 prepolymers were first formed on consumption of the majority of the monomethylsilyl groups at $t_r \leq 65$ min and then these pregel chains were scarcely linked trough a small amount of remaining monomethylsilyl groups to form the 3-dimensional gel at $t_r > 65$ min. The lack of critical gelation behavior and the small equilibrium modulus ($<< (1-\phi_{sol})\rho RT/M_{n,pre}$) on completion of gelation is consistent with this mechanism.

In Chapter 4, linear viscoelastic behavior was investigated for a PDMS gel formed through the bulk double-liquid crosslinking reaction of the 1/1 (wt/wt) mixture of the prepolymers A and B. Time-temperature superposition worked, and master curves at 20˚C were constructed for the storage and loss moduli, G' and G'', in a wide range of angular frequency ω (= 10^3-10^{-5} s^{-1}) by combining the data obtained from dynamic oscillatory tests and creep tests. With decreasing ω to 10^{-1} s^{-1}, G'' decreased in proportion to $\omega^{0.6}$ and G' rapidly

decreased to its equilibrium plateau at the modulus $G_e = 2.8\times10^3$ Pa. On a further decrease of ω well in the plateau regime of G', G'' decreased in proportion to $\omega^{0.3}$. Thus, the gel exhibited the fast and slow relaxation processes characterized with these types of power-law behavior of G''. The molecular weight between the crosslinks evaluated from the G_e data (as well as the equilibrium swelling ratio in toluene), $M_c \cong 340\times10^3$, was about ten times larger than $M_{w,pre}$. The crosslinking reaction was made in the bulk state but still gave such a scarce gel network possibly because a large amount of sol chains and dangling chains had diluted the entanglements during the reaction to suppress the trapped entanglement formation. From the analysis of the G' and G'' data on the basis of the above M_c value and the intrinsic Rouse relaxation time, the fast relaxation process was assigned as the Rouse-like constraint release (CR) process of individual gel strands. The polydispersity of the strands was found to be essential for the power-law behavior of G'' to be observed in the plateau regime of G'. The slow relaxation process was related to fluctuation of the crosslinking points, which is equivalent to cooperative Rouse-CR motion of many gel strands connected at these points.

In Chapter 5, linear viscoelastic behavior was examined for the PDMS gels scarcely crosslinked through the double-liquid reaction and subjected to the sol extraction. The gel sample after the sol extraction exhibited the fast and slow relaxation processes characterized with the power-law behavior of the dynamic loss modulus, $G''\propto\omega^{0.5}$ and $G''\propto\omega^{0.8}$ at high ω. The fast relaxation was essentially the same as that in the gel before the sol extraction and attributed to the CR-Rouse relaxation of individual gel strands having a considerable length distribution. In contrast, the slow relaxation, being related to cooperative CR involving neighboring gel strands, appeared to become faster after the sol extraction than before. This puzzling result may have reflected a spatial heterogeneity of the crosslinking density. The viscoelastic property was examined also for the as-prepared PDMS gels (containing the sol

chains) having different crosslinking densities. The CR-Rouse relaxation tail of the gel having a higher crosslinking density was found to extend to low frequencies compared to that of the scarcely crosslinked gel after the sol extraction. Thus, the CR motion of the strands appeared to be more strongly affected by the crosslinking density than by the sol chains.

In Chapter 6, nonlinear mechanical behavior was examined for the scarcely crosslinked PDMS gel (made from the 1/1 mixture of the prepolymers A and B) under constant-rate elongation and large step shear strains. The average molecular weight of the gel strands evaluated from the equilibrium modulus in the linear viscoelastic regime was $M_c = 190 \times 10^3$, and the strands had a significantly broad molecular weight distribution, $M_w/M_n \cong 600$, as estimated from fit of the linear viscoelastic moduli with a Rouse network model. In the elongational test at constant elongational rates $\dot{\varepsilon}$, the gel exhibited $\dot{\varepsilon}$-insensitive strain hardening followed by rupture at an elongational ratio of $\lambda_{max} = 4.5$. This λ_{max} was significantly smaller than the λ_{max}° nominally expected for a gel composed of monodisperse strands having $M_c = 190 \times 10^3$; $\lambda_{max}^{\circ} = 53$ and $\lambda_{max}/\lambda_{max}^{\circ} \cong 0.08$ for those strands. In contrast, a reference experiment made for a gel sample (Gel-U) composed of monodisperse strands having densely trapped entanglements indicated that λ_{max} of this gel was close to λ_{max}°; $\lambda_{max} \cong 14$, $\lambda_{max}^{\circ} = 16$, and $\lambda_{max}/\lambda_{max}^{\circ} \cong 0.9$ for Gel-U. These results suggested that the low-*M* fractions of the strands in the scarcely crosslinked gel were highly stretched and broken at λ much smaller than the λ_{max}° defined for the *average* M_c, thereby governing the nonlinear elongational/rupture behavior. Under large step shear strains γ (> 2), the scarce gel exhibited nonlinear decay of the shear stress with time. Analysis of the linear viscoelastic moduli after imposition of large strains indicated that the stress decay under large strains reflected scission of the low-*M* fractions of the gel strands as well as the motion of scission-formed long strands occurring with time. This behavior was qualitatively similar to the nonlinear elongational

behavior, although a delicate difference related to time-dependent cessation/motion of the scission-formed long strands remained between the nonlinearities under the large shear and elongation.

List of Publications

1. Publications Included in This Thesis

1. Viscoelastic Behavior of Scarcely Crosslinked Poly(dimethyl siloxane) Gel
   Hideaki TAKAHASHI, Yoshitaka ISHIMURO, Hiroshi WATANABE
   Nihon Reoroji Gakkaishi (J Soc Rheol Jpn), **2006**, 34, 135 - 145

2. Viscoelastic Behavior of Scarcely Crosslinked Poly(dimethyl siloxane) Gels: 2. Effects of Sol component and Network Strand Length
   Hideaki TAKAHASHI, Yoshitaka ISHIMURO, Hiroshi WATANABE
   Nihon Reoroji Gakkaishi (J Soc Rheol Jpn), **2007**, 35, 191 - 198

3. Nonlinear Mechanical Behavior of Scarcely Crosslinked Poly (dimethyl siloxane) Gel: Effect of Strand Length Polydispersity
   Hideaki TAKAHASHI, Yoshitaka ISHIMURO, Hiroshi WATANABE
   Polymer Journal, **2008**, 40, 465 - 474

4. Viscoelastic Behavior of Scarcely Crosslinked Poly(dimethyl siloxane) Gel: 3. Examination of Gelation Process
   Hideaki TAKAHASHI, Yoshitaka ISHIMURO, Hiroshi WATANABE
   Nihon Reoroji Gakkaishi (J Soc Rheol Jpn), in press.

2. Other Related Publications

5. Viscoelastic Behavior of an Epoxy Compound with High Fillers During Cure

   Motohiro KUROKI, Hideaki TAKAHASHI, Yoshitaka ISHIMURO

   Nihon Reoroji Gakkaishi (J Soc Rheol Japan), **1999**, 27, 235 - 241

Acknowledgements

The present study has been carried out under the direction of Professor Hiroshi Watanabe at Institute for Chemical Research in Kyoto University, from 2005 to 2009.

The author would like to express his most sincere thanks to Professor Hiroshi Watanabe for his continuous encouragement, guidance, comments, discussions and collaborations throughout the study.

The author also expresses his profound gratitude to Dr. Yoshitaka Ishimuro at Toray Research Center Inc. for providing an important opportunity to study and for his helpful advice and valuable encouragement ever since the author joined the company from 1996.

Special thanks are given to Professor Toshinobu Yoko at Institute for Chemical Research, Kyoto University and Professor Toshikazu Takigawa at Department of Material Chemistry, Graduate School of Engineering, Kyoto University for their invaluable comments.

The author is deeply indebted to Professor Kenji Urayama at Department of Material Chemistry, Graduate School of Engineering, Kyoto University for helpful discussion and generous supply of his precious material (Gel-U) and invaluable comments.

The author is indebted to Professor Tadashi Inoue at Graduate School of Science, Osaka University, Professor Yuichi Masubuchi and Professor Yumi Matsumiya at Institute for Chemical Research in Kyoto University for their helpful guidance and advice.

The author is sincerely grateful to Professor Shigeru Yamago and Ms. Eri Mishima at Institute for Chemical Research in Kyoto University for their kind support in ^{1}H-NMR measurements.

The author acknowledges with thanks the invaluable supports and advices from Dr. M. Todoki, Dr. M. Oishi, Messrs.Y. Takai, H. Kawagoe, H. Ichikawa, T. Hirano, N. Higeta, and Dr. H. Ishida of Toray Research Center Inc.

The author especially wishes to express thanks to Ms. Yukie Kajikawa, Prof. Takashi Uneyama, Messrs. Shinichi Okada, Kenji Furuichi, Quan Chen, Kazushi Horio, Takatoshi Yaoita, Takeshi Suzuki, Satoshi Tanaka, Hiroshi Kawakita, Taro Kinoshita, Motoaki Moriya, Ryo Saito, Shiro Katakura, Keisuke Hiramoto, and Ms. Akiko Uno for their continuous support and encouragement throughout this study at Watanabe laboratory. The author also wishes to express thanks to all the other past and current students of Watanabe laboratory.

Finally, the author expresses his gratitude to his wife, Chika Takahashi, his father and mother, Masaru Takahashi and Hiromi Takahashi, his sons, Ryosuke Takahashi and Yuta Takahashi, and all his relatives and friends.

March 2009

Hideaki Takahashi